TAMPEREEN TEKNILLINEN YLIOPISTO
TAMPERE UNIVERSITY OF TECHNOLOGY

Matti Virkki

Supramolecular Materials for Photocontrolled Optical Nonlinearity

Julkaisu 1413 • Publication 1413

Tampere 2016

Tampereen teknillinen yliopisto. Julkaisu 1413
Tampere University of Technology. Publication 1413

Matti Virkki

Supramolecular Materials for Photocontrolled Optical Nonlinearity

Thesis for the degree of Doctor of Science in Technology to be presented with due permission for public examination and criticism in Sähkötalo Building, Auditorium S2, at Tampere University of Technology, on the 7th of October 2016, at 12 noon.

Tampereen teknillinen yliopisto - Tampere University of Technology
Tampere 2016

ISBN 978-952-15-3811-7 (printed)
ISBN 978-952-15-3825-4 (PDF)
ISSN 1459-2045

Abstract

Photonics, the science of light, is driving another technological revolution in the 21st century just as electronics did during the previous one. Many of our current solutions in, for example, telecommunications and information storage already rely on modification of light with matter and vice versa. Still, the ever-increasing need for bandwidth and storage, while keeping the cost and power requirements down, requires continuous efforts in the improvement of existing and creation of new technologies. The development of better materials is at the core of such efforts. Modification of optical properties of matter with light brings us to the realm of nonlinear optics. The fact that organic materials have the largest and fastest nonlinear optical response gives us the reason to look into these materials.

This Thesis focuses on the study of new organic materials concepts in the search for nonlinear response that can be turned on and off at will. The scope of the studied materials extends to supramolecular polymers, small-molecule amorphous matter, and liquid-crystalline polymers. Each of these materials is characterized by relatively strong designed interactions between the constituent molecules, which give them rather unique features, most importantly the capability to resist spontaneous interactions that reduce the nonlinear optical response. Photocontrol of the nonlinear response is reached due to the phototriggered isomerization of azobenzene molecules that are used throughout the Thesis. Purely optical means are applied to realign the azobenzene molecules into an arrangement that enables second-order nonlinear response. As this realignment is fully reversible, the on–off control of nonlinear response becomes possible.

The results of this Thesis imply that the type and strength of supramolecular interactions in a polymer system have a pronounced effect on the ability to fight against harmful spontaneous interactions. While hydrogen-bonded materials are deemed unsuitable for strong photocontrolled response, the newer halogen bonding concept provides promising results and deserves further studies. Results on a new small-molecule amorphous material combined with a well-known azobenzene molecule with relatively strong nonlinear response hint that this new approach might challenge the polymer systems, which have been extensively studied for a few decades. A conceptually new liquid-crystalline polymer is also developed and its nonlinear response is reversibly controlled by light with an unprecedented contrast of 20. Although the absolute level of nonlinearity in the studied materials is moderate at best, the value of the information gained in this Thesis serves to guide the design strategies when materials applicable in photonics are sought for.

Preface

The research presented in this Thesis was carried out in the Optics Laboratory of Tampere University of Technology during the years 2011–2016. Some of the foundations for these studies were laid already during 2008–2010 while working as a research assistant towards Bachelor's and Master's degrees. I gratefully acknowledge the Graduate School of Tampere University of Technology, the Väisälä Foundation and the Graduate School of Modern Optics and Photonics for funding the research.

I would like to thank my supervisor, Professor Martti Kauranen for accepting me to his group and for his support even when I again and again pushed the work to directions that had been previously seen as endless swamps of trouble. The patience and positivity certainly pays off in the form of relating the feeling of trust to one's own skills. My sincere gratitude goes also to Professor Arri Priimagi whom I was lucky enough to get as a co-supervisor to guide me in these studies. The spring of ideas and possibilities certainly helped to push me to the completion of this work. I thank my co-authors Ossi Tuominen, Alessandra Forni, Marco Saccone, Pierangelo Metrangolo, Giuseppe Resnati, Keiji Ogawa, and Jun-ichi Mamiya for their invaluable contributions to our joint research. I thank Francisco J. Rodríguez for introducing me to all-optical poling many years back.

In the course of these studies, I got to visit several research laboratories around the world. I wish to thank Professor Atsushi Shishido from Tokyo Institute of Technology, Japan, Professor Gaetano Assanto from Roma Tre University, Italy, and Professor Pierre-François Brevet from Claude Bernard University Lyon 1, France for their hospitality. I learned much on these visits and the fruits of the collaboration are evident in this Thesis, in other common publications as well as in ongoing work.

Working in a physics laboratory on a topic owing much to photo*chemistry* might be a lonesome crusade. However, the atmosphere and group activities of our laboratory made it more of a pleasant hike among friends. I am grateful to at least Goëry, Juha, Jan, Mikko, and Caroline for organizing the social events and thank all the past and present members of the laboratory for the atmosphere. I thank Jouni for sharing the office and valuable thoughts for most of these years and my friends and colleagues from other laboratories Matti and Topi for lunch company and often broadened views on science and life.

Finally, I thank my family for their love: Mother, Grandmother, Hanna, and Sanna as well as Matti and Liisa. My deepest gratitude belongs to my wife Kirsi and my light and joy Laura for putting things to the right perspective every day already on the way home.

Tampere, September 2016

Matti Virkki

Contents

List of abbreviations and symbols

AOP	All-optical poling
DR1	Disperse Red 1
EFISHG	Electric-field-induced second-harmonic generation
LC	Liquid crystal
NLO	Nonlinear optical
P4VP	Poly(4-vinylpyridine) polymer
PS	Polystyrene polymer
SHG	Second-harmonic generation
α	Absorption coefficient
$\mathbf{A}$	Slowly varying electric field amplitude
$\mathcal{A}$	Absorbance
β	Second-order molecular polarizability
$\mathbf{B}$	Magnetic flux density
c	Speed of light
Δk	Wave vector mismatch
$\Delta\phi$	Phase difference
$\mathbf{D}$	Electric displacement field
$\frac{\partial F}{\partial t}$	Time derivative of function F
ε_0	Electric permittivity of vacuum
$\varepsilon^{(1)}$	Relative permittivity
$\mathbf{E}$	Electric field
$\mathcal{E}$	Energy
f	Local field factor
γ	Third order molecular polarizability
$\mathbf{H}$	Magnetic field

I	Intensity, precisely irradiance (power per area)
$\mathbf{J}$	Current density
$\chi^{(n)}$	Electric susceptibility of order n
k_B	Boltzmann constant
$\mathbf{k}$	Wave vector
k	Magnitude of the wave vector, $\lvert\mathbf{k}\rvert$
λ	Wavelength
μ	Dipole moment
μ_{eq}	Transition dipole moment
μ^0	Permanent dipole moment
μ_0	Magnetic permeability of vacuum
$\mathbf{M}$	Magnetization
∇	Gradient
$\nabla\cdot$	Divergence
$\nabla\times$	Curl
ν	Frequency
n	Refractive index
n_e	Refractive index for ordinary polarization direction
n_o	Refractive index for extraordinary polarization direction
N	Number density
$\lvert\cdot\rvert$	Norm
ω	Angular frequency ($2\pi \times$ frequency)
$\mathbf{O_P}$	Parity operator
$\mathbf{P}$	Electric polarization
$\mathbf{P}^{(n)}$	Electric polarization of order n
ρ	Free charge density
$\mathbf{r}$	Position vector
σ	Absorption cross section
t	Time
T	Temperature
T_g	Glass transition temperature
$\langle\cdot\rangle$	Time average

List of publications

Paper I Matti Virkki, Martti Kauranen, and Arri Priimagi, "Different chromophore concentration dependence of photoinduced birefringence and second-order susceptibility in all-optical poling," *Applied Physics Letters*, vol. 99, no. 18, p. 183309, 2011.

Paper II Matti Virkki, Ossi Tuominen, Alessandra Forni, Marco Saccone, Pierangelo Metrangolo, Giuseppe Resnati, Martti Kauranen, and Arri Priimagi, "Halogen bonding enhances nonlinear optical response in poled supramolecular polymers," *Journal of Materials Chemistry C*, vol. 3, no. 12, pp. 3003–3006, 2015.

Paper III Matti Virkki, Ossi Tuominen, Martti Kauranen, and Arri Priimagi, "Photoinduced nonlinear optical response in azobenzene-functionalized molecular glass," *Optics Express*, vol. 24, no. 5, pp. 4964–4971, 2016.

Paper IV Arri Priimagi, Keiji Ogawa, Matti Virkki, Jun-ichi Mamiya, Martti Kauranen, and Atsushi Shishido, "High-contrast photoswitching of nonlinear optical response in crosslinked ferroelectric liquid-crystalline polymers," *Advanced Materials*, vol. 24, no. 48, pp. 6410–6415, 2012.

1 Introduction

While inorganic materials continue to be the backbone of photonics applications in the 21st century, organics are slowly paving their way to common use. Efficient production [1,2] and detection [3,4] of light fully based on organic materials have matured even to device level. Due to the well-established manufacturing infrastructure and strong market position of inorganic materials, however, their complete replacement in photonics seems unlikely. Nevertheless, organic materials will complement traditional solutions, in particular, in applications that require large active areas, flexibility, or low-cost processing. In some applications, the properties of organic molecules simply overwhelm conventional inorganic materials. The large and ultrafast nonlinear optical response found in many molecules is one important example [5]. Another key feature of many organic molecules is that they exhibit photochromism, *i.e.*, exist in two forms with different spectroscopic and physical properties and can be switched between these forms reversibly by light.

Azobenzenes are perhaps the most widely studied group of photochromic molecules [6]. They exists in two forms: a rodlike *trans* isomer and a bent *cis* isomer. Isomerization in both directions can be efficiently and repeatedly driven by light. The extent of material properties that can be controlled with light using the photoisomerization reaction is extremely broad, ranging from large-scale mechanical motions like the inscription of permanent surface-relief gratings [7] and photoinduced bending [8] to the control of absorption, refractive index and nonlinear optical response [9]. Although some applications have been demonstrated using these effects [10,11], further research is needed to fully understand the mechanisms at play and to find the best possible concepts for a given application.

Nonlinear optics is the study of phenomena that occur when the optical properties of a material system are changed by the presence of light [12]. A simple, yet important example of a nonlinear effect is second-harmonic generation, where the frequency of incoming light is doubled in a nonlinear material. Another important example is the linear electro-optic effect, in which an external electric field modifies the refractive index of the material. Second-harmonic generation finds applications in the generation of laser light at new wavelengths and the electro-optic effect in the modulation of light for telecommunications. The latter has been one of the main driving forces behind research on polymer materials similar to those studied in this Thesis. For electro-optic modulators, the strong and ultrafast nonlinear optical response of organic molecules provides important opportunities: the device can be made smaller, faster and more power efficient than the inorganic counterparts [13]. Both of the aforementioned nonlinear effects have their origin in the second-order nonlinear response, which is very sensitive to material symmetries. By tuning the molecular arrangement between centrosymmetric and noncentrosymmetric states, the second-order nonlinearity can be turned on and off. This enables the possibility to realize reconfigurable photonic devices. The control of molecular arrangement through photochromism is the core of this Thesis.

1.1 Aim and scope of this work

An important challenge of organic photonics is to transfer the excellent molecular-level properties into properties of the bulk material. For high bulk response, large portion of the material should consist of the molecules with the desired optical properties. Due to interactions between individual molecules, the arrangement that produces the desired properties may not be energetically favoured and will be spontaneously lost. The introduction of specific interactions between the photoactive molecules and the surrounding matter can fight against this spontaneous relaxation, allowing high bulk response to be reached.

The research presented in this Thesis arose from the supramolecular materials concepts studied in the Optics Laboratory of Tampere University of Technology and the Department of Applied Physics of Aalto University. In these studies, the photocontrol of linear optical properties, such as the refractive index and diffraction, was considered. It was shown that these properties greatly benefit of specific interactions between the photoactive molecules and a support polymer[14,15]. This is due to the ability of the designed supramolecular interactions to fight against the disruptive effects of intermolecular interactions. This, together with the strong backround of the Nonlinear Optics Group in studying polarization-sensitive nonlinear optical phenomena, provided the interdisciplinary starting point for this Thesis.

The first goal of this research was to test the previous hydrogen-bond-based materials concept[14] in search for photocontrolled materials with high nonlinear optical response. The second goal was to investigate whether the fully new, halogen-bonded supramolecular polymers outperform hydrogen-bonded systems. This concept was only emerging at the beginning of this Thesis work and is at the leading edge of current research on supramolecular systems.

An open mind must be kept so that one will no ignore newly emerging strategies for reaching larger goals. Therefore, the introduction to fascinating nonpolymeric materials, namely *molecular glasses*, with similar properties compared to the previously studied polymers quickly lead to the adoption of this materials concept into a new goal of this research: Could these glasses perhaps surpass the properties of the polymers intensively studied already for a few decades? Lastly, one of the original goals of this study was to see whether the collective motion of liquid crystals could make the photocontrol of nonlinear response more efficient. Although the last two goals may seem to differ from the original starting point, they have more in common than might seem. Indeed, each part of this Thesis serves one common goal: creation of materials with high nonlinear optical response that can be turned on and off at will. This goal is sought for by designing and taking advantage of the intermolecular interactions present in each material.

1.2 Structure of the Thesis

This Thesis summarizes the work presented in four original articles published in peer-reviewed journals in the fields of physics, chemistry and materials science. Chapter 2 introduces some basic principles of nonlinear optics. The focus is on second-order nonlinear optical response, which scales quadratically with the input field. The importance of material symmetry for second-order effects is also introduced. The evolution of second-harmonic wave in a general nonlinear material is derived as well as the evolution of the second-harmonic wave in an all-optically-poled material.

Chapter 3 introduces the origin of the nonlinear optical response in organic materials. The reader is briefly walked through the historical evolution of molecular-level nonlinear response. Measurement methods for the molecular response are introduced. The importance of intermolecular interactions in the molecular matter is covered together with the relation of molecular and macroscopic responses. Important classes of materials are treated from the viewpoint of their applicability to nonlinear optics.

Chapter 4 is the most extensive and most important part of this Thesis. Here, the material concepts and nonlinear optical principles introduced earlier are put together and the possibility to control the nonlinear response by light is in focus. The key properties of the azobenzene molecular switches used in all parts of this work are carefully explained. Overview of earlier work on similar effects and the practical implementation of the optical measurements performed in this Thesis are presented. Finally, the main results of each publication are summarized and their implications are considered.

The Thesis is concluded in Chapter 5 where a critical review of the results is presented and future prospects for the open lines of research are considered.

1.3 Author's contribution

The research included in this Thesis has been published in four papers. **Paper I** and **Paper II** deal with supramolecular polymers whose structure is controlled by all-optical poling. In **Paper III**, this method is extended to a nonpolymeric amorphous material. In **Paper IV**, a liquid-crystal polymer is switched between two structural states, in order to control its nonlinear optical response.

Paper I This paper presents the results of a systematic study of a hydrogen-bonded supramolecular guest–host polymer where the concentration of the photoactive nonlinear guest molecule is varied in a polymer matrix. Second-harmonic generation and birefringence are studied. The author took part in planning the research, fabricated the studied samples, built the optical poling measurement setup, performed all the sample characterization and nonlinear optical experiments, and wrote most of the manuscript.

Paper II This paper is a direct continuation to **Paper I**. Here, supramolecular polymers formed by halogen bonding are studied. The strength of the guest–host interaction is studied and comparison to hydrogen bonding is made. The author took part in planning the research, built the measurement setups for all-optical poling, photoinduced birefringence and

photochemical *cis–trans* lifetime studies, performed all of the sample characterization and photochemical experiments, and most of the nonlinear optical measurements, and wrote most of the manuscript.

Paper III This paper switches from the supramolecular polymers to a molecular glass. This material has the common nonlinear chromophore with **Paper I** but covalently bound to a group that promotes the formation of an amorphous phase. The author planned the research, fabricated the studied samples, built the all-optical poling measurement setup, performed all of the sample characterization and most of the nonlinear optical experiments, and wrote most of the manuscript.

Paper IV This paper was realized in collaboration with the Chemical Resources Laboratory at Tokyo Institute of Technology after a one-month visit by the author. Here, a polymerized ferroelectric liquid crystal is studied using photoinitiated order–disorder transition aiming for photoswitched on–off control of the nonlinear optical response. The author built the measurement setups for nonlinear optical measurements, performed most of these measurements, and participated in writing the manuscript.

As is the usual case in modern science, most of the work in this Thesis has been due to joint efforts between many individuals. Collaboration inside our laboratory, inside our university, with other universities in Finland, and around the world was needed to make this progress possible. The author's contribution to the published papers is shown in greater detail in Table 1.1. The contribution is divided into three categories: **Preparation**, **Experiments** and **Reporting**. The preparation includes the recognition of the research problem, planning of the research, and laying out the needed theory and experiments. The experiments include the sample fabrication, realization of the measurement setups, and performing the measurements. The reporting includes data analysis and preparation for reporting, writing the manuscript, and handling the manuscript submission. It should be noted that while this Thesis is interdisciplinary between chemistry, materials science and physics, synthesis of new compounds is not reported in these papers. The materials were acquired either from commercial sources (**Paper I** and **Paper III**) or from the co-authors (**Paper II** and **Paper IV**) who have previously reported the synthesis procedures.

Table 1.1: Summary of author's contribution to articles included in this Thesis.

Paper	Preparation	Experiments	Reporting
I	60 %	100 %	90 %
II	50 %	80 %	80 %
III	90 %	80 %	90 %
IV	20 %	50 %	20 %

2 Nonlinear optics

Nonlinear optics is the field of science that focuses on light–matter interactions in the regime where the intensity of light is high enough to affect the optical properties of matter. Although some nonlinear optical (NLO) phenomena were observed much earlier [16], the field of nonlinear optics bloomed after the invention of the laser in 1960, as it made highly intense light readily available. The discovery of second-harmonic generation [17] was immediately followed by the detection of two-photon absorption [18], and soon a bustling new field of study was established. In this Chapter, some important NLO phenomena are conceptionally introduced as the starting point for this Thesis. The majority of this Chapter is used to obtain the equation describing how the strength of the nonlinear response is extracted from experimental data in **Paper I** and **Paper III**. The proceeding and notation presented in *Nonlinear Optics* by Robert Boyd [12] is mostly followed.

2.1 Linear optics and wave equation

We begin by introducing the important parts of notation and the linear response of matter. Interaction between light and matter is based on the modification of the charge density in matter due to the electromagnetic field of light [19]. In a simplified view, light induces oscillating electrical dipoles which in turn radiate light. The density of dipole moments, *i.e.*, the electric polarization $\widetilde{\mathbf{P}}(\mathbf{r},t)$ of a material can be represented as[†]

$$\widetilde{\mathbf{P}}(\mathbf{r},t) = \varepsilon_0 \chi^{(1)} \cdot \widetilde{\mathbf{E}}(\mathbf{r},t), \tag{2.1}$$

where ε_0 is the vacuum permittivity and $\widetilde{\mathbf{E}}(\mathbf{r},t)$ is the electric component of the optical field dependent on time t and position $\mathbf{r}$. The material response is defined by the linear susceptibility $\chi^{(1)}$, a second-rank tensor that connects the electric-field vector to the polarization vector. The optical properties of matter are not the same for every oscillation frequency of the electric field. Therefore, the field is represented by a sum of frequency components as

$$\widetilde{\mathbf{E}}(\mathbf{r},t) = \sum_n \mathbf{E}(\mathbf{r},\omega_n) e^{-i\omega_n t}, \tag{2.2}$$

where $\mathbf{E}(\mathbf{r},\omega_n)$ is the complex amplitude of the field component oscillating at frequency ω_n. Here, the summation is performed over all positive and negative frequencies present in the field in order to simplify the notation. The negative frequencies deserve a bit of attention as a negative frequency is something rather unphysical. Let us take a case with only one frequency present in the field and oscillating at frequency ω. In the present

[†]Tilde (~) is used to denote quantities rapidly oscillating in time

notation, the summation has the components ω and $-\omega$ and the field in this particular case is

$$\widetilde{\mathbf{E}}(\mathbf{r},t) = \mathbf{E}(\mathbf{r},\omega)e^{-i\omega t} + \mathbf{E}(\mathbf{r},-\omega)e^{i\omega t}. \tag{2.3}$$

As a measurable quantity, the field should be real. This requirement is satisfied by defining $\mathbf{E}(\mathbf{r},-\omega) = \mathbf{E}^*(\mathbf{r},\omega)$ for the complex amplitudes. Here * is used for complex conjugate.

The propagation of an electromagnetic wave can be described with the wave equation readily derived from Maxwell's equations. In the following, the wave equation to describe the propagation of light in a linear medium is derived. Maxwell's equations in SI units in the differential form are[12]

$$\begin{aligned} \nabla\cdot\widetilde{\mathbf{D}} &= \tilde{\rho}, & \nabla\cdot\widetilde{\mathbf{B}} &= 0, \\ \nabla\times\widetilde{\mathbf{E}} &= -\frac{\partial\widetilde{\mathbf{B}}}{\partial t}, & \nabla\times\widetilde{\mathbf{H}} &= \frac{\partial\widetilde{\mathbf{D}}}{\partial t} + \widetilde{\mathbf{J}}, \end{aligned} \tag{2.4}$$

where $\widetilde{\mathbf{D}}$ is the electric displacement field, $\widetilde{\mathbf{E}}$ is the electric field, $\widetilde{\mathbf{B}}$ is the magnetic-flux density, and $\widetilde{\mathbf{H}}$ is the magnetic field. The last two quantities, the free-charge density $\tilde{\rho}$ and current density $\widetilde{\mathbf{J}}$ describe how the fields interact with free charges within the medium. The last two equations that are needed to describe the light–matter interaction are the constitutive equations

$$\widetilde{\mathbf{D}} = \varepsilon_0\widetilde{\mathbf{E}} + \widetilde{\mathbf{P}}, \tag{2.5}$$

$$\widetilde{\mathbf{H}} = \frac{1}{\mu_0}\widetilde{\mathbf{B}} - \widetilde{\mathbf{M}}, \tag{2.6}$$

where $\widetilde{\mathbf{P}}$ is the electric polarization and $\widetilde{\mathbf{M}}$ is the magnetization. The remaining quantities, the electric permittivity ε_0 and the magnetic permeability μ_0 are universal constants related to the speed of light by $c = \sqrt{1/\varepsilon_0\mu_0}$. The materials relevant to this work are dielectric, *i.e*, containing no free charges, as well as nonmagnetic. Thus, Eqs. (2.4) are simplified as we can assume that $\tilde{\rho} = 0$ and $\widetilde{\mathbf{J}} = 0$ while Eq. (2.6) is simplified as $\widetilde{\mathbf{M}} = 0$.

With these assumptions, we take the curl of $\nabla\times\widetilde{\mathbf{E}}$ and use Eq. (2.6) to get

$$\nabla\times\nabla\times\widetilde{\mathbf{E}} = \nabla\times\left(-\frac{\partial\widetilde{\mathbf{B}}}{\partial t}\right) = -\frac{\partial}{\partial t}\nabla\times\widetilde{\mathbf{B}} = -\mu_0\frac{\partial}{\partial t}\nabla\times\widetilde{\mathbf{H}} = -\mu_0\frac{\partial^2\widetilde{\mathbf{D}}}{\partial t^2}. \tag{2.7}$$

Next, the vectorial identity $\nabla\times\nabla\times\mathbf{F} = \nabla(\nabla\cdot\mathbf{F}) - \nabla^2\mathbf{F}$ with the assumption that $\nabla\cdot\widetilde{\mathbf{E}} = 0$ is applied. This assumption is true for plane waves and $\nabla\left(\nabla\cdot\widetilde{\mathbf{E}}\right) \approx 0$ is a valid approximation also in many other cases. Together with Eq. (2.5) this yields

$$\nabla^2\widetilde{\mathbf{E}} = \varepsilon_0\mu_0\frac{\partial^2\widetilde{\mathbf{E}}}{\partial t^2} + \mu_0\frac{\partial^2\widetilde{\mathbf{P}}}{\partial t^2}. \tag{2.8}$$

With the speed of light and reorganization we get the wave equation in the form

$$\nabla^2\widetilde{\mathbf{E}} - \frac{1}{c^2}\frac{\partial^2\widetilde{\mathbf{E}}}{\partial t^2} = \frac{1}{\varepsilon_0 c^2}\frac{\partial^2\widetilde{\mathbf{P}}}{\partial t^2}. \tag{2.9}$$

With the polarization from equation (2.1) we get

$$-\nabla^2\widetilde{\mathbf{E}} + \frac{1}{c^2}\frac{\partial^2\widetilde{\mathbf{E}}}{\partial t^2} + \frac{1}{c^2}\chi^{(1)} \cdot \frac{\partial^2\widetilde{\mathbf{E}}}{\partial t^2} = 0. \tag{2.10}$$

In the case of an isotropic medium, where the susceptibility is a scalar quantity, this simplifies to

$$-\nabla^2\widetilde{\mathbf{E}} + \frac{1}{c^2}(1+\chi^{(1)})\frac{\partial^2\widetilde{\mathbf{E}}}{\partial t^2} = 0 \tag{2.11}$$

This equation has solutions in the form of plane waves. Following the field definition for a single frequency component in Eq. (2.3), the amplitude is of the form

$$\mathbf{E}(\mathbf{r},\omega) = \mathbf{A}(\mathbf{r},\omega)e^{i\mathbf{k}\cdot\mathbf{r}}. \tag{2.12}$$

Here $\mathbf{A}(\mathbf{r},\omega)$ is the slowly-varying amplitude and $\mathbf{k}$ is the wave vector. The rapid oscillation in space is contained in the exponential term of Eq. (2.12). The factor $\frac{1}{c^2}(1+\chi^{(1)})$ is related to the speed, v, at which the wave travels in the material by

$$\frac{1}{v^2} = \frac{1}{c^2}(1+\chi^{(1)}) = \frac{\varepsilon^{(1)}}{c^2}. \tag{2.13}$$

Therefore, for the speed we can write $v = c/\sqrt{1+\chi^{(1)}} = c/n$, where $n = \sqrt{1+\chi^{(1)}}$ is the refractive index of the material. The last term in Eq. (2.13) introduces the relative permittivity $\varepsilon^{(1)} = 1+\chi^{(1)}$ that is used to take the linear response into account when we focus on the nonlinear interaction. For the plane-wave solutions, the magnitude of the wave vector is

$$|\mathbf{k}| = k = \frac{n\omega}{c}. \tag{2.14}$$

According to these definitions, it follows from Poynting's theorem that the intensity (time-averaged power per area) is

$$I = 2n\varepsilon_0 \left|\mathbf{E}(\mathbf{r},\omega)\right|^2 = 2n\varepsilon_0 \left|\mathbf{A}(\mathbf{r},\omega)\right|^2. \tag{2.15}$$

2.2 Nonlinear polarization and nonlinear optical phenomena

When the electric field is sufficiently strong to affect the optical properties of the matter it is interacting with, the electric polarization is no longer linearly dependent on the electric field. If the field is not too strong (ultimately it would rip the material apart making the idea of oscillating dipoles obsolete), the polarization can be represented as a power series [12,20]

$$\widetilde{\mathbf{P}}(\mathbf{r},t) = \varepsilon_0\left[\chi^{(1)}\cdot\widetilde{\mathbf{E}}(\mathbf{r},t) + \chi^{(2)}\colon\widetilde{\mathbf{E}}^2(\mathbf{r},t) \ + \chi^{(3)}\vdots\widetilde{\mathbf{E}}^3(\mathbf{r},t) + \ldots\right] \tag{2.16}$$

$$\equiv \widetilde{\mathbf{P}}(\mathbf{r},t)^{(1)} + \widetilde{\mathbf{P}}(\mathbf{r},t)^{(2)} + \widetilde{\mathbf{P}}(\mathbf{r},t)^{(3)} + \ldots \tag{2.17}$$

Here, $\chi^{(1)}$ is again the linear susceptibility and $\chi^{(2)}$ and $\chi^{(3)}$ the second- and third-order susceptibilities, respectively. These parameters characterize the optical properties of the medium. The different terms in Eq. (2.16) have been rewritten in Eq. (2.17) as the first-, second-, and third-order polarization components. The NLO phenomena are

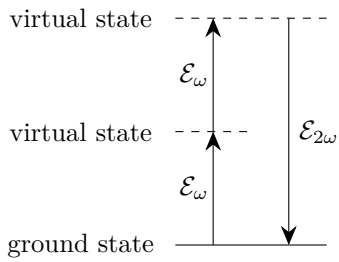

Figure 2.1: Energy-level diagram for SHG.

usually grouped by the polarization order that needs to be considered. Second-order effects stem from the second-order polarization, third-order effects from the third-order polarization and so forth. Higher-order effects generally require higher electric fields to become apparent and therefore second- and third-order effects are most often considered. Important third-order effects include intensity-dependent refractive index and self-phase modulation. The first effect causes self-focusing or self-defocusing of intense light and the second one allows, for example, the existence of short pulses that maintain their shape during propagation. In this work, we focus on second-order effects and the rest of this section is spent to cover two of them that are most relevant for the rest of this Thesis: second-harmonic generation and the electro-optic effect.

We now divide the polarization and the field into their frequency components as in Eq. (2.2) and consider second-order polarization. The polarization amplitude at the frequency $\omega_n + \omega_m$ is represented as

$$P_i^{(2)}(\mathbf{r}, \omega_n + \omega_m) = \varepsilon_0 \sum_{jk} \sum_{(mn)} \chi_{ijk}^{(2)}(\mathbf{r}, \omega_n + \omega_m; \omega_n, \omega_m) E_j(\mathbf{r}, \omega_n) E_k(\mathbf{r}, \omega_m), \qquad (2.18)$$

where the indices i, j and k refer to the Cartesian components (x, y, z) of the fields.

Perhaps the simplest second-order effect is second-harmonic generation (SHG) where two photons of an incident field are transformed into a single photon with twice the energy and hence twice the frequency (Fig. 2.1). This effect is also known as frequency doubling. Second-harmonic generation is commonly used for producing laser light at new wavelengths where suitable laser sources might not be available. The energy levels with dashed lines in Fig. 2.1 are not true energy levels of the interacting material system but so-called virtual levels. Therefore, the uncertainty principle limits the lifetime, Δt of these states by $\Delta\mathcal{E}\Delta t \sim \frac{\hbar}{2}$. As the virtual-state energy $\Delta\mathcal{E}$ here equals the photon energy, $\mathcal{E}_\omega = \hbar\omega$, the time scale of the process is close to one cycle of the optical field. For all practical purposes, the process can be considered instantaneous. In these *parametric* processes also the coherence of the input field is maintained.

Next, let us consider the particular case of SHG in a material that possesses a center of inversion, *i.e.*, in a centrosymmetric material. Such a material is invariant under the parity transformation, represented by the operation $\mathbf{O_P} : \mathbf{r} \to -\mathbf{r}$. Electric field and polarization are vector quantities that behave in the same way as the position vector under this operation:

$$\mathbf{O_P} : \widetilde{\mathbf{E}}(\mathbf{r}, t) \to -\widetilde{\mathbf{E}}(-\mathbf{r}, t), \;\; \mathbf{O_P} : \widetilde{\mathbf{P}}(\mathbf{r}, t) \to -\widetilde{\mathbf{P}}(-\mathbf{r}, t). \qquad (2.19)$$

One component of Eq. (2.18) for SHG from a field with input frequency ω reduces to a scalar equation

$$P^{(2)}(\mathbf{r}, 2\omega) = \varepsilon_0 \chi^{(2)} E^2(\mathbf{r}, \omega). \tag{2.20}$$

According to Eqs. (2.19) and (2.20), we can write for the polarization

$$\begin{aligned} P^{(2)}(\mathbf{r}, 2\omega) &= -P^{(2)}(-\mathbf{r}, 2\omega) = -\varepsilon_0 \chi^{(2)} \left(E(-\mathbf{r}, \omega)\right)^2 = -\varepsilon_0 \chi^{(2)} \left(-E(\mathbf{r}, \omega)\right)^2 \\ &= -\varepsilon_0 \chi^{(2)} \left(E(\mathbf{r}, \omega)\right)^2 = -P^{(2)}(\mathbf{r}, 2\omega), \end{aligned} \tag{2.21}$$

where inversion was performed in steps 1 and 3. As a fundamental constant, the vacuum permittivity does not change in the inversion, and neither does $\chi^{(2)}$ due to the assumption of centrosymmetric material. However, this result can hold only if $P^{(2)} = 0$ implying that $\chi^{(2)} = 0$, which leads to the important conclusion that **second-harmonic generation is forbidden in a centrosymmetric material**. More generally, a similar procedure can be used to show that any second-order NLO effect vanishes in a centrosymmetric material.

It should be noted that polarization of electric-dipole nature follows Eq. (2.19). Other types of polarization, such as those of electric-quadrupole and magnetic-dipole origin need not follow it. In addition, inversion symmetry is always broken at an interface. Therefore, the vanishing second-order response only applies in bulk matter with electric-dipole type response to light. For the purpose of this work, this restriction is not too severe as bulk properties of matter whose nonlinear response stems from organic chromophores with strong electric-dipole response is studied (Section 3.1).

The second important second-order effect for this Thesis is the linear electro-optic effect, often called the Pockels effect. In this phenomenon, a field oscillating at an optical frequency and a DC or low-frequency field interact but no new frequencies are produced. Let us take the optical field at frequency ω and the DC field at frequency 0. Performing the summation in Eq. (2.18) over the cases that yield polarization oscillating at ω we get

$$P_i^{(2)}(\mathbf{r}, \omega) = 2\varepsilon_0 \sum_{jk} \chi_{ijk}^{(2)}(\mathbf{r}, \omega; \omega, 0) E_j(\mathbf{r}, 0) E_k(\mathbf{r}, \omega). \tag{2.22}$$

Note that a factor of two appears in Eq. (2.22) in comparison to Eq. (2.20). This is due to degeneracy of the field in the case of SHG which leads to just one term at the frequency 2ω. However, in the case of the electro-optic effect, the two fields yield two terms at the frequency ω in the summation over frequencies. Due to a property called intrinsic permutation symmetry, these terms are identical and a factor of two appears. For comparison, in the case of linear interaction, the polarization can be written as

$$P_i^{(1)}(\mathbf{r}, \omega) = \varepsilon_0 \sum_{k} \chi_{ik}^{(1)}(\mathbf{r}, \omega) E_k(\mathbf{r}, \omega), \tag{2.23}$$

where $\chi_{ik}^{(1)}$ is the linear susceptibility component relating polarization in direction i to the E-field in direction k. As seen in Section 2.1, the refractive index is dependent on the linear susceptibility. Comparing Eqs. (2.22) and (2.23), one can see that $\chi_{ijk}^{(2)}(\mathbf{r}, \omega; \omega, 0) E_j(\mathbf{r}, 0)$ is analogous to $\chi_{ik}^{(1)}(\mathbf{r}, \omega)$ when considering the polarization at frequency ω caused by the field $E_k(\mathbf{r}, \omega)$. The conclusion is that due to the nonlinear interaction, a new term that affects the refractive index is produced and this new effect is dependent on the DC-field amplitude.

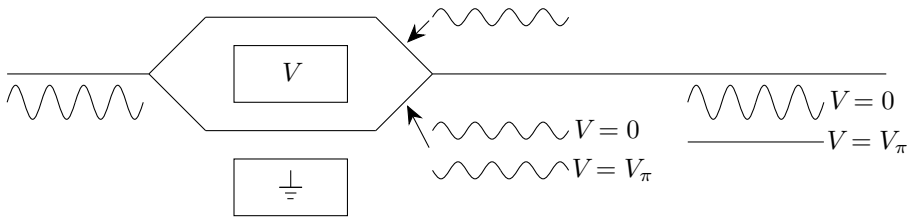

Figure 2.2: Schematic of a Mach–Zehnder electro-optic amplitude modulator. Redrawn from Refs. [13, 21].

A refractive index that depends on a DC field means that the phase shift occurring in the material for an optical field can be controlled by adjusting the DC-field amplitude. As a result, a material with second-order response can be used to build electro-optic modulators, an example of which is shown schematically in Fig. 2.2. The principle of operation for this device is rather simple. The input wave travelling in a waveguide is divided into parts travelling the upper and lower arms of the device. The lower arm contains the nonlinear material and voltage is applied over it. At a certain voltage, namely the half-wave voltage V_π, the phase of the wave exiting the lower arm will be shifted by π relative to that exiting the upper arm. The waves from the two arms are recombined and the output field becomes zero due to destructive interference. When no voltage is applied, no phase shift occurs in the lower arm relative to the upper arm and constructive interference produces an output wave similar to the input when losses are neglected. Importantly, the requirement of noncentrosymmetry applies also in the case of the electro-optic effect.

2.3 Evolution of second-harmonic wave

With the fundamentals of nonlinear polarization and the important nonlinear effects, we return to the wave equation that was found in Eq. (2.9) to be:

$$\nabla^2\widetilde{\mathbf{E}} - \frac{1}{c^2}\frac{\partial^2\widetilde{\mathbf{E}}}{\partial t^2} = \frac{1}{\varepsilon_0 c^2}\frac{\partial^2\widetilde{\mathbf{P}}}{\partial t^2}. \tag{2.24}$$

However, instead of linear polarization, we assume that the material polarization has the terms of Eq. (2.17) and represent the displacement field and polarization split into their linear and nonlinear parts:

$$\widetilde{\mathbf{D}} = \widetilde{\mathbf{D}}^{(1)} + \widetilde{\mathbf{P}}^{NL}, \tag{2.25}$$

$$\widetilde{\mathbf{P}} = \widetilde{\mathbf{P}}^{(1)} + \widetilde{\mathbf{P}}^{NL}, \tag{2.26}$$

where the linear part of $\widetilde{\mathbf{D}}$ is given by

$$\widetilde{\mathbf{D}}^{(1)} = \varepsilon_0\widetilde{\mathbf{E}} + \widetilde{\mathbf{P}}^{(1)}. \tag{2.27}$$

With equations (2.26) to (2.27), the wave equation takes the form

$$\nabla^2\widetilde{\mathbf{E}} - \frac{1}{\varepsilon_0 c^2}\frac{\partial^2\widetilde{\mathbf{D}}^{(1)}}{\partial t^2} = \frac{1}{\varepsilon_0 c^2}\frac{\partial^2\widetilde{\mathbf{P}}^{NL}}{\partial t^2}. \tag{2.28}$$

Next, we divide $\widetilde{\mathbf{E}}$, $\widetilde{\mathbf{D}}^{(1)}$ and $\widetilde{\mathbf{P}}^{NL}$ into sums of their frequency components as in Eq. (2.2). For one frequency component, oscillating at frequency ω, the wave equation can now be represented using the complex amplitudes in the time-independent form

$$\nabla^2\mathbf{E}(\mathbf{r},\omega) + \frac{\omega^2}{\varepsilon_0 c^2}\mathbf{D}^{(1)}(\mathbf{r},\omega) = -\frac{\omega^2}{\varepsilon_0 c^2}\mathbf{P}^{NL}(\mathbf{r},\omega). \tag{2.29}$$

In general, the displacement-field amplitude can be connected to the electric-field amplitude by a complex, frequency-dependent tensor $\varepsilon^{(1)}(\omega)$ with

$$\mathbf{D}^{(1)}(\mathbf{r},\omega) = \varepsilon_0\varepsilon^{(1)}(\omega)\cdot\mathbf{E}(\mathbf{r},\omega). \tag{2.30}$$

We now end up with the time-independent wave equation where $\mathbf{P}^{NL}(\mathbf{r},\omega)$ acts a source term:

$$\nabla^2\mathbf{E}(\mathbf{r},\omega) + \frac{\omega^2}{c^2}\varepsilon^{(1)}(\omega)\cdot\mathbf{E}(\mathbf{r},\omega) = -\frac{\omega^2}{\varepsilon_0 c^2}\mathbf{P}^{NL}(\mathbf{r},\omega). \tag{2.31}$$

Now, SHG is again taken into focus. Some simplifications are applied: collimated, monochromatic, continuous-wave beams travelling in z-direction in a lossless material are considered. The waves are assumed to be linearly polarized in the x-direction. In the absence of the nonlinear source term, the solutions are plane waves of the form shown in the first section and we assume that the second-harmonic wave has the amplitude

$$E_2(z,\omega_2) = A_2 e^{ik_2 z} \tag{2.32}$$

The subscript 2 is used throughout this section for the second-harmonic wave. Here A_2 is the slowly-varying amplitude, k_2 is the wave vector, now scalar for a wave travelling in the z-direction. For the wave vector k_2 and refractive index n_2 it holds that

$$k_2 = \frac{n_2\omega_2}{c},\ \ n_2^2 = \varepsilon^{(1)}_{xx}(\omega_2), \tag{2.33}$$

where ω_2 is the frequency of the second-harmonic field. The dielectric tensor was reduced into a single component as we consider only fields polarized in x-direction. It follows that the refractive index n_2 is considered for the x-polarized wave.

The nonlinear polarization is caused by an applied field which is represented identically with E_2. The subscript 1 is used for all the quantities of the fundamental wave and the wave is

$$E_1(z,\omega_1) = A_1 e^{ik_1 z}. \tag{2.34}$$

Looking back at Eq. (2.18) for this fixed geometry, a polarization source term of the form

$$P^{(2)}(z,2\omega_1) = P_2(z,\omega_2) = \varepsilon_0\chi^{(2)}_{xxx}A_1^2 e^{2ik_1 z} \tag{2.35}$$

emerges. The single susceptibility component is labelled as $\chi^{(2)}_{xxx}$ marking the susceptibility for the case of x-polarized fundamental and second-harmonic. Now equations (2.32), (2.34) and (2.35) are substituted to the nonlinear wave equation (2.31). The fields only depend on the z-coordinate which allows for the replacement of ∇^2 with $\frac{\partial^2}{\partial z^2}$ and we obtain

$$\left[\frac{\partial^2 A_2}{\partial z^2} + 2ik_2\frac{\partial A_2}{\partial z} - k_2^2 A_2 + \frac{n_2\omega_2^2}{c^2}A_2\right]e^{ik_2 z} = -\frac{\omega_2^2}{\varepsilon_0 c^2}\varepsilon_0\chi^{(2)}_{xxx}A_1^2 e^{i2k_1 z}. \tag{2.36}$$

The third and fourth terms on the left cancel each other and a further simplification is obtained by using the slowly-varying-amplitude approximation. If the fractional change in A_2 is small over a distance of one wavelength, it holds that

$$\left|\frac{\partial^2 A_2}{\partial z^2}\right| \ll k_2 \frac{\partial A_2}{\partial z} \tag{2.37}$$

and the first term in Eq. (2.36) can be neglected. This approximation and the introduction of the wave-vector mismatch $\Delta k = 2k_1 - k_2$ yield a very simple form for the evolution of the second-harmonic wave amplitude:

$$\frac{\partial A_2}{\partial z} = \frac{i\chi^{(2)}_{xxx} A_1^2 \omega_2^2}{2k_2 c^2} e^{i\Delta k z}. \tag{2.38}$$

A similar equation can be derived for the amplitude of the fundamental wave, A_1. However, when the portion of energy moving from the fundamental wave to the second-harmonic wave is small, A_1 can be assumed to be constant. This undepleted-pump approximation allows simple integration of Eq. (2.38) from 0 to L, representing the travel through a nonlinear crystal of length L.

$$A_2(L) = \frac{i\chi^{(2)}_{xxx} A_1^2 \omega_2^2}{2k_2 c^2} \int_0^L e^{i\Delta k z} dz = \frac{i\chi^{(2)}_{xxx} A_1^2 \omega_2^2}{2k_2 c^2} \left(\frac{e^{i\Delta k L} - 1}{i\Delta k}\right). \tag{2.39}$$

For the intensity of the second-harmonic wave, Eq. (2.39) is squared and $I_i = 2n_i \varepsilon_0 c \left|A_i\right|^2$ from Eq. (2.15) is used for both fields $i = 1, 2$. For a real-valued $\chi^{(2)}_{xxx}$, this yields

$$I_2(L) = \frac{(\chi^{(2)}_{xxx})^2 \omega_2^2 I_1^2}{2n_1^2 n_2 c^3 \varepsilon_0 \Delta k^2} \sin^2\left(\frac{\Delta k L}{2}\right) = \frac{(\chi^{(2)}_{xxx})^2 \omega_2^2 I_1^2 L^2}{8n_1^2 n_2 c^3 \varepsilon_0} \mathrm{sinc}^2\left(\frac{\Delta k L}{2}\right), \tag{2.40}$$

where $\mathrm{sinc}(x) = \frac{\sin(x)}{x}$ was used to obtain the second form. Note that by definition $\mathrm{sinc}(0) = 1$.

The two forms of (2.40) offer important information on the concept of phase matching. In the second form, we can set $\Delta k = 0$ which is the case of perfect phase matching and the intensity of the second-harmonic wave increases quadratically with the interaction length. When $\Delta k \neq 0$, the first form shows that the intensity varies sinusoidally reaching its first maximum after the *coherence length* $L_{coh} = \frac{\pi}{\Delta k}$. After this point, the phase mismatch causes destructive interference and the second-harmonic intensity falls to zero at point $L = 2L_{coh}$. The wave vector mismatch Δk for SHG is

$$\Delta k = 2k_1 - k_2 = \frac{2n_1\omega_1}{c} - \frac{n_2\omega_2}{c} = \frac{2n_1\omega_1}{c} - \frac{n_2 2\omega_1}{c} = \frac{2\omega_1}{c}(n_1 - n_2) = \frac{2\omega_1}{c}\Delta n. \tag{2.41}$$

Therefore, perfect phase matching can only be met if the refractive index of the material is the same at the fundamental and second-harmonic frequencies. Usually materials show normal dispersion, which means that the refractive index increases with increasing frequency and perfect phase matching is not reached. One method to circumvent this problem is to use birefringence to compensate for the dispersion. In a birefringent material, the refractive index is different for different polarization states of the interacting electromagnetic waves (Fig. 2.3(a)). If the birefringence is large enough to overcome normal dispersion, by careful choice of orientation of the crystal, the phase-matching condition can be met and high-efficiency SHG is possible.

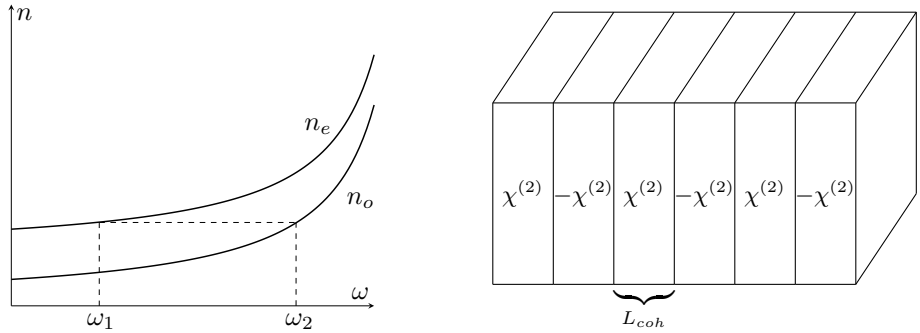

Figure 2.3: (a) Dispersion of the refractive index in a positive uniaxial crystal. The refractive indices at frequencies ω_1 and ω_2 are the same despite of normal dispersion as the polarization of the ω_1 wave has been chosen so that it experiences the extraordinary index n_e and the wave at ω_2 experiences the ordinary index n_o. (b) A quasi-phase-matched structure.

However, not all nonlinear materials show adequate birefringence for the method above. Another strategy for phase-matching is to flip the sign of $\chi^{(2)}$ after each coherence length (See Fig. 2.3(b)). This change compensates for the phase mismatch accumulated up to that point in the structure and the intensity of the second-harmonic wave continues to grow. Such *quasi-phase-matching* leads only to a decrease by a factor of $(2/\pi)^2$ for the intensity in Eq. (2.40) compared to setting $\Delta k = 0$. In principle, a quasi-phase-matched structure could be produced by breaking the nonlinear material into slices with the thickness of one coherence length, flipping every other slice, and recombining the slices. However, taking 1064 nm fundamental wavelength with the frequency $\omega_1 = 1.77 \times 10^{15}\,\frac{1}{\mathrm{s}}$ and $|\Delta n| = 0.01$, which is a reasonable value for dispersion, the coherence length is only 27 µm which makes the slicing all but impossible. However, in some materials flipping the sign of $\chi^{(2)}$ can also be reached by a method called periodic poling[22] where a spatially varying electric field is used to rearrange the material structure.

2.4 Fundamentals of all-optical poling

In general, poling refers to the process of creating a polar structure in a disordered material or one with some other initial structure. The motivation for poling in the light of this work stems from the fact that a structure with polar symmetry is one example of noncentrosymmetry, making second-order nonlinear processes allowed. A common method for reaching a polar structure is to use static electric field. However, optical fields can be used for this purpose as well when nonlinear interactions are considered. Setting $\omega_n = \omega$ and $\omega_m = -\omega$, Eq. (2.18) produces a static polarization component and the phenomenon is called optical rectification. A more intriguing result is found when the input field is the coherent combination of fields at frequencies ω and 2ω and third-order interaction is considered[23,24]. Our total field considering one polarization and propagation in z direction is now

$$\widetilde{E}_{tot} = A_1 e^{i(k_1 z - \omega t)} + A_2 e^{i(k_2 z - 2\omega t)} + c.c., \tag{2.42}$$

The field oscillating at ω is called the *writing* field and the one at 2ω is the *seeding* field. Index 1 is used for all quantities of the writing field and index 2 for the seeding field. The

third power of this field has several terms oscillating at frequencies from ω to 6ω but also two terms that are independent of time. Therefore, the time average of the field cube takes the form

$$\left\langle \widetilde{E}_{tot}^3 \right\rangle = 3A_1^2 A_2^* e^{i((2k_1-k_2)z)} + 3\left(A_1^*\right)^2 A_2 e^{-i((2k_1-k_2)z)}. \tag{2.43}$$

Taking into account the initial phase and absorption at frequency 2ω, the slowly-varying amplitudes can be written as $A_1 = |A_{1,0}|\, e^{i\phi_1}, A_2 = |A_{2,0}|\, e^{i\phi_2} e^{-\frac{\alpha}{2}z}$, where ϕ_1 and ϕ_2 are the initial phase factors and α is the absorption coefficient at frequency 2ω. The quantities $A_{1,0}$ and $A_{2,0}$ refer to the amplitudes at $z = 0$. For brevity, $\Delta k = 2k_1 - k_2$ as in the previous section and $\Delta\phi = 2\phi_1 - \phi_2$ is defined as the phase difference of the fields. Now the time-averaged field cube becomes

$$\left\langle \widetilde{E}_{tot}^3 \right\rangle = 3\left|A_{1,0}^2 A_{2,0}\right| \left(e^{i(\Delta k z + \Delta\phi)} + e^{-i(\Delta k z + \Delta\phi)}\right) e^{-\frac{\alpha}{2}z}. \tag{2.44}$$

Through some mechanism, the time-averaged field cube is connected to the creation of a long-lived second-order susceptibility to the nonlinear material. This mechanism is covered in Section 4.2 but is now taken for granted and an induced second-order susceptibility $\chi_{ind}^{(2)} \propto \left\langle E_{tot}^3 \right\rangle$ is introduced. The induced susceptibility is defined to be [25]

$$\chi_{ind}^{(2)} = \chi_{eff}^{(2)} \left(e^{i(\Delta k z + \Delta\phi)} + e^{-i(\Delta k z + \Delta\phi)}\right) e^{-\frac{\alpha}{2}z} = 2\chi_{eff}^{(2)} \cos(\Delta k z + \Delta\phi) e^{-\frac{\alpha}{2}z}, \tag{2.45}$$

where $\chi_{eff}^{(2)} \propto \left|A_{1,0}^2 A_{2,0}\right|$ is the effective second-harmonic susceptibility from which the spatial variation has been separated[‡]. A key benefit of this *all-optical poling* (AOP) can be seen from Eq. (2.45): the induced susceptibility switches its sign after propagating the distance of $\pi/\Delta k$ which means that the pattern automatically fulfils the requirement of quasi-phase-matching.

Next, the evolution of the second-harmonic wave in an all-optically poled material is derived. The field producing the second-order polarization is assumed to be identical to the one that is used for creating the induced susceptibility. This is the situation in practice as this *probing* field is the same as the writing field. The polarization source term is analogous to that in Eq. (2.35):

$$P^{(2)}(z, \omega_2) = \varepsilon_0 \chi_{ind}^{(2)} A_1^2 e^{i2k_1 z} \tag{2.46}$$

and the evolution of the the second-harmonic wave can be represented as in Eq. (2.38) with

$$\frac{\partial A_2}{\partial z} = -\frac{\alpha}{2} A_2 + \frac{i\chi_{ind}^{(2)} A_1^2 \omega_2^2}{2k_2 c^2} e^{i\Delta k z}. \tag{2.47}$$

Note that A_2 is the slowly-varying amplitude of the second-harmonic field produced by the optically poled material. All the details of the poling process, including the seeding-field amplitude, also marked with A_2, are hidden in the induced susceptibility. One modification compared to Eq. (2.38) has been performed here. The materials studied by AOP in this work have high absorbance at the second-harmonic wavelength. Therefore,

[‡]It should be noted that this definition differs from that of Fiorini et. al. [25] by a factor of 2 as their definition is $\chi_{ind}^{(2)} = \chi_{eff}^{(2)} \cos(\Delta k z + \Delta\phi) e^{-\frac{\alpha}{2}z}$.

attenuation has been included as the first term on the right-hand side of Eq. (2.47)[25]. We now inject $\chi^{(2)}_{ind}$ from Eq. (2.45) and solve for A_2 at the position z and obtain

$$A_2(z) = \frac{i\chi^{(2)}_{eff} A_1^2 \omega_2^2}{2k_2 c^2} \left[\frac{1}{2i\Delta k} e^{i\Delta\phi} \left(e^{2i\Delta k z} - 1 \right) + z e^{-i\Delta\phi} \right] e^{-\frac{\alpha}{2} z}. \tag{2.48}$$

And in terms of intensities, setting $z = L$, we get for a real $\chi^{(2)}_{eff}$

$$I_2(L) = \frac{(\chi^{(2)}_{eff})^2 \omega_2^2 I_1^2 L^2}{8 n_1^2 n_2 c^3 \varepsilon_0} \left(1 + \mathrm{sinc}^2(\Delta k L) + 2\mathrm{sinc}(\Delta k L)\cos(\Delta k L + 2\Delta\phi) \right) e^{-\alpha L}. \tag{2.49}$$

Two special cases can be deduced from this equation. For a very thick nonlinear material ($L \gg \frac{1}{\Delta k}$), the sinc terms vanish and the result is identical to the perfectly phase matched version of Eq. (2.40). For a thin material ($L \ll \frac{1}{\Delta k}$), on the other hand, the sinc terms reduce to unity and the equation becomes

$$I_2(L) = \frac{(\chi^{(2)}_{eff})^2 \omega_2^2 I_1^2 L^2}{8 n_1^2 n_2 c^3 \varepsilon_0} \left(2 + 2\cos(2\Delta\phi) \right) e^{-\alpha L}. \tag{2.50}$$

Now the second-harmonic intensity varies sinusoidally with the phase difference of the writing and seeding fields. With the right adjustment of the phase difference ($\Delta\phi = 0 + n\pi \implies \cos(2\Delta\phi) = 1$, with n an integer) we end up with

$$I_2(L) = \frac{(\chi^{(2)}_{eff})^2 \omega_2^2 I_1^2 L^2}{2 n_1^2 n_2 c^3 \varepsilon_0 10^{\mathcal{A}}}, \tag{2.51}$$

where the absorption term $e^{-\alpha L}$ was replaced with $10^{-\mathcal{A}}$ in order to use the common definition $\mathcal{A}$ for absorbance at the ω_2 wavelength.

Finally, in order to determine the value of $\chi^{(2)}_{eff}$, a reference measurement can be run using a reference material with known $\chi^{(2)}$. From Eqs. (2.40) and (2.51) we can write the second-harmonic intensity of a transparent reference material $I_{2,r}$ and for a thin sample all-optically poled $I_{2,s}$:

$$I_{2,r} = \frac{(\chi^{(2)}_{xxx,r})^2 \omega_2^2 I_1^2}{2 n_{1,r}^2 n_{2,r} c^3 \varepsilon_0 \Delta k_r^2} \quad I_{2,s} = \frac{(\chi^{(2)}_{eff,s})^2 \omega_2^2 I_1^2 L_s^2}{2 n_{1,s}^2 n_{2,s} c^3 \varepsilon_0 10^{\mathcal{A}_s}}, \tag{2.52}$$

where $L = \frac{1}{\Delta k}(\pi + 2n\pi)$ with n an integer was assumed for the reference. This requirement is easily fulfilled as shown in Section 4.2. Here the indices s and r are used for the sample and the reference for each material or sample property. These equations combine into

$$\chi^{(2)}_{eff,s} = \chi^{(2)}_{xxx,r} \left(\frac{n_{1,s}}{n_{1,r} \Delta k_r L_s} \right) \sqrt{\frac{I_{2,s}}{I_{2,r}} \frac{n_{2,s}}{n_{2,r}} 10^{\mathcal{A}_s}}, \tag{2.53}$$

similarly as found in Ref. [26]. According to this equation, only the refractive indices for both materials, the absorbance and thickness for the all-optically poled sample and the second-order susceptibility for the reference are required to deduce the effective susceptibility of the sample.

3 Organic materials in nonlinear optics

This chapter focuses on the material concepts required to understand the NLO response of the organic materials studied in this Thesis. First, the molecular-level origin of the nonlinear response is introduced. The design strategies and evolution of molecules with high optical nonlinearity are explained, followed by the measurement techniques for the molecular response. The connection between the molecular and bulk-level properties is covered conceptually in the first section and through an example as we start to focus on bulk materials. In the last two sections, the general characteristics of crystals, liquid crystals, and amorphous solids are introduced and earlier work on the nonlinear properties of these types of material systems are reviewed. The particular materials used in this Thesis are used as examples where appropriate.

3.1 Molecular-level nonlinear optical response

All condensed matter consists of atoms connected to each other by electric forces between the nuclei and their outer electrons. In many inorganic crystals, these individual bonds between atoms form a network extending all the way to the material boundaries. The arrangement of the individual atoms then dictates the properties, including optical properties, of the material. Organic materials, on the other hand, are composed of molecules. In a single organic molecule, the atoms are strongly bonded to each other just as the atoms in an inorganic material. However, the forces between molecules are in general far weaker than the bonds between atoms. This leads to an important distinction that applies to molecular matter: the NLO properties are largely dictated by those of the individual molecules[27]. Therefore, the material can be studied in the gas phase or in a solution and the results extended to the solid phase if the arrangement of the molecules in the solid is known.

Interaction between light and matter is based on the modification of the charge density in matter due to the electromagnetic field of light[19]. In a simplified view, light induces oscillating electric dipoles which in turn radiate light. The dipole moment μ_I of a molecule can be represented as a power series[28] similarly to equation (2.16) given component-wise

$$\mu_I = \mu_I^0 + \alpha_{IJ}E_J + \beta_{IJK}E_JE_K + \gamma_{IJKL}E_JE_KE_L + ... \tag{3.1}$$

where μ_I^0 is the permanent dipole moment, α_{IJ} is the linear polarizability, β_{IJK} and γ_{IJKL} are the second- and third-order polarizabilities (also denoted as first- and second-order hyperpolarizabilities) and E_J, E_K, E_L are the electric field components. The indices I, J, K and L refer to directions in the molecular coordinate system XYZ and summation over X, Y, and Z is implied.

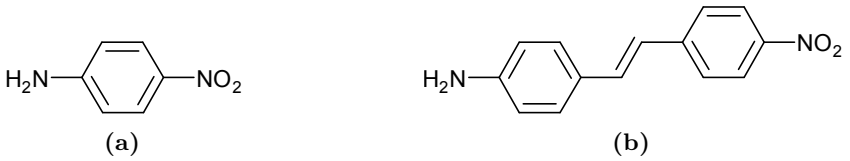

Figure 3.1: Donor–π–acceptor molecules (a) p-nitroaniline and (b) 4-nitro-4'aminostilbene.

For a strong optical response, relatively mobile electrons must be present in the molecule. An important example of highly mobile electrons are those involved in conjugated π-type bonds. In a conjugated π-electron system, single and double bonds alternate on every other bond site. In the conjugated structure, the π-electrons are not bound to a single atom but can move over the entire conjugation length. This delocalization makes the molecule's electronic structure highly deformable which results in strong NLO response [27].

Any arrangement of centrosymmetric molecules leads to a centrosymmetric bulk material. Therefore, for second-order nonlinear processes, the requirement of noncentrosymmetry (Section 2.2) applies also to the molecular structure. Exceptions to this requirement are found when the higher-order effects such as magnetic dipoles or electric quadrupoles contribute to the response [29–31]. Another important exception arises when the molecules exhibit strong intermolecular interactions leading to the possibility of charge transfer between the molecules [32,33].

Strong molecular second-order nonlinearity, *i.e.*, high β, is often found in molecules containing delocalized π-electron systems and asymmetric charge distribution. The charge imbalance is achieved by substituting strong electron-donating and/or electron-withdrawing chemical groups into the molecule. The largest values of β are found when the molecules have charge-transfer resonance states with energies close to the ground state [27]. The simplest examples of π-electron systems with charge imbalance are substituted benzenes. Early studies on this type of molecules revealed a strong correlation between the strength of the substituent's electron-donating or electron-withdrawing properties and the molecular second-order NLO response [34–36]. Disubstitution of benzene with both electron-donating and electron-withdrawing groups was found to result in mutual reinforcement and very high values of the second-order polarizability [37]. A prime example of this is p-nitroaniline shown in figure 3.1(a) with $\beta \approx 20 \times 10^{-30}$ esu = $84 \times 10^{-40} \mathrm{m}^4\ \mathrm{V}^{-1}$ [38,39†]. Moving to a longer conjugated π-system, such as stilbene, resulted in an order-of-magnitude increase in the second-order polarizability to $1100 \times 10^{-40} \mathrm{m}^4\ \mathrm{V}^{-1}$ found for 4-nitro-4'aminostilbene [36], shown in figure 3.1(b). Later on, it was shown that β increases quadratically with increasing conjugation length in disubstituted molecules [41].

Due to the aforementioned findings, a large portion of the research on second-order NLO molecules has been focused on donor–π–acceptor (D–π–A) type molecules with relatively long conjugated π-system [42]. In such molecules, an electron-donating group is connected to an electron-withdrawing group through a conjugated π system. This structure results in strong charge asymmetry as the donor group is "pushing" the electrons away and the

†The first value presented is in cgs electrostatic units. However, in this work, SI units are used. The conversion factor $\beta_{SI} = \frac{4\pi}{3 \times 10^{10}} \beta_{cgs}$ is used when moving from cgs to SI units. Some sources report β values in SI units $\mathrm{C\ m^3\ V^{-2}}$ following the convention where the vacuum permittivity is not included in the definition of electric polarization (Chapter 2). Using this convention, the β values in SI units presented here need to be multiplied with $\varepsilon_0 = 8.854 \times 10^{-12}\ \mathrm{C\ m^{-1}\ V^{-1}}$ [12,40]. Values at the 1064 nm fundamental wavelength are shown if not otherwise stated.

acceptor group is "pulling" them closer. Due to this behaviour the D–π–A type molecules are often termed as push–pull molecules[43]. While increasing donor and acceptor strength was originally found to increase β, later it was shown that for a certain conjugation bridge there is an optimal combination of donor and acceptor strengths[44]. Furthermore, bond-length alteration (the average difference in length of single and double bonds) in the conjugation bridge was found to lower β[45,46]. These findings have led to new design strategies and to molecules with very high second-order NLO response[47–49].

In the late 1990s, the right choice of donor and acceptor combined with reasonably long conjugated π-electron systems lead to values of $\beta > 10000 \times 10^{-40}\,\mathrm{m^4\,V^{-1}}$ [50]. However, translating this progress into material level has proven difficult due to dipole–dipole interactions between the molecules[51]. These interactions work against the preferred noncentrosymmetric molecular arrangement, diminishing the achievable bulk response, which is covered in the next sections. This finding has triggered molecular design strategies aiming for spherical rather than rod-like nonlinear molecules or the addition of isolation groups to mitigate the effects of the intermolecular interactions[52–56].

In addition to optimizing the NLO response, other important molecular properties must be kept in mind in the molecular design[57]. A common concern with most modern high-β molecules is that the high response is partially due to resonance enhancement. What is meant by resonance here is that the photons at the desired wavelength have energy close to the energy difference between the ground state and an excited state of the molecule. The downside of this enhancement is that absorption is increased which in turn hinders the feasibility of such molecules in SHG or electro-optic modulation. Some progress has been made in optimizing the ratio of β and absorption using dipolar molecules with several excited states contributing to the resonance enhancement[58] and with octupolar molecules[59]. Another challenge is the thermal stability of organic molecules. Many popular D–π–A molecules decompose at temperatures <250 °C which limits their feasibility as high temperatures (∼300 °C) are often required in photonic device fabrication[57,60]. A successful route to increased thermal stability has been found to lie in replacing aliphatic electron donors with aromatic ones[61].

Although weak compared to intramolecular bonds, the intermolecular interactions cannot be neglected when considering the macroscopic NLO properties of matter. The polarity of the material around the nonlinear molecule has been shown to affect the second-order polarizability considerably[39,62,63]. In the particular case where the nonlinear molecule forms hydrogen bonds, notable change in the second-order polarizability can occur. It has been shown for p-nitroaniline in different solvents that hydrogen bonding can almost double β even when the changes due to different solvent polarities has been accounted for[64].

3.2 Measurement techniques for molecular response

Studying individual molecules dissolved in an appropriate solvent is highly convenient as the concentration can be easily controlled and the molecular environment is determined by the solvent. However, in a solution, the molecules assume random orientations and thus the macroscopic order becomes centrosymmetric. External means are needed to create a macroscopic order and thus measurable second-order nonlinearity. For molecules with permanent dipole moment, macroscopic polar (and thus noncentrosymmetric) order is created by applying an external electric field to the sample solution. A method called

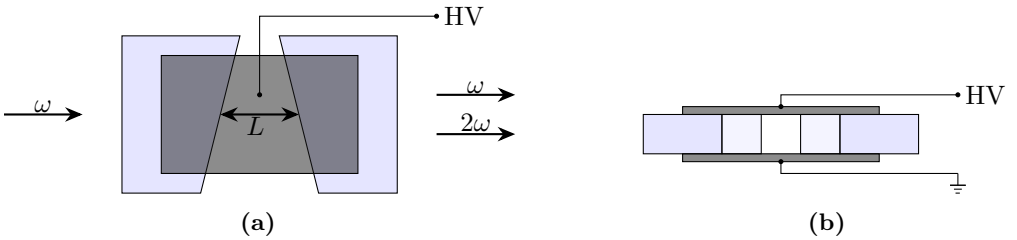

Figure 3.2: Schematic representation of an EFISHG cell. (a) Top view and (b) side view. Redrawn from Ref. [40].

electric-field-induced second-harmonic generation (EFISHG) was developed upon this idea[35].

With a fundamental field oscillating at frequency ω with amplitude A_ω and a static field E_0, the nonlinear polarization at the second-harmonic frequency 2ω is caused by a third-order interaction as[40,65]

$$P(2\omega) = \varepsilon_0 \Gamma E_0 A_\omega^2, \tag{3.2}$$

where $\Gamma = 3\chi^{(3)}_{zzzz}(-2\omega; 0, \omega, \omega)$ is the third-order macroscopic susceptibility that relates to the molecular polarizabilities by

$$\varepsilon_0 \Gamma = N f_0 f_\omega^2 f_{2\omega} \left(\gamma + \frac{\mu^0 \cdot \beta}{5 k_B T} \right). \tag{3.3}$$

Here N is the number density of the molecules and f_0, f_ω and $f_{2\omega}$ are local-field factors for the static field and fields at ω and 2ω frequencies, respectively. These factors provide a correction to the external fields to account for the influence of charges associated with neighbouring molecules[27]. Any material will produce an EFISHG signal through the third-order polarizability γ. However, molecules with permanent dipole moment $\boldsymbol{\mu^0}$ tend to align along the direction of the static field and the second term in Eq. (3.3) emerges. This term contains the scalar product of the permanent dipole moment and the second-order polarizability divided by a factor taking into account the molecular orientational distribution[40]. If $\gamma \ll \frac{\mu^0 \cdot \beta}{5 k_B T}$, the EFISHG signal will be mostly due to the second-order polarizability and we can write for the second-harmonic intensity produced by the solution:

$$I_{sol} \propto (\mu^0 \cdot \beta)^2. \tag{3.4}$$

In practice, the solution is placed into a wedge-shaped cell between high-voltage electrodes. The fundamental beam is weakly focused into the cell and the cell moved in the perpendicular direction with respect to the beam (Fig. 3.2(a)). Due to the wedge, the position shift gradually changes the length L over which the fundamental beam interacts with the solvent. The result is a sinusoidally varying second-harmonic intensity similarly to that described by Eq. (2.40) and the scalar product $\mu^0 \cdot \beta$ can be determined. Although EFISHG is a well established method for the characterization of molecular second-order polarizabilities, it has some limitations. Notably, only molecules with a permanent dipole moment can be studied and the measurement result is the scalar product $\mu^0 \cdot \beta$ instead of β.

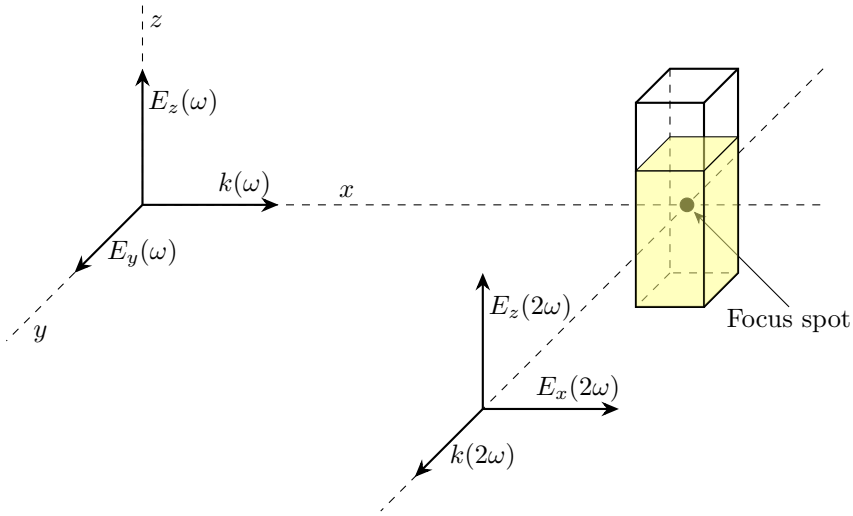

Figure 3.3: Geometry of a hyper-Rayleigh scattering setup. Redrawn from Ref. [67].

Another method for determining the second-order polarizability is hyper-Rayleigh scattering. Due to orientational fluctuations of asymmetric molecules in a solution, the solution is noncentrosymmetric over small distances and can have second-order nonlinear response[66]. Thus, the light scattered from such a solution can have a component at the second-harmonic frequency due to the molecular second-order response. This effect is called hyper-Rayleigh scattering. Let us take a measurement geometry where a z- or y-polarized fundamental beam with intensity I_ω and travelling in x-direction is focused to the center of a sample cell holding a solution with m constituents (Fig. 3.3). The intensity $I_{2\omega,i}$ of a second-harmonic wave travelling in y-direction with polarization $i = z, x$ is given by[40,67]

$$\begin{aligned} I_{2\omega,i} =& \frac{4\pi^2}{\varepsilon_0^3 n_\omega^2 c \lambda_\omega^4} f_\omega^4 f_{2\omega}^2 I_\omega^2 \\ & \times \sum_m N_m \left[\sum_{jk} \sum_{j'k'} (\hat{j} \cdot \hat{e}_\omega)(\hat{k} \cdot \hat{e}_\omega)(\hat{j}' \cdot \hat{e}_\omega)(\hat{k}' \cdot \hat{e}_\omega) \left\langle \beta_{ijk} \beta_{ij'k'} \right\rangle \right], \end{aligned} \tag{3.5}$$

where n_ω is the refractive index at the fundamental wavelength λ_ω. The terms f_ω and $f_{2\omega}$ are the local-field factors at the fundamental and second-harmonic frequency, respectively, and N_m is the concentration of constituent m. The term in brackets contains the projections of the fundamental field polarization unit vector $\hat{e}_\omega$ and the molecular coordinate axes. The last term in the brackets is the average over the molecular orientations. In the average, β_{ijk} is presented in the laboratory frame transformed from the molecular frame β_{IJK} using direction cosines.

The rather complicated expression of Eq. (3.5) can be greatly simplified assuming the molecular second-order polarizability has one dominant component which we denote β_{ZZZ} implying the choice that the molecular axis Z has been taken along the dominant component. We assume also that the second-harmonic intensity polarized in z-direction is measured. Now the direction average simplifies to $\frac{5}{35}\beta_{ZZZ}^2$ [67,68]. If the x-polarized signal was to be measured, the direction average would give $\frac{1}{35}\beta_{ZZZ}^2$ which leads to $\frac{6}{35}\beta_{ZZZ}^2$

for unpolarized detection. A practical measurement solution has only two constituents: the solvent and the solute under study. With these simpifications, we can write for the measurement signal proportional to $I_{2\omega,z}$ [39,40]

$$S_{2\omega} = G\left(N_{sv}\beta^2_{ZZZ,sv} + N_{sl}\beta^2_{ZZZ,sl}\right) I^2_{\omega}, \tag{3.6}$$

where N_{sv} and N_{sl} are the number densities and $\beta_{ZZZ,sv}$ and $\beta_{ZZZ,sl}$ are the second-order polarizabilities of the solvent and solute, respectively. Here G is a constant that takes into account the molecular orientational distribution, local field factors, physical constants and instrument factors. Importantly, with Eq. (3.6) only the second-order polarizability of the solvent is needed to determine that of the solute. In practice, $S_{2\omega}$ from a concentration series at low solute concentration is measured to obtain a straight line of the form $S_{2\omega} = aN_{sl} + b$. Fitting a line to the measurement results then allows the determination of $\beta^2_{ZZZ,sl}$ as

$$\beta^2_{ZZZ,sl} = \frac{a}{b} N_{sv}\beta^2_{ZZZ,sv} = \frac{a}{b}\frac{\rho_{sv}N_A}{M_{sv}}\beta^2_{ZZZ,sv}, \tag{3.7}$$

where ρ_{sv} is the density of the solvent, M_{sv} is the molecular mass of the solvent and N_A is the Avogadro number.

The reason to use low concentration of the solute is that the refractive index and the local-field factors remain practically unchanged from sample to sample and G remains constant. In addition, high concentration would change the density and number density of the solvent. At low concentration, all these properties can be assumed to be those for the pure solvent. For molecules that are strongly absorbing at the fundamental or second-harmonic wavelength, additional correction is needed. In the case of absorption at the second-harmonic wavelength, which is relevant for this Thesis, the absorption-corrected form of Eq. (3.6) is written as

$$S_{2\omega} = G\left(N_{sv}\beta^2_{ZZZ,sv} + N_{sl}\beta^2_{ZZZ,sl}\right) 10^{-\mathcal{A}_{2\omega}} I^2_{\omega}, \tag{3.8}$$

where $\mathcal{A}_{2\omega}$ is the absorbance of the solution over the distance it travels from the focus spot of the fundamental beam to the boundary of the sample cell before reaching the collection optics of the setup. The absorbance can be written as

$$\mathcal{A}_{2\omega} = \epsilon_{sl} c_{sl} L, \tag{3.9}$$

where ϵ_{sl} is the molecular absorption coefficient of the solute, c_{sl} is its concentration, and L is the length from the focus spot to cell boundary.

The advantage of hyper-Rayleigh scattering over EFISHG is that it allows the determination of the second-order polarizability without knowledge of the permanent dipole moment. Neither a high-voltage source or special sample are needed for hyper-Rayleigh scattering. In addition, the solvent provides an internal reference for determining the value of β. The weakness of hyper-Rayleigh scattering is mostly that the signal due to random orientational fluctuations is very weak requiring a highly sensitive detection system. As the measured signal is proportional to β^2, the sign of the second-order polarizability cannot be determined. The weak hyper-Rayleigh signal can cause additional problems due to other nonlinear phenomena often occuring in organic molecules [69]. For example, two-photon-absorption-induced fluorescence can display a significant broad-band emission in the long-wavelength side of the hyper-Rayleigh signal. This can mostly be avoided by the use of a narrow-band filter in the detection system. However, emission from a

three-photon-absorption induced fluorescence can have a notable contribution at the second-harmonic wavelength and care is needed in the examination of the hyper-Rayleigh scattering signal for reliable results.

3.3 Crystals and liquid crystals

Crystalline solids are materials whose building blocks are arranged in an ordered periodic lattice structure[70]. In inorganic materials, these building blocks are very small like the individual ions of sodium and chlorine found in table salt or the highly polar H_2O molecules constituting water. In a crystalline organic material, on the other hand, the building blocks are relatively large organic molecules that can be ionic or neutral.

For crystals, the molecular second-order polarizability β_{IJK} is connected to the bulk second-order susceptibility $\chi^{(2)}_{ijk}$ by the general equation[27,28]

$$\begin{aligned}\chi^{(2)}_{ijk}(\omega_3;\omega_1,\omega_2) = {} & N f_i(\omega_3) f_j(\omega_1) f_k(\omega_2) \\ & \times \sum_{IJK} \sum_{s=1}^{n} \cos(\theta_{i,I(s)}) \cos(\theta_{j,J(s)}) \cos(\theta_{k,K(s)}) \beta_{IJK}(\omega_3;\omega_1,\omega_2),\end{aligned} \tag{3.10}$$

where N is the density of the unit cells, $f_i(\omega_3)$, $f_j(\omega_1)$ and $f_k(\omega_2)$ are the local-field field factors at the frequencies ω_3, ω_1 and ω_2, respectively. The last term is the sum over n molecules that occupy one unit cell, and summation together with the cosine terms take care of the projection from the molecular coordinates IJK to the laboratory coordinates ijk.

In order to point out the huge potential provided by of organic materials, let us take 4-nitro-4'-aminostilbene shown in Section 3.1 with modestly high second-order polarizability and assume it is due to a single component $\beta_{ZZZ} = 1100 \times 10^{-40}\,\mathrm{m^4\,V^{-1}}$. If we were able to create a perfect crystal of this material organized such that each molecule is pointing in the same direction and choose this orientation to be in the z-direction in the laboratory frame, the component $\chi^{(2)}_{zzz}$ in Eq. (3.10) would assume the form

$$\chi^{(2)}_{zzz}(\omega_3;\omega_1,\omega_2) = N f_z(\omega_3) f_z(\omega_1) f_z(\omega_2) \beta_{ZZZ}(\omega_3;\omega_1,\omega_2) \tag{3.11}$$

The local field factors are described by Lorenz–Lorentz-type expressions[28] $f(\omega) = \frac{n_\omega^2+2}{3}$. With a reasonable refractive index of 1.5 this factor is about 1.4. Let us take this value for each frequency. Assuming the density close to that of liquid stilbene[71] ($1\,\mathrm{g\,cm^{-3}}$), the molecular weight $240\,\mathrm{g\,mol^{-1}}$ gives the number density $2.5 \times 10^{27}\,\mathrm{m^{-3}}$. With these values Eq. (3.11) gives $\chi^{(2)}_{zzz} \approx 750\,\mathrm{pm\,V^{-1}}$. This value is one order of magnitude higher than $\chi^{(2)} = 68.8\,\mathrm{pm\,V^{-1}}$ found in the commonly used inorganic material lithium niobate ($LiNbO_3$) at 1060 nm wavelength[72]. Lithium niobate, a synthetic inorganic crystal has been for decades the material of choice for many applications requiring high NLO response[73,74]. The molecular nonlinearity of 4-nitro-4'-aminostilbene is far from the best achieved and yet it would overwhelm the bulk response of lithium niobate if it were to assume perfect ordering.

Following the previous example, the highly-ordered structure of crystalline materials makes them particularly interesting for second-order NLO applications: when noncentrosymmetric molecules form a perfect crystalline structure, very strong bulk second-order response can be achieved. This requires that the molecules spontaneously form an ordered

lattice that belongs to one of the 21 (out of total 32) crystal point groups that lack a center of inversion[12]. As interactions between the molecules are weak and numerous, predicting crystallization to a noncentrosymmetric lattice is far from simple[42].

Due to the difficulty in rational design of crystalline order, research on organic crystals for second-order nonlinearity has largely been a process of trial and error. A useful tool for estimating second-order NLO properties of crystalline materials is the Kurtz powder method[75]. In this technique, the crystalline material is ground into a powder and the SHG from the powder is measured. While information on phase-matching and particle size is needed for a more accurate estimate of the second-order NLO response, the method gives a reasonable starting point for evaluating the applicability of a crystalline material for second-order NLO purposes: when the Kurtz method hints towards a large nonlinear response, the crystal is taken under further analysis.

Already in the 1970's, an early study on a single crystal of D–π–A benzene derivative 2-methyl-4-nitroaniline demonstrated several times higher bulk second-order response than lithium niobate[76]. A very potent group of crystalline organic materials, found in the 1990's, are the stilbazolium salts[77]. Many of these stilbene-like ionic molecules have been found to form good-optical-quality crystals with high second-order NLO response with particular interest focusing on 4-N,N-dimethylamino-4'-N'-methyl-stilbazolium tosylate (DAST)[78–81]. A relatively new approach takes advantage of the highly directional metal–ligand coordination bonds in metal–organic supramolecular systems to fight the tendency of centrosymmetric crystallization[82]. Amino acid crystals, discovered to be SHG-active already in the 1960's[83], continue to be of some interest. While their second-order nonlinearity is only moderately high at best, the key advantage of amino acids such as threonine and arginine and their derivatives is their tendency to form high-quality crystals transparent down to ultraviolet wavelengths[84,85].

Liquid-crystalline materials have peculiar properties between those of a traditional liquid and those of a well-organized solid crystal. A liquid crystal (LC) is generally strongly anisotropic but exhibits certain degree of fluidity, sometimes even comparable to an ordinary liquid. With a few exceptions[86,87], LCs are composed of rod-like organic molecules. The liquid-crystalline phases, also called *mesomorphic*, *i.e.*, intermediate phases, can be reached by thermal processes (*thermotropic* mesomorphism) or by the influence of solvents (*lyotropic* mesomorphism)[88]. In the case of thermotropic mesomorphism, heating the material starting from a solid does not directly lead to the formation of a isotropic liquid at a certain temperature. Instead, the process goes through one or several mesomorphic phases that may exhibit liquid crystallinity.

The thermotropic LCs are traditionally divided into nematic and smectic phases (See Fig. 3.4). In the nematic phase, the constituent molecules, *i.e.*, *mesogens* have high degree of long-range orientational order, but no long-range translational order. The nematic phase can be viewed as a liquid-like material in which all the molecules are oriented with their long axes, or *directors*, approximately parallel. The smectic phase adds translational order in the form of layer structures with thickness on the order of the length of the molecules. In the smectic A phase, the molecules are in the direction of the layer normal while, in the smectic C, their directors have certain tilt angle with respect to the layer normal[88].

While both the nematic and smetic mesophases are strongly anisotropic and exhibit, for example, strong birefringence and high nonlinear refractive index[89], their structures allow a center of inversion making them centrosymmetric and thus inactive for second-order NLO processes. This is due to the fact that while the molecular long axes are parallel in each of the structures, the molecules have equal probability to be parallel or antiparallel

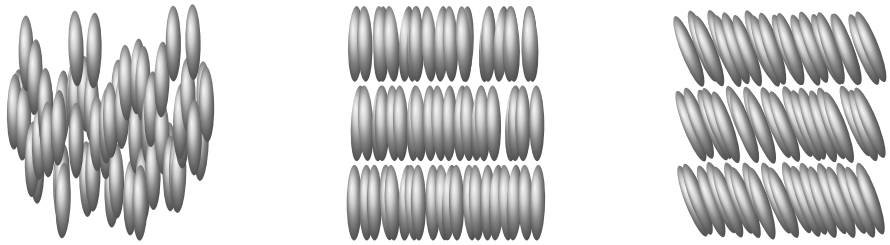

(a) Nematic **(b)** Smectic A **(c)** Smectic C

Figure 3.4: Liquid-crystalline phases.

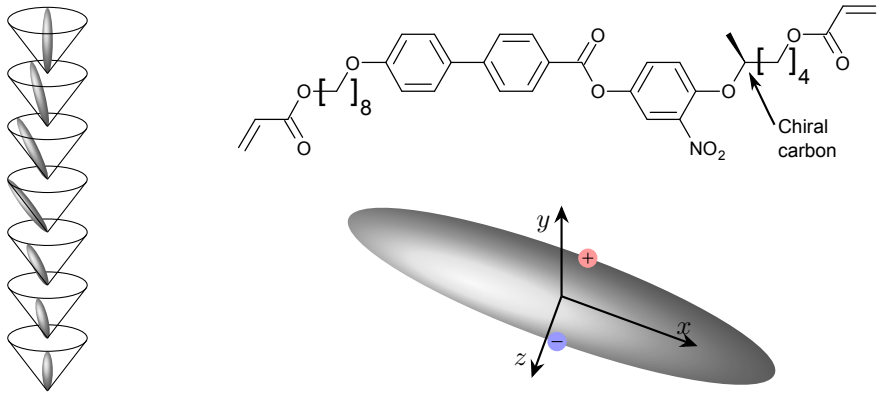

(a) **(b)**

Figure 3.5: (a) Formation of a helix structure in the chiral smectic C phase. (b) Structure of a molecule that forms the chiral smectic C phase (majority component of the material in **Paper IV**) and a schematic representation of this type of molecules.

even when the molecules themselves are noncentrosymmetric. Thus, further order is required to reach second-order NLO activity in LCs.

The required break of symmetry is found in the chiral liquid-crystalline phases, the most important examples being the chiral nematic, which is often termed *cholesteric* due to historical reasons, and the chiral smectic C. In the chiral nematic phase the director orientation gradually rotates forming a helix structure with the helix direction perpendicular to the director. In the chiral smectic phase, chirality arises from gradually changing director azimuth angle with respect to the layer normal (See Fig. 3.5(a)). This leads to a helix structure with the helix axis in the direction of the layer normal. The chiral ordering in these phases is spontaneously formed when the LC molecules are chiral (lack mirror symmetry) or even when a small portion of chiral molecules are added. In Fig. 3.5(b), the chiral carbon of a molecule that displays the chiral smectic C phase is shown. While the chiral nematic phase is the simplest example of a chiral LC and has found commercial use in thermochromic thermometers[90], the chiral smectic C is the relevant phase for this Thesis. This is due to the possibility of realizing a ferroelectric phase from this phase.[91]

In the ferroelectric liquid-crystalline phase, the chiral helix has been unwound and the

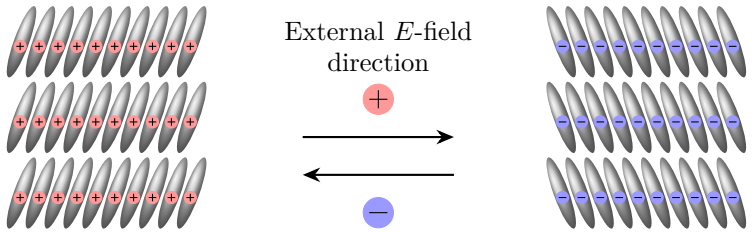

Figure 3.6: Schematic representation of a ferroelectric LC.

structure closely resembles the smectic C phase. The important difference is that in the case of chiral molecules, the only symmetry in the system is a 2-fold rotation with axis parallel to the smectic layers. The molecular chirality combined with this ordering leads to a spontaneous polarization along the symmetry axis and thus the ferroelectric phase exhibits bulk electric polarization and pyroelectricity. With external electric fields, this polarization direction can be altered (See Fig. 3.6), *i.e.*, ferroelectric behaviour is found in the LC[91]. As the helix structure is inherent to the chiral smectic C, external means must be used to reach the ferroelectric phase. The best known way is to "lock" the molecular directors through surface interactions. In this method, the LC is suspended in a cell with thickness that is less than the helical pitch of the chiral smectic C phase. If such a structure is built using LC molecules that prefer to be oriented parallel to the cell wall, only two molecular orientations are possible and a surface-stabilized ferroelectric LC is formed.[92] Another way to reach a similar structure is to use an external electric field to force the helix to unwind. The structure can then be frozen by polymerizing some of the LC molecules into a relatively rigid structure that still allows LC behaviour. This is the approach for the material system used in **Paper IV**.

Soon after polar order in ferroelectric LCs was demonstrated, investigation of the second-order NLO properties began[93]. Phase-matched SHG[94,95] was achieved but the response was orders of magnitude lower than that found in traditional inorganic crystals. This was due to low molecular second-order polarizability and poor stereocontrol, *i.e.*, selection of only one chiral enantiomer in the chiral mesogens. A notable step forward was taken when the electronic asymmetry, discussed in Section 3.1, was introduced to the mesogens[96]. In the molecule shown in Fig. 3.5(b), a nitrobenzene group provides a notable dipole moment and second-order polarizability component in the direction perpendicular to the director, enhancing the polarity and bulk second-order response in a ferroelectric LC. This concept has since been taken even further by combining a D–π–A type azobenzene molecule with high β to ferroelectric LC phase forming mesogens[97] and considerably high second-order nonlinearity has been reached[98]. While strong second-order NLO properties have been a goal in developing new ferroelectric LCs, SHG has also been found to be a versatile tool for studying the structures of liquid crystals[99].

3.4 Amorphous polymers and molecular glasses

For many molecules with high second-order polarizability, growing sufficiently large single crystals for practical applications is all but impossible. Amorphous materials offer a completely different approach towards efficient bulk second-order response. An amorphous material is a solid with no long-range order. Sometimes amorphous materials are described

as “frozen liquids” to highlight the similarity to the liquid phase. The lack of order makes the material isotropic and therefore centrosymmetric which means that, for second-order NLO response, external means are needed to break this symmetry. These means are covered at the end of this chapter after the introduction of the important amorphous material systems.

In a simplified view, polymers are large molecules composed of a high number of small repeating units called monomers. In a commercial polymer, the number of monomers is in the range of hundreds to tens of thousands, which leads to the very high molecular masses ranging from 10^4 to over 10^6 g mol^{-1}. The high number of repeating units makes the length scale of polymer molecules exceptional: while the chain is only about 1 nm in diameter, its length may be several micrometers [100]. In a polymer, the long molecules form coiled structures that are penetrated by chain segments from other molecules forming an entangled network. If the thermal energy of the molecules is high enough, long segments of the polymer chains can move relative to each other and the polymer can flow. When the temperature of such polymer melt is lowered, at a certain point, all the long-range motion ceases. This temperature is called the *glass-transition temperature*, T_g. Any material that shows this behaviour can be called a glass. For the purpose of this Thesis, the words glass and amorphous solid can be used interchangeably although also other amorphous phases exist. Some polymers fold in a manner that allows the formation of small crystalline areas surrounded by amorphous areas and these polymers are called semicrystalline [101].

A polymer material system for optical applications can be built of a polymer matrix, giving the system a rigid amorphous structure, and of strongly light-responsive organic molecules somehow embedded into the polymer. Often, the light-responsive molecules exhibit absorption in the visible spectrum giving them certain color. Therefore, these molecules are called *chromophores*, strictly meaning the color-giving part of a molecule [102], or *dyes*. A simple method for preparing an embedded system is to mix the polymer and dye in a suitable solvent. When the solvent vaporises, a solid *guest–host* system of the dye and polymer is formed. For high second-order NLO response, the polymer must be embedded with molecules with high second-order polarizability. A considerable amount of research has been focused on the guest–host systems of D–π–A type molecules (Section 3.1) and common polymers like polyacrylates [103,104], and high-T_g polyimides [105,106], that offer enhanced thermal stability of the NLO response.

A well-studied group of high-β chromophores, sometimes called NLO-phores, are the push–pull azobenzene derivatives. In addition to moderately high optical nonlinearity, the D–π–A-structure makes this type of molecules electrically polar. The structure of a push–pull azobenzene Disperse Red 1 (DR1) is shown in Fig. 3.7 together with schematic representations of molecules of this type highlighting the dipolar nature. The properties of azobenzenes are thoroughly covered in Section 4.1. The polarity has severe consequences when high bulk nonlinearity is sought through increasing the chromophore concentration in the host polymer: electrostatic interactions between the molecules favour antiparallel orientation of the molecules which leads to diminished second-order NLO response [107–109]. Other disadvantages of simple guest–host systems include lowered T_g and diffusion of the guest molecules out of the polymer matrix [110,111]. These problems can be fought against by binding the chromophores tightly to the polymer, thus reducing the chromophore mobility and lowering the chance of chromophore–chromophore interactions.

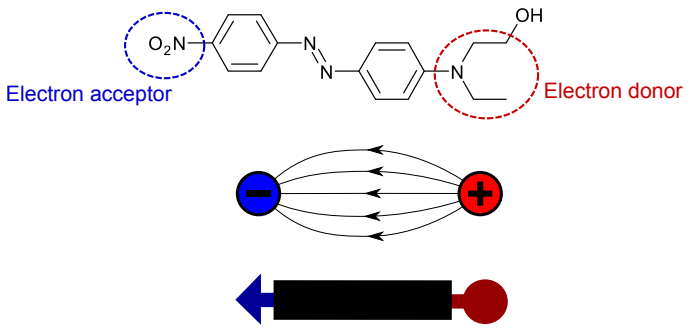

Figure 3.7: The structure of a prototype push–pull azobenzene DR1 used in **Paper I** and in **Paper III** of this Thesis and schematic representations this type of molecule.

A commonly used method for strong chromophore–polymer binding is to attach the chromophore covalently to the polymer chains. Covalent bonds have very high binding energies and chromophore mass fractions up to 50 wt. % are common in these special polymers without problems caused by chromophore–chromophore interactions[6] The downside of covalent bonding is that tedious and expensive chemical synthesis route must be found every time a new combination of a polymer and chromophore is to be studied. A way to combine the best parts of covalently-bonded systems and guest–host systems lies in the concepts of supramolecular chemistry: with relatively strong non-covalent bonds, hydrogen-bonding for example, the simplicity of just mixing a polymer with a dye and much-lowered chromophore mobility can be combined[112]. This requires that the polymer and chromophore are chosen such that non-covalent bonds spontaneously appear between them, which leads to the formation of a supramolecular structure resembling a covalently-bonded polymer. This strategy is followed in **Paper I** in the form of a hydrogen-bonded supramolecular polymer and in **Paper II** by using chromophores that form halogen bonds with the polymer matrix. The different chromophore-embedded polymer systems are depicted in Fig. 3.8. The chromophore is considered to be DR1 shown in Fig. 3.7. Importantly, this molecule has the capability of forming hydrogen bonds through its single hydroxyl group or this group can be easily used bond to the molecule covalently to a polymer chain.

Hydrogen bonding is a special case of electrostatic interaction, which forms between an electronegative atom and a hydrogen atom connected to another electronegative atom[102]. A common example of the importance of hydrogen bonding is water, where each H_2O molecule can form two hydrogen bonds and these bonds contribute to the exceptionally high boiling point of water relative to its molecular weight. Compared to the ubiquitous hydrogen bond, halogen bonding is a less-known intermolecular interaction that has been gathering notable attention only in the past 15 years[113]. Due to their electronegativity, halogen atoms in organic molecules are generally considered to be sites of high electron-density. Therefore, they act as electron donors, forming attractive interactions with electron-poor species. However, in a molecule, the electron density around a halogen atom is not evenly distributed. Instead, an area of lower electron density, called the σ-hole is found opposite to the single covalent bond[114]. Particularly with the larger halogens Br or I connected to a electron-withdrawing structure, the σ-hole can act as positive site forming attractive bonds to electron-rich species. This interaction is called the halogen bond[115]. As an example, one of the halogen-bond-forming molecules studied in **Paper II**

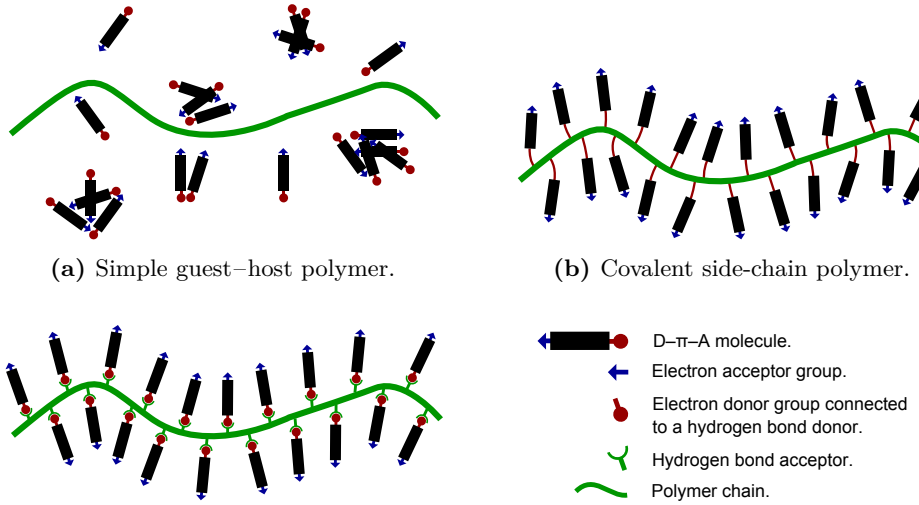

(a) Simple guest–host polymer. **(b)** Covalent side-chain polymer.

(c) Supramolecular side-chain polymer. **(d)** Explanations of figure symbols.

Figure 3.8: Polymers embedded with D–π–A chromophores with different chromophore–polymer interactions.

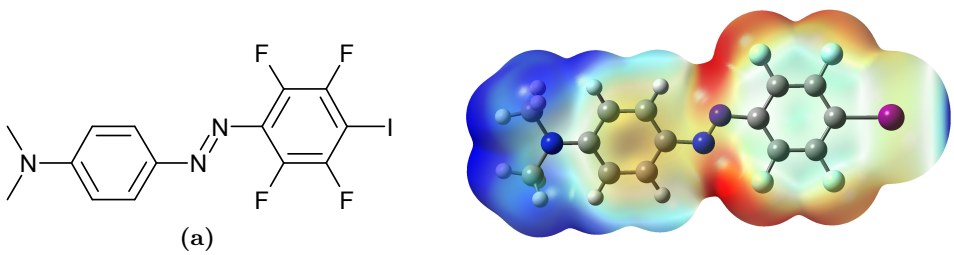

(a) **(b)**

Figure 3.9: (a) Chemical structure and (b) electrostatic potential map of the Azo-I molecule capable to halogen bonding. Negative electrostatic potential (high electron density) is shown in red and positive electrostatic potential (low electron density) in blue. Reproduced from **Paper II** with permission from the Royal Society of Chemistry.

is shown in Fig. 3.9. From the electrostatic potential map, it is evident that a narrow area of low electron density can be found at the iodine atom at the very end of the molecule. Due to the small size of the σ-hole, the halogen bond is highly directional, forming to a narrow range around the 180° angle with respect to the halogen atom's single covalent bond [116].

In addition to polymers, some smaller (molecular mass $\lesssim 1000\ \mathrm{g\,mol^{-1}}$) organic molecules form stable amorphous phases instead of crystallization. These materials are called *molecular glasses* and they started gaining considerable attention in the 1990's for organic electronic applications, for example organic light emitting diodes [117,118]. The general idea behind molecular design for a molecular glass is to reach a structure that does not easily allow packing of the molecules into an ordered lattice. Ways to approach this goal are

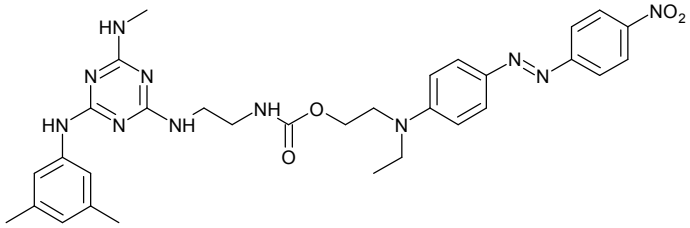

Figure 3.10: Structure of the DR1-functionalized molecular glass studied in **Paper III**.

to aim for nonplanar molecular structure and irregular shape[118,119]. If the molecule has a large amount of different conformations with similar energy in the liquid state, it is expected to show weakened ability to crystallize due to kinetic reasons[119].

The important difference between polymers and molecular glasses stems from the difference in their molecular weight and synthesis. During polymerization, the number of monomers can never be exactly chosen. Thus, a polymer always has some degree of dispersity in its molecular mass, whereas the small molecule in a molecular glass is identical to the next one. This difference leads to easier purification of the molecular glasses and better repeatability in sample fabrication compared to polymers[120,121]. Similarly to a polymer, a molecular glass could be used as the host material for guest–host systems together with NLO chromophores. However, work on NLO-active molecular glasses has focused on functionalized molecular glasses[122–125]. This approach is similar to the concept of covalent bonding of chromophores to a polymer while it maintains the advantages due to lower molecular weight. A few years ago, a new family of molecular glasses called the mexylaminotriazines was introduced[126,127]. Despite the relatively high symmetry and possibility to self-assemble through hydrogen bonding, these materials show remarkable tendency to form stable amorphous phases. Even when functionalized with chemical groups that readily crystallize when pure, the mexylaminotriazines tend to be amorphous[128]. DR1-functionalized mexylaminotriazine was recently synthesized and shown to form a stable glassy state[129]. This material, shown in Fig. 3.10, is studied in **Paper III**.

For a bulk second-order response, the isotropic order of the amorphous material must be broken. Thanks to the permanent dipole moment of D–π–A-type molecules, this order is broken by a static electric field that tends to align the molecules into polar order. The process is similar to EFISHG performed in liquids (Section 3.2). An important difference is that in a solid glassy material, the molecules are not free to rotate and their mobility must be enhanced by some means. The simplest method is to heat the material near its glass-transition temperature, where thermal energy is sufficient to allow molecular realignment. In principle, the process consists of three steps: (1) apply an electric field to the material, (2) increase the temperature close to T_g, (3) cool the sample to ambient temperature with the field on. The cooling back to the glassy state with the field on "locks" the polar structure caused by the field at the elevated temperature and the field can be turned off and the order remains. In practice, thermal relaxation will gradually reinstate the original isotropic order and the second-order nonlinear response is lost with time[110]. However, by using a high-T_g host polymer formed by crosslinking the polymer chains in the poling process, the thermal relaxation can be made very slow[105,106].

An early study with electrically-poled materials was performed in the 1980's with a LC polymer and a prototype D–π–A molecule 4-(dimethylamino)-4'-nitrostilbene (DANS). Relatively small second-order susceptibility of $\chi^{(2)} = 1\,\mathrm{pm\,V^{-1}}$ was reached in a few-minute time scale[130]. Later on, electro-optic coefficient values $\sim 10\,\mathrm{pm\,V^{-1}}$ were found with azobenzene guests in amorphous polymer hosts such as poly(methyl methacrylate) only to be overwhelmed by the covalently-bonded functionalized polymers soon reaching $40\,\mathrm{pm\,V^{-1}}$[104]. These polymers were eagerly studied in the late 1980's and early 1990's[60]. Still, the superiority of the functionalized polymers with covalent bonding is not the full story as modern chromophore guests in poly(methyl methacrylate) host have shown electro-optic coefficients exceeding $200\,\mathrm{pm\,V^{-1}}$ (1310 nm)[131]. For supramolecular binary glasses where both components possess strong molecular second-order polarizability, electro-optic coefficient exceeding $300\,\mathrm{pm\,V^{-1}}$ (1310 nm) has been reached[132].

4 Photocontrolled nonlinear optical response

This chapter is the core part of this Thesis. Here, the possibility to photocontrol the nonlinear properties of the material systems covered in Chapter 3 is introduced. In the first section, the light-induced changes at the molecular level are explained, focusing on the azobenzene moieties that are behind the photocontrolled properties of each material used in this Thesis. In the second section, previous work on photocontrolled NLO response in amorphous materials is introduced, followed by detailed description of the AOP method used in this Thesis. The main results of **Paper I**, **Paper II** and **Paper III** are reviewed. In the third section, the photoswitching of nonlinear optical response in crystals and LCs is introduced and previous work on this topic is covered. The material system and experimental methods applied in **Paper IV** are described and the main results reviewed.

4.1 Azobenzene: a photocontrolled molecular trigger

Based on the origin of the NLO response covered in Chapter 3, photocontrol of this response requires that light is either (1) able to modify the second-order polarizability of the constituent molecules or (2) change the arrangement of the molecules between centrosymmetric and noncentrosymmetric order. In both cases, some light-triggered effect is needed at the molecular level. Chemical changes triggered by light are far from uncommon in organic molecules, contributing to the broadness of an entire field called photochemistry. The light-triggered change can result in the production of a new stable compound like the photosynthesis of sugars starting from water and carbon dioxide in plants. However, for this Thesis, the relevant reaction is a reversible photoinduced change between two molecular forms, which is called *photochromism*[†]. Common photochromic changes include ring-opening and -closing reaction found in diarylethenes[134], intramolecular proton transfer found in nitrobenzyl pyridines[135] or *cis–trans* isomerization in retinal[136]. All of these mechanisms may also to produce large changes in molecular or bulk NLO properties[133,137].

One of the best-studied class of photochromic molecules are the derivatives of azobenzene. Azobenzene is an organic molecule where diazene (doubly-bonded pair of nitrogen atoms) is substituted with two benzene rings[102]. This structure gives azobenzene a reasonably long conjugated π system and absorption in the UV–visible range. Due to this absorption

[†]Strictly, photochromism refers to the photoinduced transformation between two molecular states whose absorption spectra are different. However, other molecular properties, such as the second-order polarizability, may change between the two molecular states, and the term photochromism is extended to cover any change due to the light-triggered molecular state change[133].

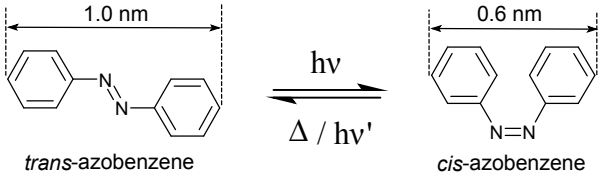

Figure 4.1: *Cis–trans* isomerization of azobenzene.

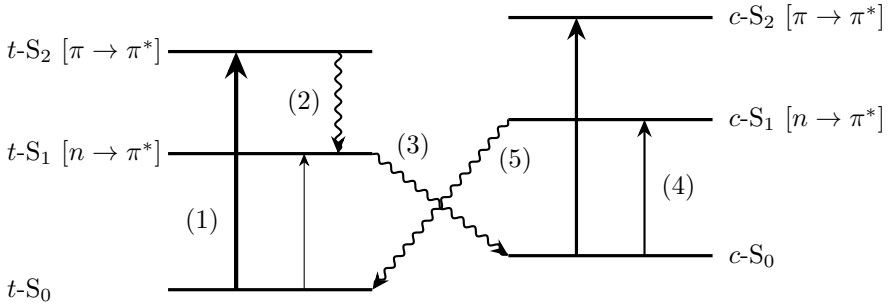

Figure 4.2: Schematic energy levels of azobenzene and a *trans–cis–trans* isomerization cycle. The eletronic transition between molecular orbitals that leads to the excited states are shown in brackets. Radiative transitions are drawn with straight arrows with broader width related to a more probable transition. Non-radiative transitions are drawn with curly arrows.

and good chemical stability, azobenzenes[‡] were originally developed and studied for the needs of dye industry. Photochromism in azobenzene is due to the reversible *cis–trans* photoisomerization (See Fig. 4.1), that changes molecular properties like the shape and dipole moment [138], as well as absorption profile [139] and second-order polarizability [140]. The *trans*-isomer is planar as drawn in Fig. 4.1, whereas the *cis*-isomer assumes a twisted geometry where the benzene rings are not in the same plane [139]. The photoisomerization in azobenzene occurs in the timescale of picoseconds through out-of-plane rotation around the N=N double bond or in-plane inversion about the N=N bond [141–145]. The debate over the mechanism has been ongoing since the 1960's [146].

A schematic energy-level diagram of azobenzene [139,141,147] is shown in Fig. 4.2. The important transitions are from the highest occupied non-bonding n and bonding π molecular orbitals to the lowest unoccupied molecular orbital which is the antibonding π^*. All of these orbitals are associated with the diazene group [148]. The *trans*-isomer has strong absorption near 320 nm (Fig. 4.3(b)) due to $\pi \rightarrow \pi^*$ transition and weak absorption near 450 nm due to symmetry-forbidden $n \rightarrow \pi^*$ transition. Absorption at 450 nm results in excitation from the ground energy level t-S_0 to the first excited level t-S_1 and absorption at 320 nm to the second excited level t-S_2, respectively. In the *cis*-isomer, the separations between the energy levels remain almost unchanged but each *cis*-isomer energy level c-S_0, c-S_1 and c-S_2 is shifted higher in energy compared to the *trans*-isomer states. In the *cis*-isomer, the $n \rightarrow \pi^*$ transition becomes more probable, which is seen as increased absorption in the visible range, and the $\pi \rightarrow \pi^*$ transition is weaker, which is seen as decreased absorption in the UV range. Based on the relative strengths of these transitions, one possible photoisomerization cycle is shown in Fig. 4.2.

[‡]Azobenzene derivatives formed by substitution of one or several of the hydrogen atoms in the benzene rings are referred to as azobenzenes

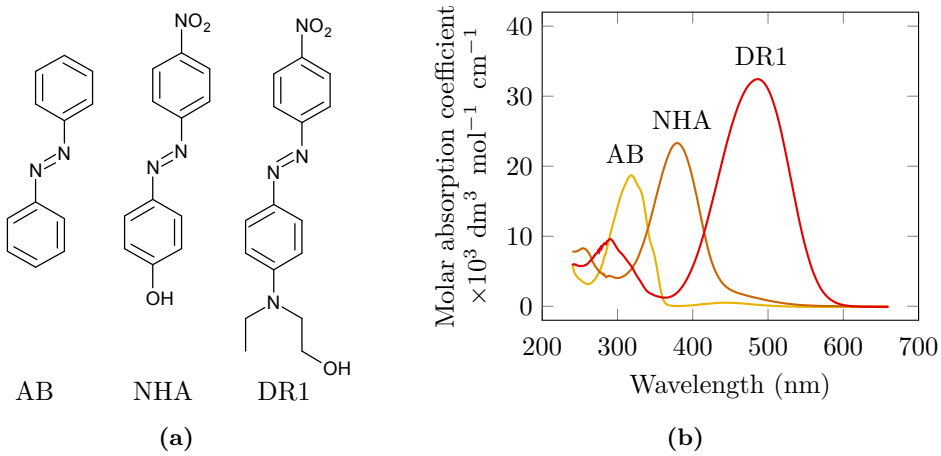

Figure 4.3: Examples of each azobenzene type: (a) Azobenzene-type unsubstituted azobenzene (AB), aminoazobenzene-type 4-nitro-4'-hydroxyazobenzene (NHA), and pseudostilbene-type 4-nitro-4'-[N-ethyl-N-(hydroxyethyl)-amino]azobenzene (DR1). (b) Molar absorption coefficients in the UV-VIS range for the molecules. The absorbances were measured in 5×10^{-5} mol dm^{-3} tetrahydrofuran solutions.

The cycle proceeds as follows: (1) a photon is absorbed at 320 nm and the molecule is excited to t-S_2, (2) non-radiative relaxation to t-S_1 occurs, (3) the molecule isomerizes to the *cis*-form non-radiatively ending up in c-S_0, (4) a photon is absorbed at 450 nm and the molecule is excited to c-S_1, and (5) the molecule isomerizes to the *trans*-form non-radiatively ending up in t-S_0. In this cycle, both isomerizations are triggered by light. However, the higher energy of the *cis* ground state makes the *trans*-isomer energetically favoured and the *cis*-isomer gradually relaxes to *trans*. Fluorescence is almost nonexistent in azobenzene[149]. The quantum yield for the $\pi \rightarrow \pi^*$ transition triggering *trans* $\rightarrow$ *cis* isomerization is about 0.15 and for the $n \rightarrow \pi^*$ transition triggering *cis* $\rightarrow$ *trans* isomerization about 0.5[139].

Substitution changes the photophysical properties of azobenzene considerably. Azobenenes are categorized into three groups (Fig. 4.3) based on the energy of the $\pi \rightarrow \pi^*$ transition which is very sensitive to substition while the energy of the $n \rightarrow \pi^*$ transition remains nearly unchanged. Examples of each azobenzene type and their absorption spectra are shown in Fig. 4.3. In azobenzene-type molecules, the $\pi \rightarrow \pi^*$ has much higher energy than the $n \rightarrow \pi^*$ transition and the energy-level diagram is similar to that shown in Fig. 4.2. For aminoazobenzene-type molecules, the $n \rightarrow \pi^*$ and $\pi \rightarrow \pi^*$ transitions occur at comparable energies meaning that the S_1 and S_2 states in Fig. 4.2 are very close to each other. The third class is the pseudostilbene-type molecules in which the energies of $\pi \rightarrow \pi^*$ and $n \rightarrow \pi^*$ transitions are again very close to each other but $\pi \rightarrow \pi^*$ has become the lowest-energy transition. In aminoazobenzenes and pseudostilbenes the weak $n \rightarrow \pi^*$ transition is easily covered by the intense $\pi \rightarrow \pi^*$ transition and cannot be resolved from absorption spectrum. In addition to the unsubstituted azobenzene, the azobenzene-type includes derivatives with, for example, alkyl or ester substituents. Substitution with amino or hydroxyl groups in the 2 or 4 positions of the benzene rings results in aminoazobenzene-type molecules[139]. A double substitution with electron-donating and electron-withdrawing groups in the opposite ends of azobenzene leads to the pseudostilbene-type molecules. Notably, this is an example of the push–pull structure that

gives rise to strong second-order polarizability discussed in Section 3.1. The substitution changes the thermal relaxation lifetimes of the *cis*-isomer drastically. Typically, the azobenzene-type molecules relax to *trans* in hours, aminoazobenzenes in minutes, and pseudostilbenes in seconds[150]. However, well-chosen substitution can increase the *cis* lifetime to at least several days[151,152].

In addition to substitution, the molecular environment can have a notable effect on the photochemical properties of azobenzenes. The pseudostilbene-type azobenzenes are particularly sensitive to the local environment. For example, for 4-(diethylamino)-4'-nitroazobenzene, the thermal relaxation of the *cis*-isomer takes 140 s when dissolved in hexane and only 2 ms when dissolved in N-methylformamide[6,153]. The polarity of the environment can notably shift the absorption peaks of the azobenzenes. This effect is known as solvatochromism. The pseudo-stilbenes show positive solvatochromism where higher polarity of the environment leads to the shift of the absorption maximum to longer wavelengths[154–156].

The properties of azobenzenes are sensitive to mutual interactions between the molecules. The spectral changes are often well described by the exciton model treating the individual molecules as point dipoles. In this model, molecular dimers and their mutual perturbation due to electrostatic interactions are considered. This leads to splitting of the molecular excited state into two states with energy difference $\Delta\mathcal{E}$[157]. In the case where the transition dipole moments of the molecules point in the same direction, the energy difference is given by

$$\Delta\mathcal{E} = \frac{2\left|\boldsymbol{\mu}_{eg}\right|^2}{r^3}\left(1 - 3\cos^2\theta\right), \tag{4.1}$$

where $\boldsymbol{\mu}_{eg}$ is the transition dipole moment from the ground state to the excited state, r is the separation between the centers of the molecules and θ is the angle between the dipole direction and the line connecting the centers of the molecules (Fig. 4.4(a)). Notably, if the transition dipole moments are out of phase, the transition becomes forbidden and only one of the energy levels can be accessed. The energy levels of the molecular dimer formed according to Eq. (4.1) are shown in Fig. 4.4(b). An important division to two regions is seen: At $\theta = 54.7°$, the energy gap disappears. For angles smaller than this value, the accessible transition has lower energy than found for the monomer and the arrangement is called J-type aggregation. For $\theta > 54.7°$, the accessible state energy is higher that that of the monomer and the arrangement is called H-type aggregation. According to Eq. (4.1), the width of the energy gap is proportional to the square of the transition dipole moment. Therefore, the effect is significant only for strong transitions which means that, in the case of azobenzenes, it needs to be considered only for the $\pi \rightarrow \pi^*$ transition. Planar molecules with strong dipole moments favour H-type aggregation into an antiparallel configuration[108]. Therefore, particularly for the pseudostilbenes, this type of aggregation is to be expected when the intermolecular distances become small. However, as discussed in Section 3.4, the antiparallel order has a devastating effect on the nonlinear optical response[109,158].

The extent of material properties and types of materials that can be controlled by light using the *cis–trans* isomerization of azobenzene is extremely broad. Photoinduced birefringence and dichroism have been studied in guest–host[159], supramolecular[160] and covalent side-chain polymers[159] as well as in Langmuir–Blodgett films[161], molecular glasses[162] and LC polymers[163]. In addition to these effects, which are caused by photoinduced molecular reorientation, large-scale mechanical effects have been observed resulting from

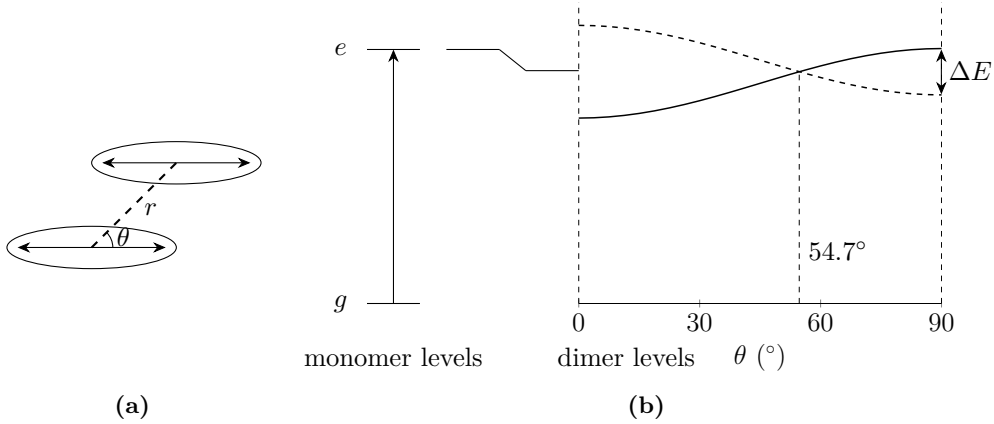

Figure 4.4: (a) Schematic geometry of the dimerization of dipolar molecules and (b) the exciton-band formation. The energy of the inaccessible state is shown with a dashed line. Redrawn from Ref. [157].

the *cis–trans* isomerization. Permanent modulations of the surface topography can be written to azobenzene polymers[7,164], molecular glasses[120,165] and even single crystals[166]. These *surface-relief gratings* copy the interference pattern that is shone onto the sample into several-hundred-nanometer-deep groove patterns. Large-scale motion in the form of photoinduced bending has been observed in LC polymers[167] and crystals[168].

The pseudostilbene-type chromophore DR1 is used both as the source of the nonlinear optical response and as the photocontrolled species in **Paper I** and **Paper III**. This well-known molecule has the second-order polarizability $\beta \approx 1000 \times 10^{-30}$ esu $= 4200 \times 10^{-40}$ m^4 V^{-1} for the *trans*-isomer[68,169]. Isomerization to *cis* decreases β by a factor of five[140] which could in principle be used to create materials with a photocontrolled nonlinear optical response. However, due to the short *cis*-lifetime of pseudostilbenes, this type of response would die out quickly. Still, the fact that both isomers of pseudostilbenes have notable absorption in the visible range, makes DR1 an efficient molecule for fast photodriven cycling between the isomers. This cycling will gradually change the molecular orientation distribution enabling new optical properties such as photoinduced birefringence and second-order NLO response, which are discussed in the next section.

4.2 All-optical poling of amorphous matter

The first notable step towards photocontrolled second-order NLO response in polymers was taken when photoassisted poling was developed as an extension to electric-field poling (Section 3.4). In photoassisted poling, the heating of a polymer system above its T_g is replaced by photoisomerization of the nonlinear molecules. The isomerization provides enhanced mobility and the molecules can align into a polar structure although the surrounding polymer is in the rigid glass-like phase[6,170]. Fully light-driven poling started developing from the observation of increasing SHG in an optical fiber exposed to high-intensity infrared light[171]. Seeding of the process with second-harmonic of the infrared light was soon found to boost the process[23] and the resulting polar, second-order NLO active structure was identified to be related to the third power of the two-frequency field[24]. The induced nonlinearities in optical fibers are relatively small but the process,

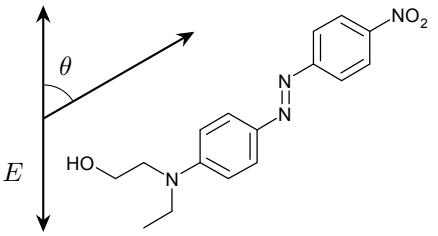

Figure 4.5: Molecular orientation angle θ with respect to linearly polarized incident field E direction.

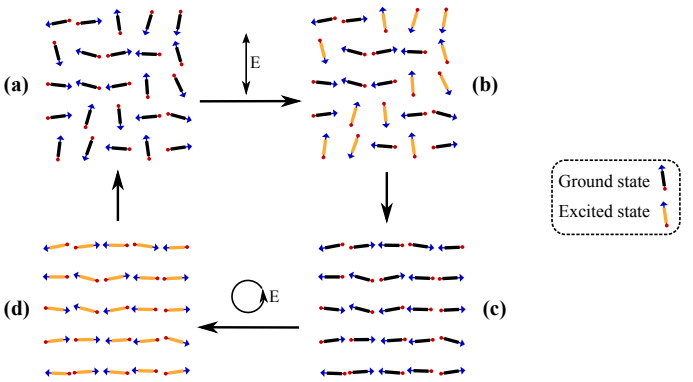

Figure 4.6: (a) → (b) → (c) Creation of an in-plane axial structure following excitation by linearly-polarized light and (c) → (d) → (a) restoration of isotropic structure following excitation by circularly-polarized light.

later conveniently named all-optical poling, was found to be suitable for poling dye-doped polymers [25,172].

In order to understand photoinduced changes in molecular arrangement, the selectivity of photoexcitation in azobenzenes needs to be considered. Let us assume that linearly polarized light with the wavelength at the absorption band of an azobenzene molecule is shone to the molecule. The molecular long axis is in angle θ with respect to the field polarization (Fig. 4.5). The rodlike *trans*-azobenzene can be approximated as a uniaxial molecule that has absorption cross section σ of the form [173]

$$\sigma(\theta) = \sigma_a \cos^2\theta + \sigma_i, \tag{4.2}$$

where σ_a and σ_i characterize the anisotropic and isotropic parts of the cross section, respectively. For a uniaxial molecule $\sigma_i \ll \sigma_a$ and according to Eq. (4.2), only the molecules that are roughly in the direction of the incident field have high probability of excitation. The photoinduced isomerization is known to affect the molecular orientation [174]. Gradually, the excited molecules rotate away from the polarization direction of the incident light and an anisotropic structure is formed. In Fig. 4.6(a) → (b) → (c), this process is shown schematically for a group of polar molecules such as DR1. Importantly, the anisotropic order can be erased by photoexcitation with no directional selectivity. In practice, this is achieved by circularly-polarized or unpolarized light and this process is shown in Fig. 4.6(c) → (d) → (a). Although the resulting structure is anisotropic showing birefringence and dichroism, the *axial* arrangement in 4.6(c) is centrosymmetric and will not show second-order NLO response.

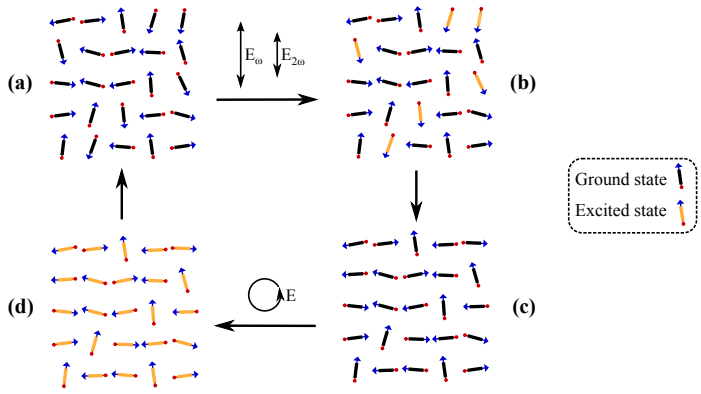

Figure 4.7: (a) → (b) → (c) Creation of an in-plane polar structure following excitation by linearly-polarized dual-frequency light and (c) → (d) → (a) restoration of isotropic structure following excitation by circularly-polarized light.

The key addition needed to realize AOP is the dual-frequency field discussed on general level in Section 2.4. In the case of a polar azobenzene, this field is chosen such that the seeding field at frequency 2ω is at the absorption band of the molecule and the fields have collinear polarization. Now, the seeding field alone would induce axial symmetry as in Fig. 4.6 through single-photon absorption and the writing field at frequency ω would create the same structure through two-photon absorption. However, the interference between these two processes has higher selectivity: the two-frequency field has different probability for the excitation of molecules pointing "up" or "down". The AOP process is schematically shown in Fig. 4.7(a) → (b) → (c). The effect of the dual-frequency excitation is exaggerated in Fig. 4.7(b): only the molecules pointing "down" are excited and reorient perpendicular to the incident field. The structure in Fig. 4.7(c) thus has excess of molecules pointing "up" making this structure polar and second-order nonlinearities allowed. It should be noted that the polar order is due to molecules remaining in the polarization direction of the optical fields[175,176]. Most of the molecules have been turned away from the polarization direction and the structure in Fig 4.7(c) will show birefringence. In **Paper I**, the second-order nonlinearity and birefringence are separately measured during AOP in order to study the differences between these quantities that are simultaneously created.

Similarly to the axial structure, the polar structure can be erased by circularly-polarized light and several poling–erasure cycles are possible. In Fig. 4.8 nine such cycles for a supramolecular polymer are shown. After a small drop from the first maximum in the second-harmonic intensity to the second one, the cycle repeats with little to no fatigue.

Despite the mechanism described above, which is sufficient for the poling process in this Thesis, AOP is far from limited to this particular case. Instead, other polarization combinations can be used[177,178] to create other types of noncentrosymmetric arrangements. In contrast to eletric-field poling, non-dipolar chromophores can be poled using AOP[179,180]. Even the requirement that the seeding beam is on the absorption band is not strictly required as interference of two-photon ($\omega + 2\omega$) and three-photon ($\omega + \omega + \omega$) absorption can create similar selectivity making AOP possible[181–183]. The main disadvantages of optically poled polymers are that the poling process is rather slow and the polar order gradually relaxes through orientational diffusion as in the case of electrically-poled polymers. Crosslinking of the polymer chains has succesfully been used to increase

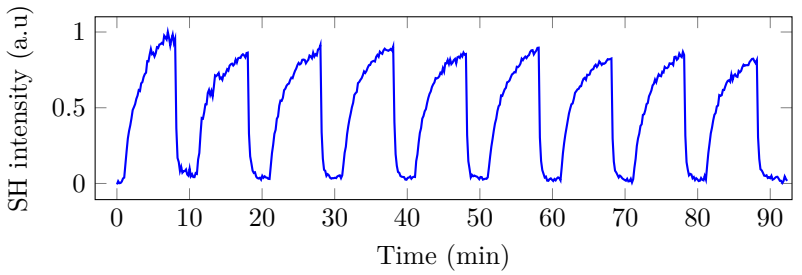

Figure 4.8: Poling–erasure cycles. Poling is started at 1 min and continued until 9 min. At 9 min, erasure is started and continued until 11 min. The cycle continues with 8 min long polings followed by 2 min long erasures.

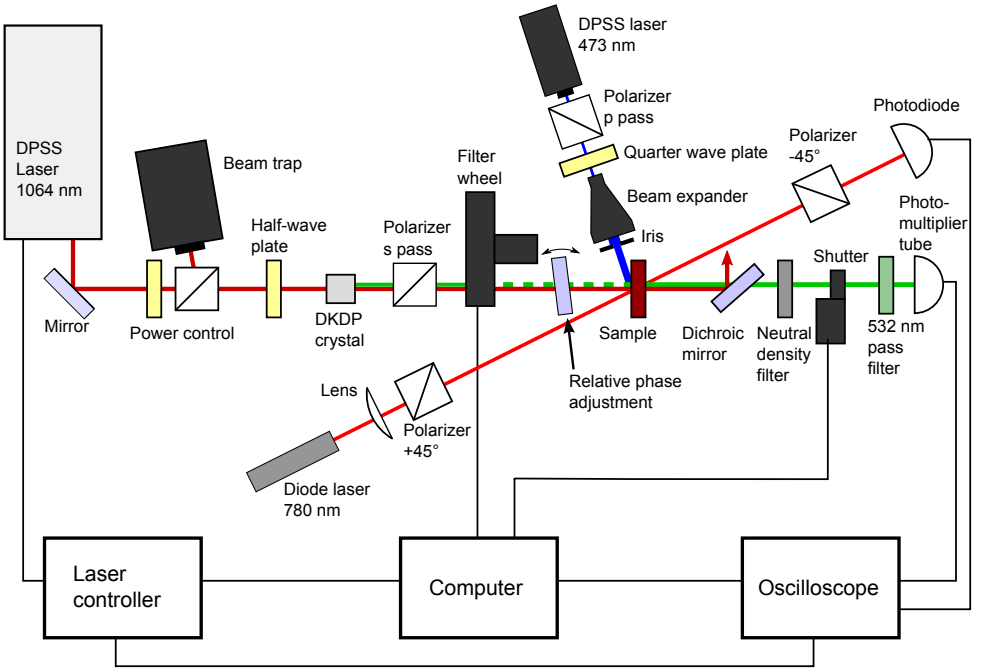

Figure 4.9: Schematic representation of the AOP setup used in **Paper I**, **Paper II** and **Paper III**.

the stability of the polar order in all-optically-poled polymers [184,185] but this process is irreversible. Longer poling time has also been shown to improve the stability of the polar order [186,187].

The experimental setup used in AOP measurements in this Thesis is shown in Fig. 4.9. The writing field at 1064 nm wavelength is produced by a diode-pumped solid-state (DPSS) laser. The laser power is adjusted using a combination of a half-wave plate and a polarizer. Another half-wave plate is used to choose the polarization direction *s* which means that the electric field points out of the plane of Fig 4.9. A deuterated potassium dihydrogen phosphate (DKDP) crystal is used to produce the weak seeding field through SHG. Collinear polarization of the two fields is verified using a polarizer that allows *s*

polarization to pass. A motorized filter wheel controls the fields that are passed to the sample. During poling, the writing and seeding fields both reach the sample and polar order is gradually formed by the mechanism previously described. Periodically, a long-pass filter is moved into the beam line by the filter wheel and the seeding beam is blocked. During this interval, the second-harmonic field produced by the sample is passed to a photomultiplier tube that records the signal. This periodic measurement is applied due to the relatively high intensity of the seeding field compared to the second-harmonic field produced by the sample. Means for continuous measurement have been developed [112,188] but the brief interruptions in the poling were found to have only a small negative effect on the second-harmonic signal that is reached, and the simple geometry allowed by the discontinuous poling was applied. In order to be sure that only the weak second-harmonic radiation at 532 nm is measured by the photomultiplier tube, the combination of a dichroic mirror, a short-pass absorptive filter and an interference filter with 10 nm band pass at 531 nm wavelength are placed in front of the photomultiplier tube. Neutral density filters are used to attenuate the second-harmonic signal to the linear range of the photomultiplier tube.

Two additional beam lines are present in the poling setup. First, a low-intensity birefringence probe beam is produced by a diode laser and weakly focused to the spot of the poling beams. Before the sample, this beam passes through a polarizer set at +45° angle with respect to *s* polarization of the poling beams. After the sample, the beam passes through another polarizer, which is set to -45°, before reaching a photodiode where its intensity is read. In the absence of a birefringent sample, no light is passed to the photodiode as the beam would need to travel through two crossed polarizers. However, birefringence of the sample rotates the polarization of the beam and the intensity passed through the second polarizer becomes [189]

$$I = I_0 \sin^2\left(\frac{\pi\,|\Delta n|\,l}{\lambda}\right), \tag{4.3}$$

where I_0 is the intensity passing the second polarizer when it has been set to +45°, *i.e.* to the same direction with respect to the first polarizer. Here $\Delta n = n_e - n_o$ is the difference of the refractive index between the extraordinary and ordinary directions. These directions are fixed by the poling beam polarization. Finally, l is the sample thickness and λ is the wavelength of the probe beam. The second additional beam line is used to erase the molecular arrangement as shown in Fig. 4.7(c) → (d) → (a). A polarizer and a quarter-wave plate are used to produre a circularly-polarized beam, which is expanded to a much larger diameter compared to the poling beam size. A top-hat profile is cut from the erasing beam and it is guided to the sample where it fully covers the poling beam area whenever applied.

All-optical poling is highly sensitive to the relative intensity between the writing and seeding fields [26]. Therefore, in **Paper II** and in **Paper III**, this ratio was carefully optimized before performing the final measurements. The reason for this sensitivity stems from the fact that, for the most efficient polar selectivity in the molecular excitation, the probability of single-photon absorption from the seeding field and two-photon absorption from the writing field should be equal. In the two-level molecule approximation, this requirement gives the equation [26]

$$\left|\frac{E_{2\omega}}{E_{\omega}^2}\right| = \frac{\Delta\mu}{2\sqrt{3}\hbar\omega}, \tag{4.4}$$

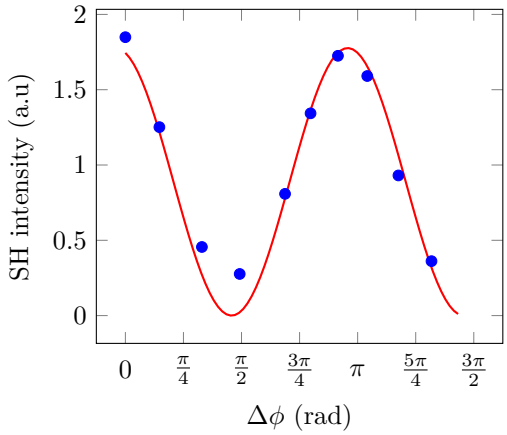

Figure 4.10: Effect of phase difference between the writing and seeding field ($\Delta\phi$) on the measured second-harmonic signal from an all-optically-poled thin polymer film. Experimental values are marked with circles and theoretical fit with a solid line.

where $E_{2\omega}$ and E_{ω} are the amplitudes of the seeding and writing fields, respectively, and $\Delta\mu$ is the difference between the dipole moments of the ground and excited states. For DR1, this equation yields the optimum ratio of $\sim 0.9 \times 10^{-10}$ m V^{-1} [26]. The ratios calculated from experimental parameters for optimized second-harmonic response in **Paper II** ($\sim 0.8 - 1.1 \times 10^{-10}$ m V^{-1}) and **Paper III** ($\sim 1.3 \times 10^{-10}$ m V^{-1}) agree well with the theoretical value even though the chromophores in **Paper II** are notably different azobenzenes compared to DR1.

In addition to relative intensity, for thin samples, the relative phase between the writing and seeding fields has a large effect on the achieved second-harmonic response. This effect is evident from Eq. (2.50). In the experiments in **Paper II** and **Paper III**, the phase difference $\Delta\phi$ was controlled by rotating a 5 mm thick BK7 glass slab that was placed right before the sample. Using the definition $\Delta\phi = 2\phi_1 - \phi_2$ The additional phase difference due to travel through the slab is

$$\Delta\phi = (2k_1 - k_2)\,(l(\theta) - l_0)\,, \tag{4.5}$$

where k_1 and k_2 are the magnitudes of the wave vectors for the writing and seeding fields, respectively, l is the length the fields travel in the slab when it is at the angle θ, and l_0 is the thickness of the slab. With some geometrical considerations, application of Snell's law and approximating for small angles θ, we get

$$\Delta\phi = \frac{\pi\Delta n l_0 \theta^2}{\lambda_{2\omega} n_{2\omega}^2}, \tag{4.6}$$

where $\Delta n = n_{\omega} - n_{2\omega}$ is the difference between the refractive indices for the writing and seeding fields in the glass and $\lambda_{2\omega}$ is the wavelength of the seeding field. Based on Eq. (2.50), for a thin sample, the measured second-harmonic signal should show the dependence $I_{SH} \propto 1 + \cos(2\Delta\phi)$. The phase control was tested with a 140 nm thick sample of DR1 side-chain polymer (Fig. 4.10). The BK7 glass slab was rotated stepwise between one and nine degrees and the the additional phase shift was calculated from Eq. (4.6) using $n_{\omega} = 1.5066$ and $n_{2\omega} = 1.5195$ obtained from Ref. [190]. At each phase difference,

the sample was poled for ten minutes and the final value of the second-harmonic signal is shown in Fig. 4.10. In order to compare to the theoretical behaviour, the function $a(1+\cos(2\Delta\phi+b))$ was fitted to the measurement points. Here parameter a takes into account the arbitrary scale of the signal and parameter b the unknown phase difference between the fields when they reach the glass slab. As seen in Fig. 4.10, the fit with only these two free parameters describes the experimental findings well. Based on this agreement with theory, it was concluded that optimization of the phase difference is indeed required to get reliable results when thin films are poled by AOP. The optimization routine was set so that four measurements are run at different angles of the glass slab. The chosen angles were 0, 4°, 5°30′ and 6° 50′ which yield $\Delta\phi = 0$, $\frac{\pi}{4}$, $\frac{\pi}{2}$ and $\frac{3\pi}{4}$. With these choices, in the worst possible case that the phase difference before entering the glass slab is $\frac{\pi}{8}$, the highest value that will be measured is $\frac{1+\sqrt{2}}{2} \approx 0.85 = 85\,\%$ of the maximum signal. Therefore, this process removes most of the ambiguity caused by the unknown absolute phase difference without increasing the needed number of AOP measurements to an impractical level.

It should be noted that the phase optimization described above was not performed in **Paper I**. This is due to the fact that the theoretically expected phase behaviour seen in Fig. 4.10 was not found with the light source used in **Paper I**. Although the expected periodic change according to $\cos(2\Delta\phi)$ was evident, the contrast was far lower than seen Fig. 4.10. The reason for this deviation was not fully confirmed but the probable causes are the less-than-optimal coherence properties of the Q-switched laser used in these measurements. Spatially multimode beam profile and difficulties in differentiating interference patterns with this light source support this conclusion. As the effect of phase difference was found to be small, the optimization procedure was deemed unnecessary. The experiments in **Paper II** and **Paper III** were run using a mode-locked laser, which is expected to have much better coherence properties and as seen in Fig. 4.10, the expected behaviour was found when this light source was used.

In order to determine the second-order susceptibility, a reference measurement was run for **Paper I** and **Paper III**. The reference signal is determined by placing a y-cut quartz wedge in the place of the sample. The geometry of the reference measurement is shown in Fig. 4.11(a). The quartz wedge is moved in z-direction which changes the interaction length of the fundamental field E_ω in the material. As a result, sinusoidal variation in the second-harmonic field $E_{2\omega}$ is seen as described by Eq. (2.40) (Fig. 4.11(b)). Based on this equation, a theoretical fit of the form $I_{SH} \propto a\sin^2(\frac{\Delta kL}{2}+b)$ has been fitted to the data. Parameter a takes into account the arbitrary scale of the second-harmonic intensity and parameter b the unknown exact thickness of the wedge at zero position. The third free parameter is Δk for which the fitting yields $-1.537\times10^5\,\mathrm{m}^{-1}$. This value is in excellent agreement with $-1.512\times10^5\,\mathrm{m}^{-1}$ calculated using Eq. (2.41) for SHG with 1064 nm fundamental wavelength. The refractive indices $n_1 = 1.5341$ and $n_2 = 1.5469$ from Ref. [191] were used for quartz at 1064 nm and 532 nm wavelengths, respectively. While the period of the oscillation matches the theoretically expected, the lowest recorded values in Fig. 4.11(b) are higher than zero. This is due to fact that the beam size in the measurements is in the mm range and therefore, the whole beam does not interact with exactly the same thickness of quartz. This small discrepancy was ignored and the peak values found with the reference method were used as $I_{2,r}$ when Eq. (2.53) was used to determine the effective susceptibilities of the all-optically-poled samples. The value $\chi_{xxx,r} = 0.6\,\mathrm{pm\,V}^{-1}$ for quartz[12] was used based on the reference measurement geometry.

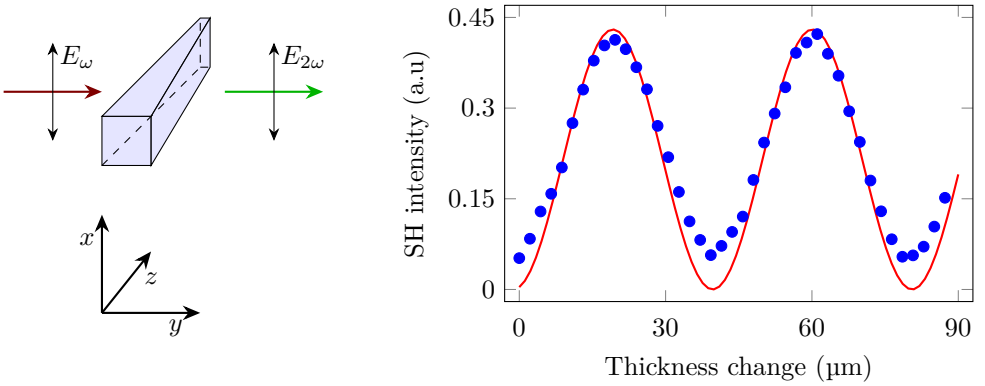

Figure 4.11: (a) Geometry of the reference measurement with a quartz wedge. (b) Reference measurement recorded for **Paper I**. Experimental values are marked with circles and theoretical fit with a solid line.

Several guest–host polymers [192,193] and particularly covalent side-chain polymers [184,186,194] have been studied in the search for efficient second-order nonlinear response by AOP. However, carefully chosen chromophore–polymer interactions for supramolecular polymer systems have remained rather unexplored. The right choice of polymer host has been shown to lead to a large increase in the electro-optic coefficient caused by electric-field poling [195]. Although part of this effect was attributed to resonance enhancement and local-field effects, most of the benefit was due to specific chromophore–polymer interactions, namely hydrogen bonding. These interactions mitigate the effects of chromophore–chromophore interactions, which eventually lead to aggregation and diminished second-order nonlinear response. Hydrogen-bonded guest–host polymers have been studied for photoinduced birefringence [14] and surface-relief gratings [15,196]. In these studies, the photocontrolled properties have been made more efficient by increased chromophore content up to high values of doping. These findings provide the starting point for **Paper I**, where a hydrogen-bonded supramolecular polymer is studied using AOP.

The supramolecular polymer system in **Paper I** is formed by hydrogen bonding between DR1 and poly(4-vinylpyridine) (P4VP) shown in Fig. 4.12(a). The concentration of DR1 was varied from 13 to 59 weight % and birefringence and second-order susceptibility were determined for each composition. All-optical poling was performed until the measured response was close to saturation and the final value was used for each composition. The main results of **Paper I** are shown in Fig. 4.12. The conclusions that can be made of these two simple figures are many: First, the hydrogen bonding clearly mitigates the effect of aggregation when birefringence caused by AOP is considered. In a simple guest–host system, already 20 wt.% of DR1 causes severe problems and lowered birefringence [14], while only saturation of the increase in birefringence is seen here even at 59 wt.%. Second, the level of birefringence reached is only slightly lower than that found in an experiment especially designed for birefringence [14]. Finally and most importantly, the second-order susceptibility shows a clear maximum at 23 wt.% chromophore concentration and then starts to decline. The sensitivity of dipolar chromophores to chromophore–chromophore interactions is well known, and causes this decline after 23 wt.%. However, the fact that a large difference is seen in the limiting concentrations for birefringence and for

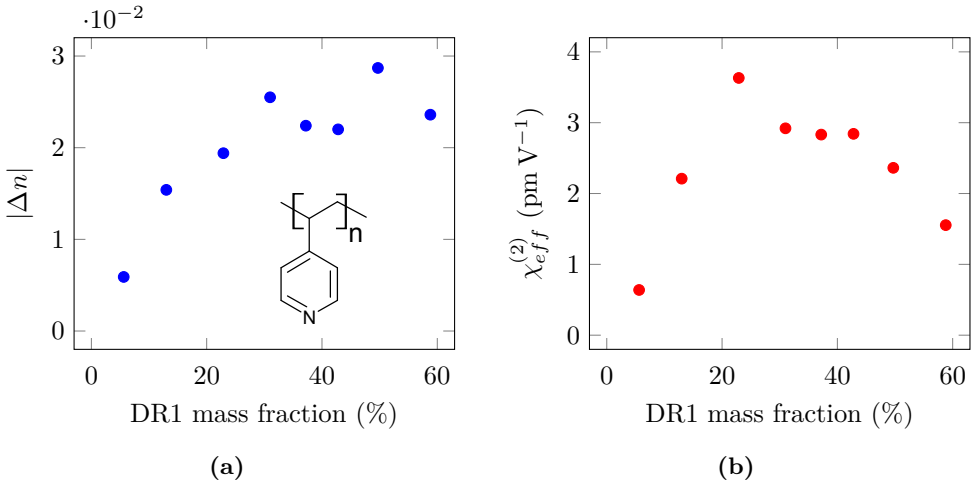

Figure 4.12: Main results of **Paper I**. (a) The dependence of birefringence and (b) second-order susceptibility on the mass fraction of DR1 azobenzene chromophore in a polymer matrix (P4VP, inset in (a)) that forms hydrogen bonds with the chromophore.

second-order susceptibility is unique for this study. Both measurable quantities are caused by a single process, which implies that there is no reason at all to be concerned about the comparability of the measurements. For the feasibility of this type of supramolecular polymers for NLO applications, the conclusion is unfortunate: although hydrogen bonding can prevent large-scale aggregation up to high chromophore concentrations, the sensitivity of second-order effects to chromophore–chromophore interactions is too high to be fought by the chromophore–polymer bonding at least in this system.

Among the new interest in the halogen bond [113], it has been applied also to photoresponsive supramolecular polymers. It has been shown that a halogen-bonded side-chain azobenzene polymer surpasses the analogous hydrogen-bonded system in the performance of surface-relief-grating inscription [197]. This finding triggered the study published in **Paper II**, where supramolecular polymers formed by hydrogen bonding (Azo-H) or halogen bonding (Azo-Br and Azo-I) between azobenzene chromophores and P4VP polymer are compared. The naming and chemical structures of the chromophores are shown in Fig. 4.13(c). A second polymer, polystyrene (PS) is used as a reference host with each chromophore in order to compare the different bonding schemes to the case where the chromophore–polymer interactions are weak. The main results of this study are shown in Figs. 4.13(a) and 4.13(b), where the evolution of second-harmonic signal during AOP for each chromophore–polymer system is drawn. The conclusions that can be made from these results are again many: First, each chromophore shows higher NLO response when embedded in P4VP, which forms specific bonds with the chromophore. Second, the halogen-bond-forming chromophores Azo-I and Azo-Br exhibit clearly higher nonlinearity compared to the hydrogen-bond-forming Azo-H. Third, among the halogen-bond formers, Azo-I reaches notably higher level of the NLO response compared to Azo-Br. This behaviour should be seen in the light that the halogen bond between Azo-I and P4VP is stronger than that between Azo-Br and P4VP. Finally, as clear differences remain between the chromophores when embedded in PS, this system cannot be considered as one without any chromophore–polymer interactions. Instead, notable interactions are present particularly between the halogen-bond formers and PS. This is attributed to bonding between the halogen atoms

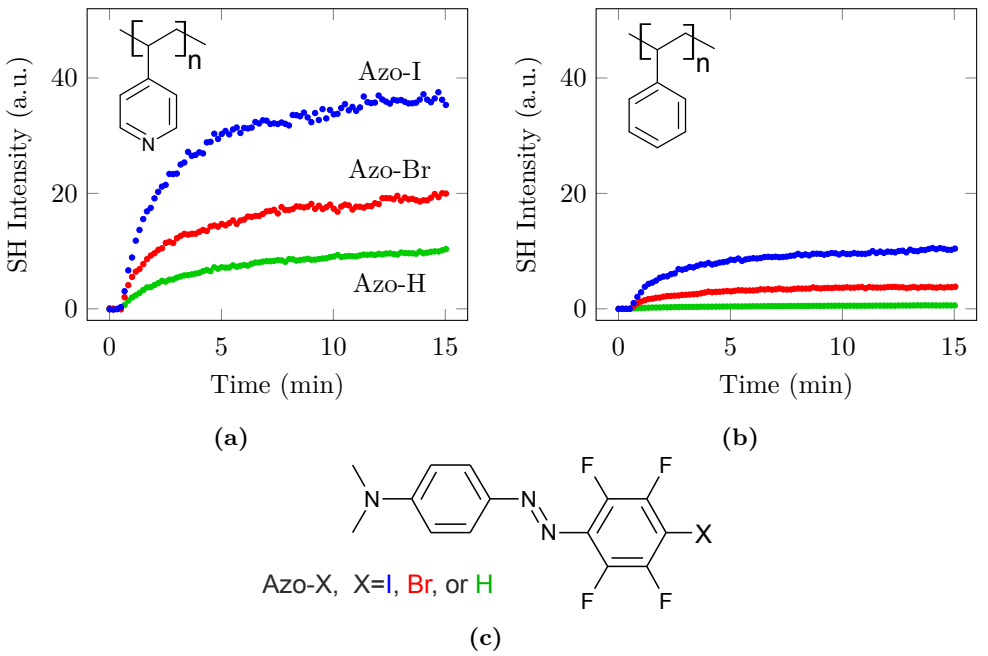

Figure 4.13: Main results of **Paper II**. The evolution of second-harmonic signal during AOP in (a) P4VP and (b) PS host polymer. Results for Azo-I are in blue, Azo-Br in red and Azo-H in green. The chemical structures of the polymers are shown in the insets. (c) The chemical structures of the chromophores.

and the π-electrons of the benzene ring in PS. Nevertheless, as confirmed by numerical modelling in **Paper II**, this interaction is weaker than those found in P4VP and the benefits of supramolecular interactions for the NLO response are highlighted by these results.

As discussed in Section 3.1, the intermolecular interactions can affect the second-order polarizability of nonlinear chromophores. Therefore, to fully understand the results in Fig. 4.13, possible changes in the properties on the molecular level should be taken into account. Results on halogen-bond-forming stilbenes[198] and numerical modelling in **Paper II** hint that the changes due to halogen bonding are far smaller than would be required to explain the results for AOP. Nevertheless, in continuation to **Paper II**, hyper-Rayleigh scattering experiments were performed on the Azo-X chromophores in order to confirm this. Two solvents were used: (1) chloroform that does not have a halogen-bond acceptor present and (2) dimethylformamide (DMF) that has a halogen-bond acceptor in the form of free electron pairs of oxygen. Solutions of each Azo-X chromophore with 10 µM concentration were prepared in these solvents. The experiments were performed using 800 nm fundamental wavelength, which yields 400 nm for the second-harmonic. At the 10 µM concentration, the absorbance at 400 nm through the applied 5 mm wide cuvette was determined to be < 0.1. The approximately 2.5 mm travel inside the cuvette thus yields at most a 10 % correction to the signal due to absorbance. As this correction is small and similar for each chromophore, it can be safely neglected. In the hyper-Rayleigh experiments, the Azo-X series is completed with Azo-F that is otherwise similar to the other halogenated molecules but is not expected to form a halogen bond as the σ-hole (Section 3.1) is not readily formed to fluorine.

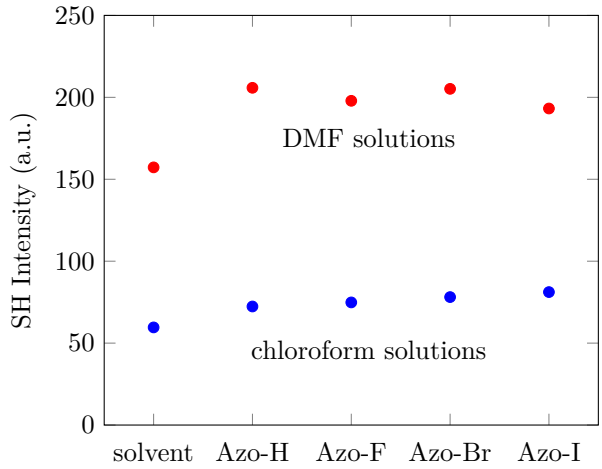

Figure 4.14: Hyper-Rayleigh scattering results for the Azo-X chromophores dissolved in chloroform and DMF.

Due to the single concentration used in these preliminary experiments, opposed to the fitting method described in Section 3.2 for hyper-Rayleigh scattering, the results should be viewed with caution and the second-order polarizabilities were not determined from this data. The results of these unpublished experiments are shown in Fig. 4.14. The first data point is for the pure solvent and the following as labelled for the Azo-X chromophores in 10 µM solution. The signal from pure DMF is approximately three times as high as that from chloroform. Still, it is evident that the second-harmonic signal from the chromophores is notably higher when dissolved in DMF. This result is as expected due to the increased polarity of the solvent when moving from chloroform to DMF. In chloroform, no bonding is expected and thus any differences between the molecules should be mostly inherent to the properties of the free molecules. Little difference in the second-harmonic signal is seen from molecule to molecule. The key result in Fig. 4.14 is that also in DMF, the differences between the molecules are small and close to the level of experimental uncertainties. Therefore, these preliminary results strongly support the conclusions made in **Paper II** that the differences between the solid materials are mostly due to the effect of the specific noncovalent interactions on the possibility to realize the desired molecular order. Dynamic infrared spectroscopy has also been used to study the photo-orientation of similar supramolecular polymers [199]. The conclusion was that halogen bonding promotes the orientation of the azobenzene and the support polymer leading to higher order when compared to hydrogen bonding.

Although efforts have been made to create molecular glasses with high NLO response, only a single report exists on AOP of a non-polymeric organic material [200]. Therefore, the newly available combination of the DR1 chromophore, well-suited for AOP and mexylaminotriazine with extremely good glass-forming properties is a promising starting point, which was studied in **Paper III**. The key results of this study are shown in Fig. 4.15. First, the evolution of the second-harmonic signal during AOP and the decay of the response were studied (Fig. 4.15(a)). The molecular glass was compared to two well-known DR1 side-chain polymers: a homopolymer with very high, 85 %, chromophore content and a copolymer with 47 % chromophore content. The latter is close to the value of 50 % found in the molecular glass. Based on the thickness-normalized second-harmonic

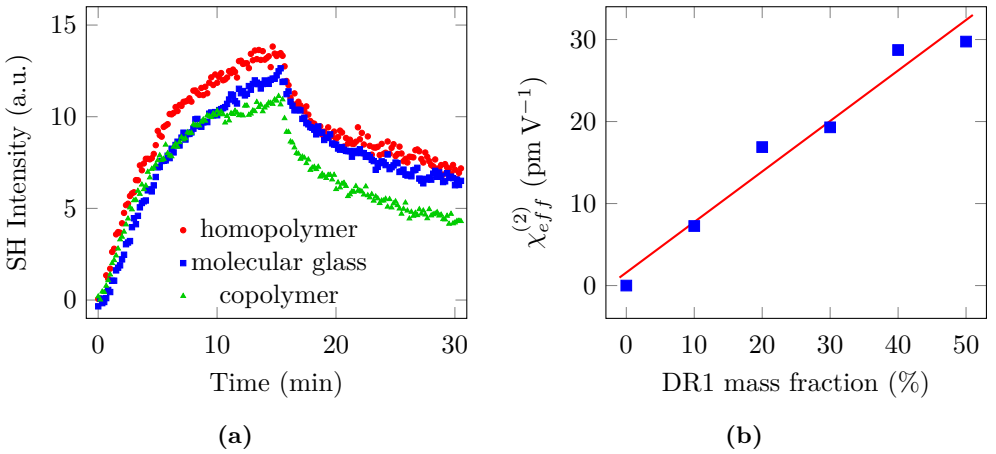

Figure 4.15: Main results of **Paper III**. (a) The evolution of second-harmonic signal during AOP in the studied molecular glass and reference polymers. Poling is stopped at 15 minutes and thermal decay is followed until 30 minutes. (b) Second-order susceptibility of molecular glass mixtures versus DR1 mass fraction. Experimental values are marked with squares and a linear fit with a solid line.

signals in Fig. 4.15(a), the molecular glass has almost equal dynamics and level of nonlinearity compared to the polymers. Furthermore, the DR1 content of the molecular glass was lowered by mixing it with another mexylaminotriazine with otherwise similar properties but no absorption in the visible range. The purpose here was to find out at which chromophore content the dipolar interactions start to limit the NLO response in the molecular glass. Interestingly, as shown in Fig. 4.15(b), almost steady increase was seen up to the 50 % content in the pure DR1-functionalized glass. Therefore, compared to the hydrogen-bonded supramolecular system in Fig. 4.12(b), the molecular glass is able to resist the harmful effects of chromophore aggregation up to a much higher concentration. Even comparison to a side-chain DR1 polymer is in favour of the molecular glass, as the highest nonlinearity has been found at 30–40 % chromophore content in the polymer [201].

4.3 Photoswitching in crystals and liquid crystals

A large number of organic crystals with good NLO properties has been developed (Section 3.3). However, reversible control of the NLO response in crystals has proven difficult [202]. The first reports on reversible modification of the NLO response by light in a bulk crystal are less than 20 years old [203,204]. In these reports, the switching of SHG was caused by photochromic molecular changes: due to photoinitiated intermolecular proton transfer, the molecular properties, most importantly the second-order polarizability, are changed without breaking the crystalline order. Although fully reversible and nearly bistable switching was reached, the recorded change in SHG was less than 60 %. Redox-driven switching in a Langmuir–Blodgett film has also been demonstrated but only a few switching cycles were possible until irreversible changes were seen [205]. Much of recent work has focused on organic–inorganic hybrid materials, where large and reversible modulation of the NLO response with temperature has been found [206–209]. In these materials, the switching is based on reversible phase transitions between a centrosymmetric and noncentrosymmetric state but the second-order susceptibility in the

"on" state remains below 1 pm V^{-1}. Recently, a metal-organic network with photoinitiated electron transfer was demonstrated [202]. Reversible change in second-order nonlinearity was shown with contrast of 3 after 35 minutes of illumination with visible light.

In contrast to solid crystals, the mobility of the constituent molecules in LCs is high. Therefore, LCs provide an excellent basis for externally induced changes in molecular orientation. A small amount of photochromic molecules, for example azobenzene derivatives, can be mixed with the mesogens to enable light-responsive behaviour. The formation of the liquid-crystalline phase will occur mostly undisturbed when the photochromic additive is rod-like resembling the other mesogens. The shape of azobenzene derivatives changes from a rod-like *trans*-isomer into a bent *cis*-isomer upon excitation with light. In an ordered LC system, this change in the small fraction of the additives is enough to break the order. Photoinduced switching between nematic and isotropic phases has been demonstrated in such a system [210]. Similar switching in microsecond time scale has been found in a system where the mesogens themselves are photoactive azobenzene derivatives [211].

As described in Section 3.3, the nematic phase as well as the isotropic phase are centrosymmetric and cannot exhibit second-order NLO effects. Therefore, a material system exhibiting photoinduced switching between a centrosymmetric and a noncentrosymmetric phase should be found to realize switching of second-order optical nonlinearity in LCs. Photoinduced switching of the spontaneous polarization in the noncentrosymmetric ferroelectric LC phase has been found using an azobenzene dopant [212,213] and even bistability of the switching has been reached using a dithienylethene dopant [214]. The switching between ferroelectric and isotropic phases that is behind the change in electric polarization should also lead to on–off switching of the second-order NLO response. Probing by SHG was not realized in the reported experiments and the mesogens were not optimized for strong nonlinearity, which might lead to very small response even in the polar ferroelectric phase. Recently, LCs with bent- or banana-shaped mesogens have gained increasing interest and electrically-induced switching to a polar structure has been probed using SHG [215]. Second-harmonic generation has been used as a probe for general studies of ferroelectric LCs and even for switching behavior in them [216], but photoinduced modification of the NLO properties is unexplored.

In **Paper IV**, the photoinitiated order–disorder transition is studied in a ferroelectric LC polymer. The material consists of three polymerizable mesogens one of which has a photoactive azobenzene core. In the sample fabrication, the monomer liquids and a small amount of photoinitiator are mixed and the mixture is injected into a LC cell. The cell consists of two glass plates covered with unidirectionally rubbed polyimide layers. Upon heating, the mixture assumes isotropic phase and during slow cooling to room temperature, the chiral smectic C phase is assumed. A DC electric field is applied across the sample perpendicular to the glass slides and the helix structure inherent to chiral smectic C is unwound and the polar ferroelectric phase is formed. Finally, the polar order is frozen by photopolymerization and the external DC field can be removed. Second-harmonic generation from 800 nm fundamental field produced with a femtosecond pulsed laser is used to probe of level of second-order nonlinearity. A schematic representation of the measurement setup is shown in Fig. 4.16. Second-harmonic generation from the sample was seen only when the sample was set to an oblique angle of incidence. This verifies that the polar axis lies perpendicular to the sample normal.

A 20 mol% portion of the mesogens are with an azobenzene core (Fig. 4.17), which is photoexcited through two-photon absoption by the 800 nm field. The molecular director

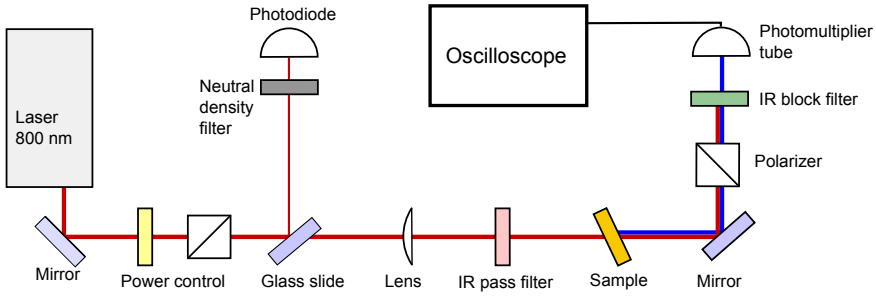

Figure 4.16: Schematic representation of the experimental setup used in **Paper IV**.

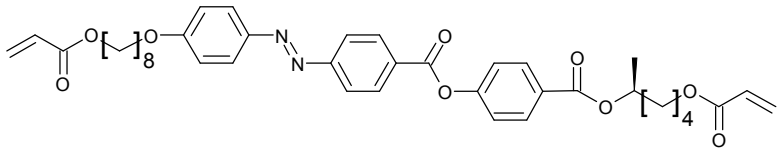

Figure 4.17: Chemical structure of the photocontrollable azobenzene mesogen of **Paper IV**.

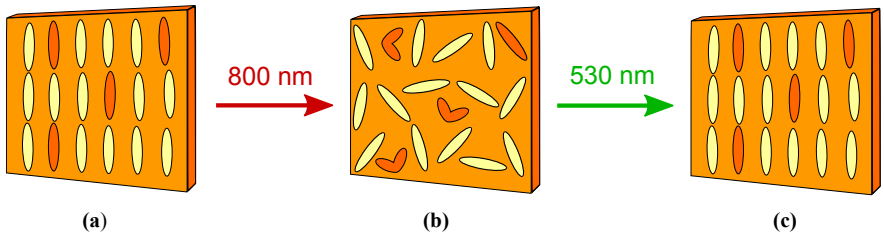

Figure 4.18: (a) → (b) Schematic representation of order–disorder transition triggered by two-photon-absorption-induced *trans–cis* isomerization using 800 nm light. (b) → (c) disorder–order transition triggered by absorption-induced *cis–trans* isomerization using 530 nm light. The azobenzene mesogens are represented with dark orange rods and the other mesogens with light yellow rods.

of the mesogens lies in the plane of the glass slides. Therefore, for a linearly-polarized 800 nm field, the photoexcitation is seen only when the azimuthal angle is chosen such that the direction of the LC director coincides with the input field polarization. When this condition is fulfilled, two-photon-absorption-induced photoexcitation followed by *trans–cis* isomerization of the azobenzene moieties occurs. This change in morphology has catastrophic effect on the liquid-crystalline order: the collective alignment with a single director direction is lost as the bent *cis*-form azobenzene does not easily fit to this configuration. This process is schematically shown in Fig. 4.18 (a) → (b). An interesting feature of the polymer-stabilized LC is that the linked polymer network tends to restore the thermodynamically stable polar arrangement. Therefore, as *cis–trans* isomerization of the azobenzene moieties removes the disturbance, the original order is returned. In **Paper IV** this process was photodriven by unpolarized light at 530 nm and is shown in Fig. 4.18(b) → (c).

The main results of **Paper IV** are shown in Fig. 4.19(a). Three cycles of 800 nm two-photon-absorption-induced order–disorder transitions followed by 530 nm single-photon-absorptio-induced disorder–order transitions are shown. The SHG produced

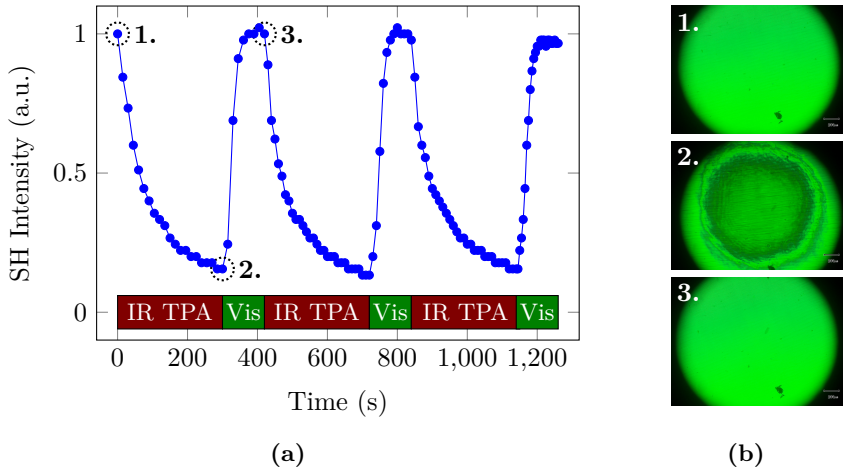

Figure 4.19: Main results of **Paper IV**. (a) The evolution of second-harmonic signal during cyclic irradiation with 800 nm light giving rise to two-photon-absorption-induced *trans–cis* isomerization (IR TPA) and during irradiation with 530 nm light causing absorption-induced *cis–trans* isomerization (Vis). (b) Polarized-optical microscope images taken at the ordered and disordered states. At point 2., reduced order is seen in the microscope image in the area of the 800 nm beam.

by the sample is decreased to about 10 % of the original value during the five-minute irradiation with 800 nm light. The original level of second-harmonic signal is fully restored during two-minute irradiation with 530 nm light. Note that in these experiments, the femtosecond-pulsed 800 nm field has a dual purpose: it is the fundamental field for SHG and the trigger for the photoisomerization. These functionalities could be easily decoupled by using another light source for probing the second-order nonlinearity. In Fig. 4.19(b), polarized-optical microscope images of the sample are also shown. These images were taken by placing the sample between two crossed polarizers with the LC director at 45° angle with respect to the polarizer transmission directions. This configuration allows the examination of the level of birefringence in different parts of the sample. In the ordered state, birefringence is expected to be higher than in the disordered state (See Fig. 4.6 and related discussion). Therefore, the polarized microscope images provide a confirmation to the origin of the changes in second-harmonic signal: at the low-SHG state, reduced birefringence is seen in the area where the 800 nm beam hits the sample. The original image is fully restored after illumination with 530 nm which restores the original order and the second-harmonic signal. The observed behaviour in Fig. 4.19(a) is neatly explained by the reversible order–disorder mechanism and the on–off contrast of SHG is as high as 10. Extended exposure with 800 nm light leads to the contrast of 20. Based on these results, the studied concept provides a versatile platform for solid materials with photocontrollable NLO response.

5 Conclusions and outlook

In this Thesis, the nonlinear optical response of supramolecular organic materials was studied using second-harmonic generation. The common feature of each part was that the nonlinear response is controlled through photoisomerization of azobenzene molecules followed by large-scale molecular rearrangement. The main method applied was all-optical poling where a dual-frequency optical field introduces bulk-level polar order due to selective excitation and molecular reorientation.

In **Paper I**, a hydrogen-bonded guest–host polymer was studied using all-optical poling. It was shown that hydrogen bonding between pyridine and hydroxyl moieties is not able to resist dipole–dipole interactions between push–pull-type azobenzenes when the chromophore loading becomes high. This result was seen despite the fact that the simultaneously probed birefringence was not greatly limited by aggregation. The result highlights the particular sensitivity of second-order nonlinear response to the spontaneous formation of centrosymmetric pairs of dipolar chromophores. The results of **Paper I** serve the closing of one line of research: the applied material system is not feasible for further study of second-order nonlinearity. Nevertheless, the results provided valuable information on the different behaviour of the two phenomena that rely on different symmetry properties of the structure.

The work on supramolecular polymers was continued in **Paper II** by the application of halogen-bonded guest–host system. It was shown that halogen bonding clearly supersedes hydrogen bonding when strong nonlinear optical response is sought for. This difference cannot be explained by changes in the molecular second-order polarizability. Instead, it was attributed to the directional nature of halogen bonding, which is by some mechanism beneficial to the arrangement of the molecules in a nonsymmetric fashion without the downsides of aggregation. A possible mechanism is that the directional bond more easily converts the orientation change of the azobenzene chromophore into a change in the orientation of the support polymer. Therefore, the entire system instead of only the chromophores assumes the new arrangement. One would assume that this mechanism leads to better stability of the molecular orientation. However, the dynamics of the halogen-bonded systems in **Paper II** are essentially equal to the hydrogen-bonded system. Still, the level of response found in the halogen-bonded system is clearly superior and new questions for further study arise. Will these improved properties hold for chromophores with higher second-order polarizability? Can the chromophore content be increased from 5–10 mol.% without adverse aggregation effects? Increase from 5 to 10 mol% only highlighted the good properties of strong halogen bonding in **Paper II**. Will stronger halogen bonding using, for example, the electron-withdrawing properties of alkynes further improve the halogen-bonded system from these first findings?

The possibility to replace the polymer network as a support structure by an amorphous material consisting of small molecules was also studied. In **Paper III**, a hydrogen-bond-forming molecular glass was shown to reach a nonlinear optical response that is comparable to well-known polymers intensively studied previously in the field of organic nonlinear materials. It was found that up to at least 50 wt.% chromophore concentration, increasing trend in the bulk second-order nonlinearity is seen. This leads to a clear point for further study: will this system resist the dipolar interactions of nonlinear chromophores with even higher molecular nonlinearity? Synthesis of new mexylaminotriazine derivatives and change in methodology is required for this as most nonlinear chromophores do not share the efficient photoisomerization cycle of push–pull azobenzene that is required for all-optical poling.

Finally, a novel ferroelectric liquid-crystalline polymer was studied for reversible on–off switching of the nonlinear optical response. It was shown in **Paper IV** that two-photon-absorption-induced photoisomerization is able to break the polar arrangement inherent to the applied material and reduce the second-harmonic generation by a factor of 20. Due to the restoring forces of the crosslinked polymer network, light-triggered back-isomerization fully restored the original level of response. The results in **Paper IV** were rather a proof-of-principle as the material system was not optimized for nonlinear response. The limits of the studied switching scheme should be addressed in future work. For high second-order nonlinear response, the mesogens used here should be replaced with ones with strong push–pull character. The stability of the disordered state is another concern: the *cis*-isomer relaxes thermally to *trans* in the timescale of tens of minutes and the ordered state is spontaneously regained. However, as the *cis* lifetime of azobenzenes can be made very long by suitable substitution, this is not a fundamental problem. Another possible strategy for stable switching is to replace the azobenzene trigger with a bistable one such as diarylethene. Furthermore, changes in the relative amounts of the constituent molecules allows control of the rigidity of the polymer network providing another approach for optimized dynamics.

Based on the view gained in course of these studies, the most promising branch for continuation lies with the halogen-bonded supramolecular polymers. To this point, they have shown favourable performance in any photoinitiated property that was put under the scope. Importantly, the point of comparison here are the hydrogen-bonded polymers which are already a notable step forward from guest–host systems with no designed interactions. Therefore, progress with these material may well end up with clear overtake of covalent polymers and finally established inorganic materials. More importantly, discovery of yet unknown applicable properties seems more than likely, and as a field of study, these materials have a lot to give to the curious mind. In light of molecular arrangement, which was the core of this work, the directional nature of the halogen bond may have a lot more to give: the right double functionalization at the opposite ends of the nonlinear molecule will favour head-to-tail organization and aggregation at high concentration could ultimately lead to *enhanced* second-order nonlinearity.

In conclusion, this work has led to advancements in the design of novel organic materials with high nonlinear optical response. The absolute level of nonlinearity reached with the studied materials is not yet high enough for practical applications. The value of the new information gained in this Thesis lies in the added understanding on the effects of intermolecular interactions on the nonlinear response. This information can serve to guide the design strategies when applicable materials in photonics are sought for.

Bibliography

[1] L. Zhou, A. Wanga, S.-C. Wu, J. Sun, S. Park, and T. N. Jackson, "All-organic active matrix flexible display," *Applied Physics Letters*, vol. 88, no. 8, p. 083502, 2006. [Online]. Available: http://link.aip.org/link/?APL/88/083502/1

[2] S. Reineke, F. Lindner, G. Schwartz, N. Seidler, K. Walzer, B. Lüssem, and K. Leo, "White organic light-emitting diodes with fluorescent tube efficiency," *Nature*, vol. 459, no. 7244, pp. 234–238, 2009.

[3] T. Someya, Y. Kato, S. Iba, Y. Noguchi, T. Sekitani, H. Kawaguchi, and T. Sakurai, "Integration of organic fets with organic photodiodes for a large area, flexible, and lightweight sheet image scanners," *IEEE Transactions on Electron Devices*, vol. 52, no. 11, pp. 2502–2511, 2005.

[4] J. Lee, P. Jadhav, and M. A. Baldo, "High efficiency organic multilayer photodetectors based on singlet exciton fission," *Applied Physics Letters*, vol. 95, no. 3, p. 033301, 2009. [Online]. Available: http://link.aip.org/link/?APL/95/033301/1

[5] J. Clark and G. Lanzani, "Organic photonics for communications," *Nature Photonics*, vol. 4, no. 7, pp. 438–446, 2010. [Online]. Available: http://www.nature.com/nphoton/journal/v4/n7/full/nphoton.2010.160.html

[6] Z. Sekkat and W. Knoll, *Photoreactive organic thin films*. San Diego: Academic Press, 2002.

[7] K. Viswanathan, Nirmal, D. Yu Kim, S. Bian, J. Williams, W. Liu, L. Li, L. Samuelson, J. Kumar, and S. K. Tripathy, "Surface relief structures on azo polymer films," *Journal of Materials Chemistry*, vol. 9, pp. 1941–1955, 1999. [Online]. Available: http://dx.doi.org/10.1039/A902424G

[8] T. Ikeda, J.-i. Mamiya, and Y. Yu, "Photomechanics of liquid-crystalline elastomers and other polymers," *Angewandte Chemie International Edition*, vol. 46, no. 4, pp. 506–528, 2007. [Online]. Available: http://dx.doi.org/10.1002/anie.200602372

[9] A. Natansohn and P. Rochon, "Photoinduced motions in azo-containing polymers," *Chemical Reviews*, vol. 102, no. 11, pp. 4139–4176, 2002. [Online]. Available: http://pubs.acs.org/doi/abs/10.1021/cr970155y

[10] A. Rodriguez, G. Vitrant, P. A. Chollet, and F. Kajzar, "Optical control of an integrated interferometer using a photochromic polymer," *Applied Physics Letters*, vol. 79, no. 4, pp. 461–463, 2001. [Online]. Available: http://link.aip.org/link/?APL/79/461/1

[11] A. Perschke and T. Fuhrmann, "Molecular azo glasses as grating couplers and resonators for optical devices," *Advanced Materials*, vol. 14, no. 11, pp. 841–843, 2002. [Online]. Available: http://dx.doi.org/10.1002/1521-4095(20020605)14:11<841::AID-ADMA841>3.0.CO;2-O

[12] R. W. Boyd, *Nonlinear Optics*. San Diego: Academic Press, 2008.

[13] L. R. Dalton, P. A. Sullivan, and D. H. Bale, "Electric field poled organic electro-optic materials: State of the art and future prospects," *Chemical Reviews*, vol. 110, no. 1, pp. 25–55, 2010. [Online]. Available: http://dx.doi.org/10.1021/cr9000429

[14] A. Priimagi, M. Kaivola, F. J. Rodriguez, and M. Kauranen, "Enhanced photoinduced birefringence in polymer-dye complexes: Hydrogen bonding makes a difference," *Applied Physics Letters*, vol. 90, no. 12, p. 121103, 2007. [Online]. Available: http://apl.aip.org/resource/1/applab/v90/i12/p121103_s1

[15] A. Priimagi, K. Lindfors, M. Kaivola, and P. Rochon, "Efficient surface-relief gratings in hydrogen-bonded polymer–azobenzene complexes," *ACS Applied Materials & Interfaces*, vol. 1, no. 6, pp. 1183–1189, 2009. [Online]. Available: http://pubs.acs.org/doi/abs/10.1021/am9002149

[16] J. Kerr, "A new relation between electricity and light: Dielectrified media birefringent," *Philosophical Magazine Series 4*, vol. 50, no. 332, pp. 337–348, 1875. [Online]. Available: http://www.tandfonline.com/doi/abs/10.1080/14786447508641302

[17] P. A. Franken, A. E. Hill, C. W. Peters, and G. Weinreich, "Generation of optical harmonics," *Physical Review Letters*, vol. 7, pp. 118–119, 1961. [Online]. Available: http://link.aps.org/doi/10.1103/PhysRevLett.7.118

[18] W. Kaiser and C. G. B. Garrett, "Two-photon excitation in CaF_2:Eu^{2+}," *Physical Review Letters*, vol. 7, pp. 229–231, Sep 1961. [Online]. Available: http://link.aps.org/doi/10.1103/PhysRevLett.7.229

[19] E. Hecht, *Optics*, 4th ed. San Fransisco: Addison Wesley, 2002.

[20] Y. Shen, *The principles of nonlinear optics*. New York: Wiley-Interscience, 1984, vol. 1.

[21] R. S. Jacobsen, K. N. Andersen, P. I. Borel, J. Fage-Pedersen, L. H. Frandsen, O. Hansen, M. Kristensen, A. V. Lavrinenko, G. Moulin, H. Ou, C. Peucheret, B. Zsigri, and A. Bjarklev, "Strained silicon as a new electro-optic material," *Nature*, vol. 441, no. 7090, pp. 199–202, May 2006. [Online]. Available: http://dx.doi.org/10.1038/nature04706

[22] M. Yamada, N. Nada, M. Saitoh, and K. Watanabe, "First-order quasi-phase matched LiNbO3 waveguide periodically poled by applying an external field for efficient blue second-harmonic generation," *Applied Physics Letters*, vol. 62, no. 5, pp. 435–436, 1993. [Online]. Available: http://scitation.aip.org/content/aip/journal/apl/62/5/10.1063/1.108925

[23] R. H. Stolen and H. W. K. Tom, "Self-organized phase-matched harmonic generation in optical fibers," *Optics Letters*, vol. 12, no. 8, pp. 585–587, Aug 1987. [Online]. Available: http://ol.osa.org/abstract.cfm?URI=ol-12-8-585

[24] N. B. Baranova and B. Y. Zel'dovich, "Physical effects in optical fields with nonzero average cube, $< E >^3 \neq 0$," *Journal of the Optical Society of America B: Optical Physics*, vol. 8, no. 1, pp. 27–32, 1991. [Online]. Available: http://josab.osa.org/abstract.cfm?URI=josab-8-1-27

[25] C. Fiorini, F. Charra, J. M. Nunzi, and P. Raimond, "Photoinduced non centrosymmetry in azo–dye polymers," *Nonlinear Optics*, vol. 9, pp. 339–347, 1995.

[26] C. Fiorini, F. Charra, J. M. Nunzi, and P. Raimond, "Quasi-permanent all-optical encoding of noncentrosymmetry in azo-dye polymers," *Journal of the Optical Society of America B: Optical Physics*, vol. 14, no. 8, pp. 1984–2003, 1997. [Online]. Available: http://www.opticsinfobase.org/josab/abstract.cfm?URI=josab-14-8-1984

[27] P. N. Prasad and D. J. Williams, *Introduction to nonlinear optical effects in molecules and polymers*. New York: Wiley, 1991.

[28] K. D. Singer, M. G. Kuzyk, and J. E. Sohn, "Second-order nonlinear-optical processes in orientationally ordered materials: relationship between molecular and macroscopic properties," *Journal of the Optical Society of America B: Optical Physics*, vol. 4, no. 6, pp. 968–976, 1987. [Online]. Available: http://josab.osa.org/abstract.cfm?URI=josab-4-6-968

[29] N. Bloembergen, R. K. Chang, S. S. Jha, and C. H. Lee, "Optical second-harmonic generation in reflection from media with inversion symmetry," *Physical Review*, vol. 174, pp. 813–822, Oct 1968. [Online]. Available: http://link.aps.org/doi/10.1103/PhysRev.174.813

[30] P. Guyot-Sionnest and Y. R. Shen, "Bulk contribution in surface second-harmonic generation," *Physical Review B*, vol. 38, pp. 7985–7989, Oct 1988. [Online]. Available: http://link.aps.org/doi/10.1103/PhysRevB.38.7985

[31] B. Koopmans, A.-M. Janner, H. T. Jonkman, G. A. Sawatzky, and F. van der Woude, "Strong bulk magnetic dipole induced second-harmonic generation from C_{60}," *Physical Review Letters*, vol. 71, pp. 3569–3572, Nov 1993. [Online]. Available: http://link.aps.org/doi/10.1103/PhysRevLett.71.3569

[32] G. J. Ashwell, G. Jefferies, D. Hamilton, D. Lynch, M. Roberts, G. Bahra, and C. R. Brown, "Strong second-harmonic generation from centrosymmetric dyes," *Nature*, vol. 375, no. 6530, pp. 385–388, Jun. 1995. [Online]. Available: http://dx.doi.org/10.1038/375385a0

[33] G. J. Ashwell, "Centrosymmetric molecules for second harmonic generation," *Advanced Materials*, vol. 8, no. 3, pp. 248–250, 1996. [Online]. Available: http://dx.doi.org/10.1002/adma.19960080314

[34] B. F. Levine, "Conjugated electron contributions to the second order hyperpolarizability of substituted benzene molecules," *The Journal of Chemical Physics*, vol. 63, no. 1, pp. 115–117, 1975. [Online]. Available: http://link.aip.org/link/?JCP/63/115/1

[35] B. F. Levine and C. G. Bethea, "Second and third order hyperpolarizabilities of organic molecules," *The Journal of Chemical Physics*, vol. 63, no. 6, pp. 2666–2682, 1975. [Online]. Available: http://link.aip.org/link/?JCP/63/2666/1

[36] J. L. Oudar, "Optical nonlinearities of conjugated molecules. Stilbene derivatives and highly polar aromatic compounds," *The Journal of Chemical Physics*, vol. 67, no. 2, pp. 446–457, 1977. [Online]. Available: http://link.aip.org/link/?JCP/67/446/1

[37] A. Dulcic and C. Sauteret, "The regularities observed in the second order hyperpolarizabilities of variously disubstituted benzenes," *The Journal of Chemical Physics*, vol. 69, no. 8, pp. 3453–3457, 1978. [Online]. Available: http://link.aip.org/link/?JCP/69/3453/1

[38] C. C. Teng and A. F. Garito, "Dispersion of the nonlinear second-order optical susceptibility of organic systems," *Physical Review B*, vol. 28, pp. 6766–6773, Dec 1983. [Online]. Available: http://link.aps.org/doi/10.1103/PhysRevB.28.6766

[39] K. Clays and A. Persoons, "Hyper-Rayleigh scattering in solution," *Physical Review Letters*, vol. 66, pp. 2980–2983, Jun 1991. [Online]. Available: http://link.aps.org/doi/10.1103/PhysRevLett.66.2980

[40] R. L. Sutherland, *Handbook of nonlinear optics*. New York: CRC press, 2003.

[41] A. Dulcic, C. Flytzanis, C. L. Tang, D. Pepin, M. Fetizon, and Y. Hoppilliard, "Length dependence of the second-order optical nonlinearity in conjugated hydrocarbons," *The Journal of Chemical Physics*, vol. 74, no. 3, pp. 1559–1563, 1981. [Online]. Available: http://link.aip.org/link/?JCP/74/1559/1

[42] L. R. Dalton, A. W. Harper, R. Ghosn, W. H. Steier, M. Ziari, H. Fetterman, Y. Shi, R. V. Mustacich, A. K.-Y. Jen, and K. J. Shea, "Synthesis and processing of improved organic second-order nonlinear optical materials for applications in photonics," *Chemistry of Materials*, vol. 7, no. 6, pp. 1060–1081, 1995. [Online]. Available: http://pubs.acs.org/doi/abs/10.1021/cm00054a006

[43] M. Barzoukas, C. Runser, A. Fort, and M. Blanchard-Desce, "A two-state description of (hyper) polarizabilities of push-pull molecules based on a two-form model," *Chemical Physics Letters*, vol. 257, no. 5–6, pp. 531–537, 1996. [Online]. Available: http://www.sciencedirect.com/science/article/pii/0009261496005866

[44] S. R. Marder, D. N. Beratan, and L. T. Cheng, "Approaches for optimizing the first electronic hyperpolarizability of conjugated organic molecules," *Science*, vol. 252, no. 5002, pp. 103–106, 1991. [Online]. Available: http://www.sciencemag.org/content/252/5002/103.abstract

[45] C. B. Gorman and S. R. Marder, "An investigation of the interrelationships between linear and nonlinear polarizabilities and bond-length alternation in conjugated organic molecules," *Proceedings of the National Academy of Sciences of the United States of America*, vol. 90, no. 23, pp. 11 297–11 301, 1993. [Online]. Available: http://www.pnas.org/content/90/23/11297.abstract

[46] G. Bourhill, J.-L. Bredas, L.-T. Cheng, S. R. Marder, F. Meyers, J. W. Perry, and B. G. Tiemann, "Experimental demonstration of the dependence of the first hyperpolarizability of donor-acceptor-substituted polyenes on the ground-state polarization and bond length alternation," *Journal of the American Chemical Society*, vol. 116, no. 6, pp. 2619–2620, 1994. [Online]. Available: http://pubs.acs.org/doi/abs/10.1021/ja00085a052

[47] S. R. Marder, L.-T. Cheng, B. G. Tiemann, A. C. Friedli, M. Blanchard-Desce, J. W. Perry, and J. Skindhøj, "Large first hyperpolarizabilities in push-pull polyenes by tuning of the bond length alternation and aromaticity," *Science*, vol. 263, no. 5146, pp. 511–514, 1994. [Online]. Available: http://www.sciencemag.org/content/263/5146/511.abstract

[48] M. Blanchard-Desce, V. Alain, P. V. Bedworth, S. R. Marder, A. Fort, C. Runser, M. Barzoukas, S. Lebus, and R. Wortmann, "Large quadratic hyperpolarizabilities with donor-acceptor polyenes exhibiting optimum bond length alternation: Correlation between structure and hyperpolarizability," *Chemistry A European Journal*, vol. 3, no. 7, pp. 1091–1104, 1997. [Online]. Available: http://dx.doi.org/10.1002/chem.19970030717

[49] J.-M. Raimundo, P. Blanchard, N. Gallego-Planas, N. Mercier, I. Ledoux-Rak, R. Hierle, and J. Roncali, "Design and synthesis of push-pull chromophores for second-order nonlinear optics derived from rigidified thiophene-based π-conjugating spacers," *The Journal of Organic Chemistry*, vol. 67, no. 1, pp. 205–218, 2002. [Online]. Available: http://pubs.acs.org/doi/abs/10.1021/jo010713f

[50] B. Robinson, L. Dalton, A. Harper, A. Ren, F. Wang, C. Zhang, G. Todorova, M. Lee, R. Aniszfeld, S. Garner, A. Chen, W. Steier, S. Houbrecht, A. Persoons, I. Ledoux, J. Zyss, and A. Jen, "The molecular and supramolecular engineering of polymeric electro-optic materials," *Chemical Physics*, vol. 245, no. 1–3, pp. 35–50, 1999. [Online]. Available: http://www.sciencedirect.com/science/article/pii/S0301010499000798

[51] L. R. Dalton, A. W. Harper, and B. H. Robinson, "The role of London forces in defining noncentrosymmetric order of high dipole moment–high hyperpolarizability chromophores in electrically poled polymeric thin films," *Proceedings of the National Academy of Sciences of the United States of America*, vol. 94, no. 10, pp. 4842–4847, 1997. [Online]. Available: http://www.pnas.org/content/94/10/4842.abstract

[52] H. Ma, B. Chen, T. Sassa, L. R. Dalton, and A. K.-Y. Jen, "Highly efficient and thermally stable nonlinear optical dendrimer for electrooptics," *Journal of the American Chemical Society*, vol. 123, no. 5, pp. 986–987, 2001. [Online]. Available: http://dx.doi.org/10.1021/ja003407c

[53] L. R. Dalton, B. H. Robinson, A. K. Jen, W. Steier, and R. Nielsen, "Systematic development of high bandwidth, low drive voltage organic electro-optic devices and their applications," *Optical Materials*, vol. 21, no. 1–3, pp. 19–28, 2003. [Online]. Available: http://www.sciencedirect.com/science/article/pii/S0925346702001076

[54] J. Luo, M. Haller, H. Ma, S. Liu, T.-D. Kim, Y. Tian, B. Chen, S.-H. Jang, L. R. Dalton, and A. K.-Y. Jen, "Nanoscale architectural control and macromolecular engineering of nonlinear optical dendrimers and polymers for electro-optics," *The Journal of Physical Chemistry B*, vol. 108, no. 25, pp. 8523–8530, 2004. [Online]. Available: http://dx.doi.org/10.1021/jp036714o

[55] P. A. Sullivan, H. Rommel, Y. Liao, B. C. Olbricht, A. J. P. Akelaitis, K. A. Firestone, J.-W. Kang, J. Luo, J. A. Davies, D. H. Choi, B. E. Eichinger, P. J. Reid, A. Chen, A. K.-Y. Jen, B. H. Robinson, and L. R. Dalton, "Theory-guided design and synthesis of multichromophore dendrimers: An analysis of the electro-optic

effect," *Journal of the American Chemical Society*, vol. 129, no. 24, pp. 7523–7530, 2007. [Online]. Available: http://dx.doi.org/10.1021/ja068322b

[56] H. L. Rommel, , and B. H. Robinson, "Orientation of electro-optic chromophores under poling conditions: A spheroidal model," *The Journal of Physical Chemistry C*, vol. 111, no. 50, pp. 18 765–18 777, 2007. [Online]. Available: http://dx.doi.org/10.1021/jp0738006

[57] T. Verbiest, S. Houbrechts, M. Kauranen, K. Clays, and A. Persoons, "Second-order nonlinear optical materials: recent advances in chromophore design," *Journal of Materials Chemistry*, vol. 7, no. 11, pp. 2175–2189, 1997.

[58] C. R. Moylan, S. Ermer, S. M. Lovejoy, I.-H. McComb, D. S. Leung, R. Wortmann, P. Krdmer, and R. J. Twieg, "(Dicyanomethylene)pyran derivatives with C2v symmetry: An unusual class of nonlinear optical chromophores," *Journal of the American Chemical Society*, vol. 118, no. 51, pp. 12 950–12 955, 1996. [Online]. Available: http://pubs.acs.org/doi/abs/10.1021/ja962673g

[59] J. Zyss and I. Ledoux, "Nonlinear optics in multipolar media: theory and experiments," *Chemical Reviews*, vol. 94, no. 1, pp. 77–105, 1994. [Online]. Available: http://pubs.acs.org/doi/abs/10.1021/cr00025a003

[60] D. M. Burland, R. D. Miller, and C. A. Walsh, "Second-order nonlinearity in poled-polymer systems," *Chemical Reviews*, vol. 94, no. 1, pp. 31–75, 1994. [Online]. Available: http://pubs.acs.org/doi/abs/10.1021/cr00025a002

[61] C. R. Moylan, R. J. Twieg, V. Y. Lee, S. A. Swanson, K. M. Betterton, and R. D. Miller, "Nonlinear optical chromophores with large hyperpolarizabilities and enhanced thermal stabilities," *Journal of the American Chemical Society*, vol. 115, no. 26, pp. 12 599–12 600, 1993. [Online]. Available: http://pubs.acs.org/doi/abs/10.1021/ja00079a055

[62] M. Stähelin, D. Burland, and J. Rice, "Solvent dependence of the second order hyperpolarizability in p-nitroaniline," *Chemical Physics Letters*, vol. 191, no. 3–4, pp. 245–250, 1992. [Online]. Available: http://www.sciencedirect.com/science/article/pii/000926149285295L

[63] J. N. Woodford, M. A. Pauley, and C. H. Wang, "Solvent dependence of the first molecular hyperpolarizability of p-nitroaniline revisited," *Journal of Physical Chemistry A*, vol. 101, no. 11, pp. 1989–1992, 1997. [Online]. Available: http://dx.doi.org/10.1021/jp9639861

[64] F. L. Huyskens, P. L. Huyskens, and A. Persoons, "Influence of solvent-solute H-bonds of p-nitroanilines on the hyper-Rayleigh scattering in solutions. Preferential environment for non-linear optically active molecules in binary solvent mixtures," *Journal of Molecular Structure*, vol. 448, no. 2–3, pp. 161–170, 1998, horizons in Hydrogen Bond Research 1997. [Online]. Available: http://www.sciencedirect.com/science/article/pii/S0022286098003469

[65] C. G. Bethea, "Experimental technique of dc induced SHG in liquids: measurement of the nonlinearity of CH_2I_2," *Applied Optics*, vol. 14, no. 6, pp. 1447–1451, Jun 1975. [Online]. Available: http://ao.osa.org/abstract.cfm?URI=ao-14-6-1447

[66] R. W. Terhune, P. D. Maker, and C. M. Savage, "Measurements of nonlinear light scattering," *Physical Review Letters*, vol. 14, pp. 681–684, Apr 1965. [Online]. Available: http://link.aps.org/doi/10.1103/PhysRevLett.14.681

[67] G. J. T. Heesink, A. G. T. Ruiter, N. F. van Hulst, and B. Bölger, "Determination of hyperpolarizability tensor components by depolarized hyper Rayleigh scattering," *Physical Review Letters*, vol. 71, pp. 999–1002, Aug 1993. [Online]. Available: http://link.aps.org/doi/10.1103/PhysRevLett.71.999

[68] J. Campo, F. Desmet, W. Wenseleers, and E. Goovaerts, "Highly sensitive setup for tunable wavelength hyper-Rayleigh scattering with parallel detection and calibration data for various solvents," *Optics Express*, vol. 17, no. 6, pp. 4587–4604, Mar 2009. [Online]. Available: http://www.opticsexpress.org/abstract.cfm?URI=oe-17-6-4587

[69] S. Stadler, G. Bourhill, and C. Bräuchle, "Problems associated with hyper-Rayleigh scattering as a means to determine the second-order polarizability of organic chromophores," *The Journal of Physical Chemistry*, vol. 100, no. 17, pp. 6927–6934, 1996. [Online]. Available: http://dx.doi.org/10.1021/jp9535102

[70] H. P. Myers, *Introductory solid state physics*. New York: CRC Press, 1997.

[71] W. M. Haynes, ed., *CRC Handbook of Chemistry and Physics, 96th Edition*. Boca Raton, FL: CRC Press/Taylor and Francis, Internet Version 2016. [Online]. Available: http://www.hbcpnetbase.com/

[72] M. M. Choy and R. L. Byer, "Accurate second-order susceptibility measurements of visible and infrared nonlinear crystals," *Physical Review B*, vol. 14, pp. 1693–1706, Aug 1976. [Online]. Available: http://link.aps.org/doi/10.1103/PhysRevB.14.1693

[73] R. S. Weis and T. K. Gaylord, "Lithium niobate: Summary of physical properties and crystal structure," *Applied Physics A*, vol. 37, pp. 191–203, 1985. [Online]. Available: http://dx.doi.org/10.1007/BF00614817

[74] E. Wooten, K. Kissa, A. Yi-Yan, E. Murphy, D. Lafaw, P. Hallemeier, D. Maack, D. Attanasio, D. Fritz, G. McBrien, and D. Bossi, "A review of lithium niobate modulators for fiber-optic communications systems," *Selected Topics in Quantum Electronics, IEEE Journal of*, vol. 6, no. 1, pp. 69–82, Jan 2000.

[75] S. K. Kurtz and T. T. Perry, "A powder technique for the evaluation of nonlinear optical materials," *Journal of Applied Physics*, vol. 39, no. 8, pp. 3798–3813, Jul 1968.

[76] B. F. Levine, C. G. Bethea, C. D. Thurmond, R. T. Lynch, and J. L. Bernstein, "An organic crystal with an exceptionally large optical second-harmonic coefficient: 2-methyl-4-nitroaniline," *Journal of Applied Physics*, vol. 50, no. 4, pp. 2523–2527, 1979. [Online]. Available: http://link.aip.org/link/?JAP/50/2523/1

[77] S. R. Marder, J. W. Perry, and C. P. Yakymyshyn, "Organic salts with large second-order optical nonlinearities," *Chemistry of Materials*, vol. 6, no. 8, pp. 1137–1147, 1994. [Online]. Available: http://pubs.acs.org/doi/abs/10.1021/cm00044a012

[78] F. Pan, M. S. Wong, C. Bosshard, and P. Günter, "Crystal growth and characterization of the organic salt 4-N,N-dimethylamino-4'-N-methyl-stilbazolium tosylate (dast)," *Advanced Materials*, vol. 8, no. 7, pp. 592–595, 1996. [Online]. Available: http://dx.doi.org/10.1002/adma.19960080714

[79] F. Pan, G. Knopfle, C. Bosshard, S. Follonier, R. Spreiter, M. S. Wong, and P. Gunter, "Electro-optic properties of the organic salt 4-N,N-dimethylamino-4'-N'-methyl-stilbazolium tosylate," *Applied Physics Letters*, vol. 69, no. 1, pp. 13–15, 1996. [Online]. Available: http://link.aip.org/link/?APL/69/13/1

[80] R. M. Kumar, D. R. Babu, G. Ravi, and R. Jayavel, "Growth and characterization of 4-dimethylamino-N-methyl-4-stilbazolium tosylate (dast) single crystals," *Journal of Crystal Growth*, vol. 250, no. 1–2, pp. 113–117, 2003, proceedings of the Fourteenth American Conference on Crystal Growth and Epitaxy. [Online]. Available: http://www.sciencedirect.com/science/article/pii/S0022024802022364

[81] Z. Yang, S. Aravazhi, A. Schneider, P. Seiler, M. Jazbinsek, and P. Günter, "Synthesis and crystal growth of stilbazolium derivatives for second-order nonlinear optics," *Advanced Functional Materials*, vol. 15, no. 7, pp. 1072–1076, 2005. [Online]. Available: http://dx.doi.org/10.1002/adfm.200500036

[82] O. R. Evans and W. Lin, "Crystal engineering of NLO materials based on metal-organic coordination networks," *Accounts of Chemical Research*, vol. 35, no. 7, pp. 511–522, 2002. [Online]. Available: http://pubs.acs.org/doi/abs/10.1021/ar0001012

[83] K. E. Rieckhoff and W. L. Peticolas, "Optical second-harmonic generation in crystalline amino acids," *Science*, vol. 147, no. 3658, pp. 610–611, 1965. [Online]. Available: http://www.sciencemag.org/content/147/3658/610.abstract

[84] J. J. Rodrigues Jr., L. Misoguti, F. D. Nunes, C. R. Mendonça, and S. C. Zilio, "Optical properties of L-threonine crystals," *Optical Materials*, vol. 22, no. 3, pp. 235–240, 2003. [Online]. Available: http://www.sciencedirect.com/science/article/pii/S0925346702002707

[85] U. Charoen-In, P. Ramasamy, and P. Manyum, "Unidirectional growth of organic nonlinear optical L-arginine maleate dihydrate single crystal by Sankaranarayanan–Ramasamy (SR) method and its characterization," *Journal of Crystal Growth*, vol. 318, no. 1, pp. 745–750, 2011. [Online]. Available: http://www.sciencedirect.com/science/article/pii/S0022024810009759

[86] S. Chandrasekhar and G. S. Ranganath, "Discotic liquid crystals," *Reports on Progress in Physics*, vol. 53, no. 1, p. 57, 1990. [Online]. Available: http://stacks.iop.org/0034-4885/53/i=1/a=002

[87] G. Pelzl, S. Diele, and W. Weissflog, "Banana-shaped compounds – a new field of liquid crystals," *Advanced Materials*, vol. 11, no. 9, pp. 707–724, 1999. [Online]. Available: http://dx.doi.org/10.1002/(SICI)1521-4095(199906)11:9<707::AID-ADMA707>3.0.CO;2-D

[88] S. Chandrasekhar, *Liquid Crystals*. Cambridge: Cambridge University Press, 1977.

[89] I. Khoo, "Nonlinear optics of liquid crystalline materials," *Physics Reports*, vol. 471, no. 5–6, pp. 221–267, 2009. [Online]. Available: http://www.sciencedirect.com/science/article/pii/S0370157309000271

[90] C. R. Smith, D. R. Sabatino, and T. J. Praisner, "Temperature sensing with thermochromic liquid crystals," *Experiments in Fluids*, vol. 30, pp. 190–201, 2001. [Online]. Available: http://dx.doi.org/10.1007/s003480000154

[91] P. Collings and M. Hird, *Introduction to liquid crystals chemistry and physics*. London: Taylor & Francis Ltd, 1997.

[92] D. M. Walba, *Advances in the synthesis and reactivity of solids*. London: JAI Press, 1991, vol. I, ch. Ferroeletric liquid crystals, pp. 173–235.

[93] A. N. Vtyurin, V. P. Ermaeov, B. I. Ostrovskii, and V. F. Shabanov, "Study of optical second harmonic generation in ferroelectric liquid crystal," *Physica Status Solidi B: Basic Solid State Physics*, vol. 107, no. 2, pp. 397–402, 1981. [Online]. Available: http://dx.doi.org/10.1002/pssb.2221070202

[94] N. M. Shtykov, M. I. Barnik, L. A. Beresnev, and L. M. Blinov, "A study of a ferroelectric liquid crystal using second optical harmonic generation," *Molecular Crystals and Liquid Crystals*, vol. 124, no. 1, pp. 379–390, 1985. [Online]. Available: http://www.tandfonline.com/doi/abs/10.1080/00268948508079489

[95] J. Y. Liu, M. G. Robinson, K. M. Johnson, and D. Doroski, "Second-harmonic generation in ferroelectric liquid crystals," *Optics Letters*, vol. 15, no. 5, pp. 267–269, 1990. [Online]. Available: http://ol.osa.org/abstract.cfm?URI=ol-15-5-267

[96] D. M. Walba, M. Blanca Ros, N. A. Clark, R. Shao, M. G. Robinson, J. Y. Liu, K. M. Johnson, and D. Doroski, "Design and synthesis of new ferroelectric liquid crystals. 14. an approach to the stereocontrolled synthesis of polar organic thin films for nonlinear optical applications," *Journal of the American Chemical Society*, vol. 113, no. 14, pp. 5471–5474, 1991. [Online]. Available: http://pubs.acs.org/doi/abs/10.1021/ja00014a059

[97] D. M. Walba, D. J. Dyer, T. Sierra, P. L. Cobben, R. Shao, and N. A. Clark, "Ferroelectric liquid crystals for nonlinear optics: Orientation of the disperse red 1 chromophore along the ferroelectric liquid crystal polar axis," *Journal of the American Chemical Society*, vol. 118, no. 5, pp. 1211–1212, 1996. [Online]. Available: http://pubs.acs.org/doi/abs/10.1021/ja952387p

[98] Y. Zhang, J. Martinez-Perdiguero, U. Baumeister, C. Walker, J. Etxebarria, M. Prehm, J. Ortega, C. Tschierske, M. J. O'Callaghan, A. Harant, and M. Handschy, "Laterally azo-bridged H-shaped ferroelectric dimesogens for second-order nonlinear optics: Ferroelectricity and second harmonic generation," *Journal of the American Chemical Society*, vol. 131, no. 51, pp. 18 386–18 392, 2009. [Online]. Available: http://pubs.acs.org/doi/abs/10.1021/ja9069166

[99] D. Hermann, "Second-harmonic generation in chiral liquid crystals," *Molecular Crystals and Liquid Crystals*, vol. 358, no. 1, pp. 167–183, 2001. [Online]. Available: http://www.tandfonline.com/doi/abs/10.1080/10587250108028279

[100] D. Bower, *An introduction to polymer physics*. New York: Cambridge University Press, 2002.

[101] J. Fried, *Polymer science and technology*. Upper Saddle River, NJ: Pearson Education, 2003.

[102] "IUPAC. Compendium of Chemical Terminology, 2nd ed. (the "Gold Book"). Compiled by A. D. McNaught and A. Wilkinson. Blackwell Scientific Publications, Oxford (1997). XML on-line corrected version: (2006–) created by M. Nic, J. Jirat, B. Kosata; updates compiled by A. Jenkins." [Online]. Available: http://goldbook.iupac.org

[103] K. D. Singer, M. G. Kuzyk, W. R. Holland, J. E. Sohn, S. J. Lalama, R. B. Comizzoli, H. E. Katz, and M. L. Schilling, "Electro-optic phase modulation and optical second-harmonic generation in corona-poled polymer films," *Applied Physics Letters*, vol. 53, no. 19, pp. 1800–1802, 1988. [Online]. Available: http://link.aip.org/link/?APL/53/1800/1

[104] L. M. Hayden, G. F. Sauter, F. R. Ore, P. L. Pasillas, J. M. Hoover, G. A. Lindsay, and R. A. Henry, "Second-order nonlinear optical measurements in guest-host and side-chain polymers," *Journal of Applied Physics*, vol. 68, no. 2, pp. 456–465, 1990. [Online]. Available: http://link.aip.org/link/?JAP/68/456/1

[105] J. F. Valley, J. W. Wu, S. Ermer, M. Stiller, E. S. Binkley, J. T. Kenney, G. F. Lipscomb, and R. Lytel, "Thermoplasticity and parallel-plate poling of electro-optic polyimide host thin films," *Applied Physics Letters*, vol. 60, no. 2, pp. 160–162, 1992. [Online]. Available: http://scitation.aip.org/content/aip/journal/apl/60/2/10.1063/1.107473

[106] M. Stähelin, C. A. Walsh, D. M. Burland, R. D. Miller, R. J. Twieg, and W. Volksen, "Orientational decay in poled second-order nonlinear optical guest-host polymers: Temperature dependence and effects of poling geometry," *Journal of Applied Physics*, vol. 73, no. 12, pp. 8471–8479, 1993. [Online]. Available: http://scitation.aip.org/content/aip/journal/jap/73/12/10.1063/1.353421

[107] A. W. Harper, S. Sun, L. R. Dalton, S. M. Garner, A. Chen, S. Kalluri, W. H. Steier, and B. H. Robinson, "Translating microscopic optical nonlinearity into macroscopic optical nonlinearity: the role of chromophore–chromophore electrostatic interactions," *Journal of the Optical Society of America B: Optical Physics*, vol. 15, no. 1, pp. 329–337, Jan 1998. [Online]. Available: http://josab.osa.org/abstract.cfm?URI=josab-15-1-329

[108] F. Würthner, S. Yao, T. Debaerdemaeker, and R. Wortmann, "Dimerization of merocyanine dyes. Structural and energetic characterization of dipolar dye aggregates and implications for nonlinear optical materials," *Journal of the American Chemical Society*, vol. 124, no. 32, pp. 9431–9447, 2002, pMID: 12167038. [Online]. Available: http://pubs.acs.org/doi/abs/10.1021/ja020168f

[109] A. Datta and S. K. Pati, "Dipole orientation effects on nonlinear optical properties of organic molecular aggregates," *The Journal of Chemical Physics*, vol. 118, no. 18, pp. 8420–8427, 2003. [Online]. Available: http://link.aip.org/link/?JCP/118/8420/1

[110] C. A. Walsh, D. M. Burland, V. Y. Lee, R. D. Miller, B. A. Smith, R. J. Twieg, and W. Volksen, "Orientational relaxation in electric field poled guest-host and side-chain polymers below Tg," *Macromolecules*, vol. 26, no. 14, pp. 3720–3722, 1993. [Online]. Available: http://pubs.acs.org/doi/abs/10.1021/ma00066a035

[111] S. K. Yesodha, C. K. S. Pillai, and N. Tsutsumi, "Stable polymeric materials for nonlinear optics: a review based on azobenzene systems," *Progress in Polymer Science*, vol. 29, no. 1, pp. 45–74, 2004. [Online]. Available: http://www.sciencedirect.com/science/article/pii/S0079670003000789

[112] A. Priimagi, S. Cattaneo, R. H. A. Ras, S. Valkama, O. Ikkala, and M. Kauranen, "Polymer–dye complexes: A facile method for high doping level and aggregation control of dye molecules," *Chemistry of Materials*, vol. 17, no. 23, pp. 5798–5802, 2005.

[113] G. Cavallo, P. Metrangolo, R. Milani, T. Pilati, A. Priimagi, G. Resnati, and G. Terraneo, "The halogen bond," *Chemical Reviews*, vol. 116, no. 4, pp. 2478–2601, 2016. [Online]. Available: http://dx.doi.org/10.1021/acs.chemrev.5b00484

[114] T. Clark, "σ-holes," *Wiley Interdisciplinary Reviews: Computational Molecular Science*, vol. 3, no. 1, pp. 13–20, 2013. [Online]. Available: http://dx.doi.org/10.1002/wcms.1113

[115] G. R. Desiraju, P. S. Ho, L. Kloo, A. C. Legon, R. Marquardt, P. Metrangolo, P. Politzer, G. Resnati, and K. Rissanen, "Definition of the halogen bond (IUPAC Recommendations 2013)," *Pure and Applied Chemistry*, vol. 85, no. 8, pp. 1711–1713, 2013.

[116] M. Saccone, G. Cavallo, P. Metrangolo, A. Pace, I. Pibiri, T. Pilati, G. Resnati, and G. Terraneo, "Halogen bond directionality translates tecton geometry into self-assembled architecture geometry," *CrystEngComm*, vol. 15, pp. 3102–3105, 2013. [Online]. Available: http://dx.doi.org/10.1039/C3CE40268A

[117] K. Naito and A. Miura, "Molecular design for nonpolymeric organic dye glasses with thermal stability: relations between thermodynamic parameters and amorphous properties," *The Journal of Physical Chemistry*, vol. 97, no. 23, pp. 6240–6248, 1993. [Online]. Available: http://dx.doi.org/10.1021/j100125a025

[118] Y. Shirota, "Organic materials for electronic and optoelectronic devices," *Journal of Materials Chemistry*, vol. 10, pp. 1–25, 2000. [Online]. Available: http://dx.doi.org/10.1039/A908130E

[119] I. Alig, D. Braun, R. Langendorf, H. O. Wirth, M. Voigt, and J. H. Wendorff, "Vitrigens," *Journal of Materials Chemistry*, vol. 8, pp. 847–851, 1998. [Online]. Available: http://dx.doi.org/10.1039/A706955C

[120] T. Fuhrmann, , and T. Tsutsui, "Synthesis and properties of a hole-conducting, photopatternable molecular glass," *Chemistry of Materials*, vol. 11, no. 8, pp. 2226–2232, 1999. [Online]. Available: http://dx.doi.org/10.1021/cm9901820

[121] P. Strohriegl and J. Grazulevicius, "Charge-transporting molecular glasses," *Advanced Materials*, vol. 14, no. 20, pp. 1439–1452, 2002. [Online]. Available: http://dx.doi.org/10.1002/1521-4095(20021016)14:20<1439::AID-ADMA1439>3.0.CO;2-H

[122] E. Ishow, C. Bellaïche, L. Bouteiller, K. Nakatani, and J. A. Delaire, "Versatile synthesis of small NLO-active molecules forming amorphous materials with spontaneous second-order NLO response," *Journal of the American Chemical Society*, vol. 125, no. 51, pp. 15 744–15 745, 2003, pMID: 14677955. [Online]. Available: http://dx.doi.org/10.1021/ja038207q

[123] A. Carella, R. Centore, L. Mager, A. Barsella, and A. Fort, "Crosslinkable organic glasses with quadratic nonlinear optical activity," *Organic Electronics*, vol. 8, no. 1, pp. 57–62, 2007. [Online]. Available: http://www.sciencedirect.com/science/article/pii/S1566119906001480

[124] M. J. Cho, S. K. Lee, D. H. Choi, and J.-I. Jin, "Star-shaped, nonlinear optical molecular glass bearing," *Dyes and Pigments*, vol. 77, no. 2, pp. 335–342, 2008. [Online]. Available: http://www.sciencedirect.com/science/article/pii/S0143720807001295

[125] K. Traskovskis, I. Mihailovs, A. Tokmakovs, A. Jurgis, V. Kokars, and M. Rutkis, "Triphenyl moieties as building blocks for obtaining molecular glasses with nonlinear optical activity," *Journal of Materials Chemistry*, vol. 22, pp. 11 268–11 276, 2012. [Online]. Available: http://dx.doi.org/10.1039/C2JM30861D

[126] O. Lebel, T. Maris, M.-E. Perron, E. Demers, and J. D. Wuest, "The dark side of crystal engineering: Creating glasses from small symmetric molecules that form multiple hydrogen bonds," *Journal of the American Chemical Society*, vol. 128, no. 32, pp. 10 372–10 373, 2006. [Online]. Available: http://dx.doi.org/10.1021/ja063353s

[127] J. D. Wuest and O. Lebel, "Anarchy in the solid state: structural dependence on glass-forming ability in triazine-based molecular glasses," *Tetrahedron*, vol. 65, no. 36, pp. 7393–7402, 2009. [Online]. Available: http://www.sciencedirect.com/science/article/pii/S0040402009010618

[128] A. Meunier and O. Lebel, "A glass forming module for organic molecules: Making tetraphenylporphyrin lose its crystallinity," *Organic Letters*, vol. 12, no. 9, pp. 1896–1899, 2010. [Online]. Available: http://dx.doi.org/10.1021/ol100139t

[129] R. Kirby, R. G. Sabat, J.-M. Nunzi, and O. Lebel, "Disperse and disordered: a mexylaminotriazine-substituted azobenzene derivative with superior glass and surface relief grating formation," *Journal of Materials Chemistry C*, vol. 2, pp. 841–847, 2014. [Online]. Available: http://dx.doi.org/10.1039/C3TC32034K

[130] G. R. Meredith, J. VanDusen, and D. J. Williams, "Optical and nonlinear optical characterization of molecularly doped thermotropic liquid crystalline polymers," *Macromolecules*, vol. 15, no. 5, pp. 1385–1389, 1982. [Online]. Available: http://pubs.acs.org/doi/abs/10.1021/ma00233a033

[131] J. Luo, Y.-J. Cheng, T.-D. Kim, S. Hau, S.-H. Jang, Z. Shi, X.-H. Zhou, and A. K.-Y. Jen, "Facile synthesis of highly efficient phenyltetraene-based nonlinear optical chromophores for electrooptics," *Organic Letters*, vol. 8, no. 7, pp. 1387–1390, 2006. [Online]. Available: http://pubs.acs.org/doi/abs/10.1021/ol060178b

[132] T.-D. Kim, J.-W. Kang, J. Luo, S.-H. Jang, J.-W. Ka, N. Tucker, J. B. Benedict, L. R. Dalton, T. Gray, R. M. Overney, D. H. Park, W. N. Herman, and A. K.-Y. Jen, "Ultralarge and thermally stable electro-optic activities from supramolecular self-assembled molecular glasses," *Journal of the American Chemical Society*, vol. 129, no. 3, pp. 488–489, 2007. [Online]. Available: http://dx.doi.org/10.1021/ja067970s

[133] J. A. Delaire and K. Nakatani, "Linear and nonlinear optical properties of photochromic molecules and materials," *Chemical Reviews*, vol. 100, no. 5, pp. 1817–1846, 2000. [Online]. Available: http://pubs.acs.org/doi/abs/10.1021/cr980078m

[134] J. A. Delaire, I. Fanton-Maltey, J. Chauvin, K. Nakatani, and M. Irie, "Nonlinear optical properties of diarylethenes," *Molecular Crystals and Liquid Crystals Science and Technology. Section A. Molecular Crystals and Liquid Crystals*, vol. 345, no. 1, pp. 233–238, 2000. [Online]. Available: http://dx.doi.org/10.1080/10587250008023924

[135] S. Houbrechts, K. Clays, A. Persoons, Z. Pikramenou, and J.-M. Lehn, "Hyper-rayleigh scattering investigation of nitrobenzyl pyridine model compounds

for optical modulation of the hyperpolarisability," *Chemical Physics Letters*, vol. 258, no. 3–4, pp. 485–489, 1996. [Online]. Available: http://www.sciencedirect.com/science/article/pii/0009261496006768

[136] E. Hendrickx, K. Clays, A. Persoons, C. Dehu, and J. L. Bredas, "The bacteriorhodopsin chromophore retinal and derivatives: An experimental and theoretical investigation of the second-order optical properties," *Journal of the American Chemical Society*, vol. 117, no. 12, pp. 3547–3555, 1995. [Online]. Available: http://dx.doi.org/10.1021/ja00117a024

[137] B. J. Coe, "Molecular materials possessing switchable quadratic nonlinear optical properties," *Chemistry A European Journal*, vol. 5, no. 9, pp. 2464–2471, 1999. [Online]. Available: http://dx.doi.org/10.1002/(SICI)1521-3765(19990903)5:9<2464::AID-CHEM2464>3.0.CO;2-L

[138] G. Kumar and D. Neckers, "Photochemistry of azobenzene-containing polymers," *Chemical Reviews*, vol. 89, no. 8, pp. 1915–1925, 1989. [Online]. Available: http://pubs.acs.org/doi/abs/10.1021/cr00098a012

[139] H. M. D. Bandara and S. C. Burdette, "Photoisomerization in different classes of azobenzene," *Chemical Society Reviews*, vol. 41, pp. 1809–1825, 2012. [Online]. Available: http://dx.doi.org/10.1039/C1CS15179G

[140] R. Loucif-Saibi, K. Nakatani, J. A. Delaire, M. Dumont, and Z. Sekkat, "Photoisomerization and second harmonic generation in disperse red one-doped and-functionalized poly(methyl methacrylate) films," *Chemistry of Materials*, vol. 5, no. 2, pp. 229–236, 1993. [Online]. Available: http://pubs.acs.org/doi/abs/10.1021/cm00026a014

[141] I. K. Lednev, T.-Q. Ye, R. E. Hester, and J. N. Moore, "Femtosecond time-resolved UV–visible absorption spectroscopy of trans-azobenzene in solution," *The Journal of Physical Chemistry*, vol. 100, no. 32, pp. 13 338–13 341, 1996. [Online]. Available: http://pubs.acs.org/doi/abs/10.1021/jp9610067

[142] T. Nägele, R. Hoche, W. Zinth, and J. Wachtveitl, "Femtosecond photoisomerization of cis-azobenzene," *Chemical Physics Letters*, vol. 272, no. 5–6, pp. 489–495, 1997. [Online]. Available: http://www.sciencedirect.com/science/article/B6TFN-3SHJ5V1-1V/2/d50aa1dd9a66bc74d262f4ecc10dc9c4

[143] P. Cattaneo and M. Persico, "An abinitio study of the photochemistry of azobenzene," *Physical Chemistry Chemical Physics*, vol. 1, no. 20, pp. 4739–4743, 1999. [Online]. Available: http://www.rsc.org/delivery/_ArticleLinking/DisplayArticleForFree.cfm?doi=a905055h&JournalCode=CP

[144] C. Ciminelli, G. Granucci, and M. Persico, "The photoisomerization mechanism of azobenzene: A semiclassical simulation of nonadiabatic dynamics," *Chemistry A European Journal*, vol. 10, no. 9, pp. 2327–2341, 2004. [Online]. Available: http://www3.interscience.wiley.com/journal/108070222/abstract?CRETRY=1&SRETRY=0

[145] E. M. M. Tan, S. Amirjalayer, S. Smolarek, A. Vdovin, F. Zerbetto, and W. J. Buma, "Fast photodynamics of azobenzene probed by scanning excited-state potential energy surfaces using slow spectroscopy," *Nature communications*, vol. 6, 2015.

[146] J. F. Rabek and G. W. Scott, *Photochemistry and photophysics*. Boca Raton, Florida: CRC Press, 1989, vol. 2.

[147] J. Ronayette, R. Arnaud, and J. Lemaire, "Isomérisation photosensibilisée par des colorants et photoréduction de l'azobenzène en solution. II," *Canadian Journal of Chemistry*, vol. 52, no. 10, pp. 1858–1867, 1974. [Online]. Available: http://article.pubs.nrc-cnrc.gc.ca/RPAS/rpv?hm=HInit&calyLang=eng&journal=cjc&volume=52&afpf=v74-265.pdf

[148] J. Griffiths, "II. photochemistry of azobenzene and its derivatives," *Chem. Soc. Rev.*, vol. 1, pp. 481–493, 1972. [Online]. Available: http://dx.doi.org/10.1039/CS9720100481

[149] C. M. Stuart, R. R. Frontiera, and R. A. Mathies, "Excited-state structure and dynamics of cis- and trans-azobenzene from resonance raman intensity analysis," *Journal of Physical Chemistry A*, vol. 111, no. 48, pp. 12 072–12 080, 2007. [Online]. Available: http://dx.doi.org/10.1021/jp0751460

[150] K. G. Yager and C. J. Barrett, "Novel photo-switching using azobenzene functional materials," *Journal of Photochemistry and Photobiology, A: Chemistry*, vol. 182, no. 3, pp. 250–261, 2006, proceedings of 7th AIST International Symposium on Photoreaction Control and Photofunctional Materials, 7th AIST International Symposium on Photoreaction Control and Photofunctional Materials. [Online]. Available: http://www.sciencedirect.com/science/article/B6TGY-4K18VSP-1/2/c00807901259cd303aba19c5442fe822

[151] S. Samanta, A. A. Beharry, O. Sadovski, T. M. McCormick, A. Babalhavaeji, V. Tropepe, and G. A. Woolley, "Photoswitching azo compounds in vivo with red light," *Journal of the American Chemical Society*, vol. 135, no. 26, pp. 9777–9784, 2013. [Online]. Available: http://dx.doi.org/10.1021/ja402220t

[152] C. Knie, M. Utecht, F. Zhao, H. Kulla, S. Kovalenko, A. M. Brouwer, P. Saalfrank, S. Hecht, and D. Bléger, "ortho-fluoroazobenzenes: Visible light switches with very long-lived Z isomers," *Chemistry A European Journal*, vol. 20, no. 50, pp. 16 492–16 501, 2014. [Online]. Available: http://dx.doi.org/10.1002/chem.201404649

[153] D. G. Whitten, P. D. Wildes, J. G. Pacifici, and G. I. Jr., "Solvent and substituent on the thermal isomerization of substituted azobenzenes. Flash spectroscopic study," *Journal of the American Chemical Society*, vol. 93, no. 8, pp. 2004–2008, 1971. [Online]. Available: http://dx.doi.org/10.1021/ja00737a027

[154] S. Kobayashi, H. Yokoyama, and H. Kamei, "Substituent and solvent effects on electronic absorption spectra and thermal isomerization of push-pull-substituted cis-azobenzenes," *Chemical Physics Letters*, vol. 138, no. 4, pp. 333–338, 1987. [Online]. Available: http://www.sciencedirect.com/science/article/pii/0009261487803949

[155] C. Reichardt, "Solvatochromic dyes as solvent polarity indicators," *Chemical Reviews*, vol. 94, no. 8, pp. 2319–2358, 1994. [Online]. Available: http://pubs.acs.org/doi/abs/10.1021/cr00032a005

[156] E. Rusu, D.-O. Dorohoi, and A. Airinei, "Solvatochromic effects in the absorption spectra of some azobenzene compounds," *Journal of Molecular Structure*, vol. 887, no. 1–3, pp. 216–219, 2008. [Online]. Available: http://www.sciencedirect.com/science/article/pii/S0022286008001865

[157] M. Kasha, H. R. Rawls, and M. A. El-Bayoumi, "The exciton model in molecular spectroscopy," *Pure and Applied Chemistry*, vol. 11, no. 3–4, pp. 371–392, 1965. [Online]. Available: http://www.iupac.org/publications/pac/11/3/0371/

[158] A. M. Kelley, "A multimode vibronic treatment of absorption, resonance Raman, and hyper-Rayleigh scattering of excitonically coupled molecular dimers," *The Journal of Chemical Physics*, vol. 119, no. 6, pp. 3320–3331, 2003. [Online]. Available: http://jcp.aip.org/resource/1/jcpsa6/v119/i6/p3320_s1

[159] O.-K. Song, C. H. Wang, and M. A. Pauley, "Dynamic processes of optically induced birefringence of azo compounds in amorphous polymers below Tg," *Macromolecules*, vol. 30, no. 22, pp. 6913–6919, 1997. [Online]. Available: http://dx.doi.org/10.1021/ma9701649

[160] A. Priimagi, J. Vapaavuori, F. J. Rodriguez, C. F. J. Faul, M. T. Heino, O. Ikkala, M. Kauranen, and M. Kaivola, "Hydrogen-bonded polymer–azobenzene complexes: Enhanced photoinduced birefringence with high temporal stability through interplay of intermolecular interactions," *Chemistry of Materials*, vol. 20, no. 20, pp. 6358–6363, 2008. [Online]. Available: http://pubs.acs.org/doi/abs/10.1021/cm800908m

[161] S. Yokoyama, M. aki Kakimoto, and Y. Imai, "Photochemically inducible and erasable dichroism by molecular reorientation of an azobenzene pendant unit in a polyimide Langmuir–Blodgett film," *Langmuir*, vol. 10, no. 12, pp. 4594–4598, 1994. [Online]. Available: http://dx.doi.org/10.1021/la00024a034

[162] K. E. Snell, R. Hou, E. Ishow, and F. Lagugné-Labarthet, "Enhanced rates of photoinduced molecular orientation in a series of molecular glassy thin films," *Langmuir*, vol. 31, no. 26, pp. 7296–7305, 2015. [Online]. Available: http://dx.doi.org/10.1021/acs.langmuir.5b01319

[163] C. Wang, H. Fei, Y. Qiu, Y. Yang, Z. Wei, Y. Tian, Y. Chen, and Y. Zhao, "Photoinduced birefringence and reversible optical storage in liquid-crystalline azobenzene side-chain polymers," *Applied Physics Letters*, vol. 74, no. 1, pp. 19–21, 1999. [Online]. Available: http://scitation.aip.org/content/aip/journal/apl/74/1/10.1063/1.123138

[164] P. Rochon, E. Batalla, and A. Natansohn, "Optically induced surface gratings on azoaromatic polymer films," *Applied Physics Letters*, vol. 66, no. 2, pp. 136–138, 1995. [Online]. Available: http://apl.aip.org/resource/1/applab/v66/i2/p136_s1

[165] H. Nakano, T. Takahashi, T. Kadota, and Y. Shirota, "Formation of a surface relief grating using a novel azobenzene-based photochromic amorphous molecular material," *Advanced Materials*, vol. 14, no. 16, pp. 1157–1160, 2002. [Online]. Available: http://dx.doi.org/10.1002/1521-4095(20020816)14:16<1157::AID-ADMA1157>3.0.CO;2-Z

[166] H. Nakano, T. Tanino, and Y. Shirota, "Surface relief grating formation on a single crystal of 4-(dimethylamino)azobenzene," *Applied Physics Letters*, vol. 87, no. 6, 2005. [Online]. Available: http://scitation.aip.org/content/aip/journal/apl/87/6/10.1063/1.2009065

[167] T. Ikeda, M. Nakano, Y. Yu, O. Tsutsumi, and A. Kanazawa, "Anisotropic bending and unbending behavior of azobenzene liquid-crystalline gels by light

exposure," *Advanced Materials*, vol. 15, no. 3, pp. 201–205, 2003. [Online]. Available: http://dx.doi.org/10.1002/adma.200390045

[168] H. Koshima, N. Ojima, and H. Uchimoto, "Mechanical motion of azobenzene crystals upon photoirradiation," *Journal of the American Chemical Society*, vol. 131, no. 20, pp. 6890–6891, 2009. [Online]. Available: http://dx.doi.org/10.1021/ja8098596

[169] P. Kaatz and D. P. Shelton, "Polarized hyper-Rayleigh light scattering measurements of nonlinear optical chromophores," *The Journal of Chemical Physics*, vol. 105, no. 10, pp. 3918–3929, 1996. [Online]. Available: http://scitation.aip.org/content/aip/journal/jcp/105/10/10.1063/1.472264

[170] Z. Sekkat and M. Dumont, "Photoassisted poling of azo dye doped polymeric films at room temperature," *Applied Physics B: Lasers and Optics*, vol. 54, no. 5, pp. 486–489, 1992. [Online]. Available: http://www.springerlink.com/content/l3n11132t4212763/

[171] U. Österberg and W. Margulis, "Dye laser pumped by Nd:YAG laser pulses frequency doubled in a glass optical fiber," *Optics Letters*, vol. 11, no. 8, pp. 516–518, Aug 1986. [Online]. Available: http://ol.osa.org/abstract.cfm?URI=ol-11-8-516

[172] F. Charra, F. Kajzar, J. M. Nunzi, P. Raimond, and E. Idiart, "Light-induced second-harmonic generation in azo-dye polymers," *Optics Letters*, vol. 18, no. 12, pp. 941–943, 1993. [Online]. Available: http://ol.osa.org/abstract.cfm?URI=ol-18-12-941

[173] J. Peretti, J. Biteau, J. P. Boilot, F. Chaput, V. I. Safarov, J. M. Lehn, and A. Fernandez-Acebes, "Remanent photoinduced birefringence in thin photochromic sol–gel films," *Applied Physics Letters*, vol. 74, no. 12, pp. 1657–1659, 1999. [Online]. Available: http://apl.aip.org/applab/v74/i12/p1657_s1

[174] Z. Sekkat, J. Wood, and W. Knoll, "Reorientation mechanism of azobenzenes within the trans $\longrightarrow$ cis photoisomerization," *The Journal of Physical Chemistry*, vol. 99, no. 47, pp. 17 226–17 234, 1995. [Online]. Available: http://pubs.acs.org/doi/abs/10.1021/j100047a029

[175] X. Zhong, X. Yu, Q. Li, S. Luo, Y. Chen, Y. Sui, and J. Yin, "Identification of the alignment of azobenzene molecules induced by all-optical poling in polymer film," *Optics Communications*, vol. 190, no. 1–6, pp. 333–337, 2001. [Online]. Available: http://www.sciencedirect.com/science/article/pii/S0030401801010495

[176] X. Yu, X. Zhong, Q. Li, S. Luo, Y. Chen, Y. Sui, and J. Yin, "Method of improving optical poling efficiency in polymer films," *Optics Letters*, vol. 26, no. 4, pp. 220–222, 2001. [Online]. Available: http://ol.osa.org/abstract.cfm?URI=ol-26-4-220

[177] S. Brasselet and J. Zyss, "Control of the polarization dependence of optically poled nonlinear polymer films," *Optics Letters*, vol. 22, no. 19, pp. 1464–1466, Oct 1997. [Online]. Available: http://ol.osa.org/abstract.cfm?URI=ol-22-19-1464

[178] A. C. Etilé, C. Fiorini, F. Charra, and J. M. Nunzi, "Phase-coherent control of the molecular polar order in polymers using dual-frequency interferences between circularly polarized beams," *Physical Review A*, vol. 56, no. 5, pp. 3888–3896, 1997.

[179] C. Fiorini, F. Charra, J.-M. Nunzi, I. D. W. Samuel, and J. Zyss, "Light-induced second-harmonic generation in an octupolar dye," *Optics Letters*, vol. 20, no. 24, pp. 2469–2471, Dec 1995. [Online]. Available: http://ol.osa.org/abstract.cfm?URI=ol-20-24-2469

[180] S. Brasselet and J. Zyss, "Multipolar molecules and multipolar fields: probing and controlling the tensorial nature of nonlinear molecular media," *Journal of the Optical Society of America B: Optical Physics*, vol. 15, no. 1, pp. 257–288, Jan 1998. [Online]. Available: http://josab.osa.org/abstract.cfm?URI=josab-15-1-257

[181] C. Fiorini, F. Charra, P. Raimond, A. Lorin, and J. M. Nunzi, "All-optical induction of noncentrosymmetry in a transparent nonlinear polymer rod," *Optics Letters*, vol. 22, no. 24, pp. 1846–1848, 1997. [Online]. Available: http://ol.osa.org/abstract.cfm?URI=ol-22-24-1846

[182] K. Kitaoka, J. Si, T. Mitsuyu, and K. Hirao, "Optical poling of azo-dye-doped thin films using an ultrashort pulse laser," *Applied Physics Letters*, vol. 75, no. 2, pp. 157–159, 1999. [Online]. Available: http://link.aip.org/link/?APL/75/157/1

[183] J. Si, J. Qiu, K. Kitaoka, and K. Hirao, "Photoinduced phase-matched second-harmonic generation in azodye-doped polymer films," *Journal of Applied Physics*, vol. 89, no. 4, pp. 2029–2032, 2001. [Online]. Available: http://jap.aip.org/japiau/v89/i4/p2029_s1

[184] G. Xu, J. Si, X. Liu, Q. Yang, P. Ye, Z. Li, and Y. Shen, "Permanent optical poling in polyurethane via thermal crosslinking," *Optics Communications*, vol. 153, no. 1–3, pp. 95–98, 1998. [Online]. Available: http://www.sciencedirect.com/science/article/pii/S0030401898002533

[185] A. Apostoluk, J.-M. Nunzi, V. Boucher, A. Essahlaoui, R. Seveno, H. Gundel, C. Monnereau, E. Blart, and F. Odobel, "Permanent light-induced polar orientation via all-optical poling and photothermal cross-linking in a polymer thin film," *Optics Communications*, vol. 260, no. 2, pp. 708 – 711, 2006. [Online]. Available: http://www.sciencedirect.com/science/article/pii/S0030401805012319

[186] S. Chan, J.-M. Nunzi, A. Quatela, and M. Casalboni, "Retardation of orientation relaxation of azo-dye doped amorphous polymers upon all-optical poling," *Chemical Physics Letters*, vol. 428, no. 4–6, pp. 371–375, 2006. [Online]. Available: http://www.sciencedirect.com/science/article/B6TFN-4KDJVSM-4/2/b9e8d1cbd165fd54a4bfb637d4dccaf8

[187] A. Priimagi, M. Kaivola, M. Virkki, F. J. Rodríguez, and M. Kauranen, "Suppression of chromophore aggregation in amorphous polymeric materials: Towards more efficient photoresponsive behavior," *Journal of Nonlinear Optical Physics and Materials*, vol. 19, no. 1, pp. 57–73, 2010.

[188] V. M. Churikov, M. F. Hung, and C. C. Hsu, "Real-time monitoring of all-optical poling of azo-dye polymer thin film," *Optics Letters*, vol. 25, no. 13, pp. 960–962, 2000. [Online]. Available: http://ol.osa.org/abstract.cfm?URI=ol-25-13-960

[189] T. Todorov, L. Nikolova, and N. Tomova, "Polarization holography. 1: A new high-efficiency organic material with reversible photoinduced birefringence," *Applied Optics*, vol. 23, no. 23, pp. 4309–4312, 1984. [Online]. Available: http://www.opticsinfobase.org/abstract.cfm?&id=28024

[190] M. N. Polyanskiy, "Refractive index database," adapted from SCHOTT optical glass data sheets 2015-07-22, (accessed Feb. 30 2016). [Online]. Available: http://refractiveindex.info

[191] M. N. Polyanskiy, "Refractive index database," adapted from G. Ghosh. Dispersion-equation coefficients for the refractive index and birefringence of calcite and quartz crystals, *Optical Communications*, vol. 163, pp. 95–102, 1999, (accessed Feb. 30 2016). [Online]. Available: http://refractiveindex.info

[192] J. Si, J. Qiu, J. Zhai, Y. Shen, Z. Meng, and K. Hirao, "Phase-matched second-harmonic generation in bulk azodye-doped polymers by all-optical poling," *Journal of Applied Physics*, vol. 95, no. 7, pp. 3837–3839, 2004. [Online]. Available: http://scitation.aip.org/content/aip/journal/jap/95/7/10.1063/1.1667271

[193] N. Tsutsumi and T. Shingu, "$\chi^{(2)}$ holography induced by all-optical poling," *Chemical Physics Letters*, vol. 403, no. 4–6, pp. 420–424, 2005. [Online]. Available: http://www.sciencedirect.com/science/article/pii/S0009261405000904

[194] J. Si, T. Mitsuyu, P. Ye, Y. Shen, and K. Hirao, "Optical poling and its application in optical storage of a polyimide film with high glass transition temperature," *Applied Physics Letters*, vol. 72, p. 762, 1998. [Online]. Available: http://apl.aip.org/applab/v72/i7/p762_s1

[195] M. J. Banach, M. D. Alexander, S. Caracci, and R. A. Vaia, "Enhancement of electrooptic coefficient of doped films through optimization of chromophore environment," *Chemistry of Materials*, vol. 11, no. 9, pp. 2554–2561, 1999. [Online]. Available: http://pubs.acs.org/doi/abs/10.1021/cm9902725

[196] J. Vapaavuori, V. Valtavirta, T. Alasaarela, J.-I. Mamiya, A. Priimagi, A. Shishido, and M. Kaivola, "Efficient surface structuring and photoalignment of supramolecular polymer-azobenzene complexes through rational chromophore design," *Journal of Materials Chemistry*, vol. 21, pp. 15 437–15 441, 2011. [Online]. Available: http://dx.doi.org/10.1039/C1JM12642C

[197] A. Priimagi, G. Cavallo, A. Forni, M. Gorynsztejn-Leben, M. Kaivola, P. Metrangolo, R. Milani, A. Shishido, T. Pilati, G. Resnati, and G. Terraneo, "Halogen bonding versus hydrogen bonding in driving self-assembly and performance of light-responsive supramolecular polymers," *Advanced Functional Materials*, vol. 22, no. 12, pp. 2572–2579, 2012. [Online]. Available: http://dx.doi.org/10.1002/adfm.201200135

[198] E. Cariati, A. Forni, S. Biella, P. Metrangolo, F. Meyer, G. Resnati, S. Righetto, E. Tordin, and R. Ugo, "Tuning second-order NLO responses through halogen bonding," *Chem. Commun.*, pp. 2590–2592, 2007. [Online]. Available: http://dx.doi.org/10.1039/B702724A

[199] J. Vapaavuori, I. T. S. Heikkinen, V. Dichiarante, G. Resnati, P. Metrangolo, R. G. Sabat, C. G. Bazuin, A. Priimagi, and C. Pellerin, "Photomechanical energy transfer to photopassive polymers through hydrogen and halogen bonds," *Macromolecules*, vol. 48, no. 20, pp. 7535–7542, 2015. [Online]. Available: http://dx.doi.org/10.1021/acs.macromol.5b01813

[200] N. Tsutsumi and K. Nakatani, "$\chi^{(2)}$ polarization induced in molecular glass of conjugated compound by all-optical poling," *Optics Communications*, vol. 259, no. 2, pp. 852 – 855, 2006. [Online]. Available: http://www.sciencedirect.com/science/article/pii/S0030401805009363

[201] F. Kajzar, O. Krupka, G. Pawlik, A. Mitus, and I. Rau, "Concentration variation of quadratic NLO susceptibility in PMMA-DR1 side chain polymer," *Molecular Crystals and Liquid Crystals*, vol. 522, no. 1, pp. 180–190, 2010. [Online]. Available: http://www.informaworld.com/smpp/content~db=all~content=a922642233

[202] P.-X. Li, M.-S. Wang, M.-J. Zhang, C.-S. Lin, L.-Z. Cai, S.-P. Guo, and G.-C. Guo, "Electron-transfer photochromism to switch bulk second-order nonlinear optical properties with high contrast," *Angewandte Chemie International Edition*, vol. 53, no. 43, pp. 11 529–11 531, 2014. [Online]. Available: http://dx.doi.org/10.1002/anie.201406554

[203] K. Nakatani and J. A. Delaire, "Reversible photoswitching of second-order nonlinear optical properties in an organic photochromic crystal," *Chemistry of Materials*, vol. 9, no. 12, pp. 2682–2684, 1997. [Online]. Available: http://pubs.acs.org/doi/abs/10.1021/cm970369w

[204] M. Sliwa, S. Létard, I. Malfant, M. Nierlich, P. G. Lacroix, T. Asahi, H. Masuhara, P. Yu, and K. Nakatani, "Design, synthesis, structural and nonlinear optical properties of photochromic crystals: Toward reversible molecular switches," *Chemistry of Materials*, vol. 17, no. 18, pp. 4727–4735, 2005. [Online]. Available: http://pubs.acs.org/doi/abs/10.1021/cm050929o

[205] L. Boubekeur-Lecaque, B. J. Coe, K. Clays, S. Foerier, T. Verbiest, and I. Asselberghs, "Redox-switching of nonlinear optical behavior in Langmuir–Blodgett thin films containing a ruthenium(ii) ammine complex," *Journal of the American Chemical Society*, vol. 130, no. 11, pp. 3286–3287, 2008. [Online]. Available: http://dx.doi.org/10.1021/ja711170q

[206] P. Serra-Crespo, M. A. van der Veen, E. Gobechiya, K. Houthoofd, Y. Filinchuk, C. E. A. Kirschhock, J. A. Martens, B. F. Sels, D. E. D. Vos, F. Kapteijn, and J. Gascon, "NH_2-MIL-53(Al): A high-contrast reversible solid-state nonlinear optical switch," *Journal of the American Chemical Society*, vol. 134, no. 20, pp. 8314–8317, 2012. [Online]. Available: http://dx.doi.org/10.1021/ja300655f

[207] Z. Sun, J. Luo, S. Zhang, C. Ji, L. Zhou, S. Li, F. Deng, and M. Hong, "Solid-state reversible quadratic nonlinear optical molecular switch with an exceptionally large contrast," *Advanced Materials*, vol. 25, no. 30, pp. 4159–4163, 2013. [Online]. Available: http://dx.doi.org/10.1002/adma.201301685

[208] C. Ji, Z. Sun, S. Zhang, S. Zhao, T. Chen, Y. Tang, and J. Luo, "A host-guest inclusion compound for reversible switching of quadratic nonlinear optical properties," *Chem. Commun.*, vol. 51, pp. 2298–2300, 2015. [Online]. Available: http://dx.doi.org/10.1039/C4CC08711A

[209] T. Chen, Z. Sun, S. Zhao, C. Ji, and J. Luo, "An organic-inorganic hybrid co-crystal complex as a high-performance solid-state nonlinear optical switch," *J. Mater. Chem. C*, vol. 4, pp. 266–271, 2016. [Online]. Available: http://dx.doi.org/10.1039/C5TC03278D

[210] T. Ikeda, T. Sasaki, and H. B. Kim, ""Intrinsic" response of polymer liquid crystals in photochemical phase transition," *The Journal of Physical Chemistry*, vol. 95, no. 2, pp. 509–511, 1991. [Online]. Available: http://pubs.acs.org/doi/abs/10.1021/j100155a003

[211] T. Ikeda and O. Tsutsumi, "Optical switching and image storage by means of azobenzene liquid-crystal films," *Science*, vol. 268, no. 5219, pp. 1873–1875, 1995. [Online]. Available: http://www.sciencemag.org/content/268/5219/1873.abstract

[212] T. Ikeda, T. Sasaki, and K. Ichimura, "Photochemical switching of polarization in ferroelectric liquid-crystal films," *Nature*, vol. 361, no. 6411, pp. 428–430, 1993.

[213] A. Langhoff and F. Giesselmann, "Photoferroelectric smectic-C* liquid crystal mixtures," *Ferroelectrics*, vol. 244, no. 1, pp. 283–293, 2000. [Online]. Available: http://dx.doi.org/10.1080/00150190008228440

[214] K. E. Maly, M. D. Wand, and R. P. Lemieux, "Bistable ferroelectric liquid crystal photoswitch triggered by a dithienylethene dopant," *Journal of the American Chemical Society*, vol. 124, no. 27, pp. 7898–7899, 2002. [Online]. Available: http://pubs.acs.org/doi/abs/10.1021/ja025954z

[215] L. Guo, S. Dhara, B. K. Sadashiva, S. Radhika, R. Pratibha, Y. Shimbo, F. Araoka, K. Ishikawa, and H. Takezoe, "Polar switching in the smectic-A_dP_A phase composed of asymmetric bent-core molecules," *Physical Review E*, vol. 81, p. 011703, Jan 2010. [Online]. Available: http://link.aps.org/doi/10.1103/PhysRevE.81.011703

[216] Y. G. Fokin, T. V. Murzina, O. A. Aktsipetrov, S. Soria, and G. Marowsky, "Switching behaviour of ferroelectric liquid crystals probed by optical second-harmonic generation," *Applied Physics B: Lasers and Optics*, vol. 74, pp. 777–781, 2002. [Online]. Available: http://dx.doi.org/10.1007/s00340-002-0921-9

Publications

Paper I

Matti Virkki, Martti Kauranen, and Arri Priimagi

"Different chromophore concentration dependence of photoinduced birefringence and second-order susceptibility in all-optical poling"

Reprinted from
Applied Physics Letters, vol. 99, no. 18, p. 183309, 2011
with the permission of AIP Publishing

Different chromophore concentration dependence of photoinduced birefringence and second-order susceptibility in all-optical poling

Matti Virkki,[1,a)] Martti Kauranen,[1] and Arri Priimagi[2,3]
[1]*Department of Physics, Tampere University of Technology, P.O. Box 692, FI-33101 Tampere, Finland*
[2]*Department of Applied Physics, Aalto University, P.O. Box 13500, FI-00076 Aalto, Finland*
[3]*Chemical Resources Laboratory, Tokyo Institute of Technology, Japan*

(Received 7 September 2011; accepted 13 October 2011; published online 2 November 2011)

We study photoinduced axial and polar ordering in Disperse Red 1 azobenzene–poly(4-vinylpyridine) polymer systems by monitoring both birefringence and second-harmonic generation during all-optical poling. The two responses are found to exhibit very distinct dependences on chromophore concentration: the photoinduced birefringence increasing up to 51 wt. % concentration and the second-order response reaching its peak already at 23 wt. %. The results show that the polar order required for second-order response is highly sensitive to chromophore-chromophore intermolecular interactions, whereas the birefringence is much more robust against such effects. © *2011 American Institute of Physics*. [doi:10.1063/1.3657829]

The linear and nonlinear optical properties of azobenzene-containing polymeric materials arise from the reversible photoisomerization of the azobenzene derivatives.[1] The isomerization process provides the possibility to photo-orient the chromophores with polarized light[2] and to induce macroscopic mass transport in the material.[3] Such photoinduced motions render azo-polymers promising for optical data storage, switching, diffractive optics, and nanotechnology.[3–6]

The light-induced molecular ordering in azo-polymers is greatly affected by the properties of the exciting light. Excitation with a single linearly polarized beam orients the molecules perpendicular to the polarization direction, and the resulting anisotropic ordering gives rise to birefringence.[2] On the other hand, excitation with a superposition of beams at a fundamental frequency and its second-harmonic gives rise to two- and one-photon excitation of the chromophores redistributing the molecules into a noncentrosymmetric polar ordering (Fig. 1). This process is known as *all-optical poling*.[7,8]

The polar ordering depends delicately on electrostatic interactions between the chromophores. Such interactions account for the fact that the second-order nonlinear optical response of azo-polymers does not increase linearly with chromophore concentration, but exhibits a maximum at a concentration value dictated by the dipole moment of the chromophores.[9,10] This optimal concentration has been studied in noncovalently[11] and covalently[12,13] coupled azo-polymer systems using electric field poling. On the other hand, we have shown that, as long as chromophore aggregation can be suppressed, the photoinduced birefringence increases linearly with concentration[14] and that intermolecular interactions can even enhance the photo-orientation process when efficient packing of the molecules is possible.[15,16] Hence, chromophore-chromophore interactions seem to play a distinct role in the axial and polar molecular alignment. All-optical poling leads to polar as well as axial molecular ordering.[8] Hence, it is important to understand whether the same or different mechanisms constrain the birefringence and second-order response that can be achieved by all-optical poling.

In this letter, we simultaneously monitor the photoinduced birefringence and second-harmonic generation (SHG) during all-optical poling and show that the two processes exhibit distinct concentration dependences. The photoinduced birefringence levels off only at very high azobenzene concentrations. The photoinduced noncentrosymmetry, on the other hand, reaches its maximum at much lower concentration. This result provides important information about the molecular-level interactions that take place in azo-polymer systems during photoinduced chromophore redistribution, and highlights the different role of electrostatic interactions in photoinduced birefringence and all-optical poling.

In order to access a wide concentration range, we take advantage of the selective hydrogen bonding between the chromophores and the polymer matrix, which allows high chromophore concentration without deteriorating sample quality.[17,18] Thin film samples were fabricated from Disperse Red 1 (DR1) and poly(4-vinylpyridine) (P4VP, $M_w = 22\,000$ g/mol), which were used as received. Their molecular structures are show in

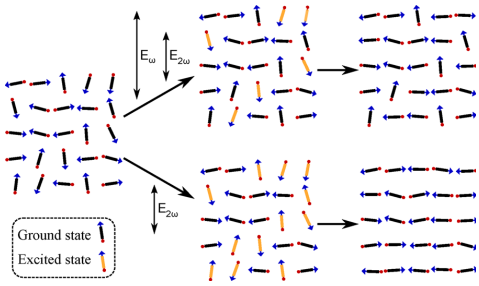

FIG. 1. (Color online) Redistribution of the in-plane molecular alignment of an isotropic structure (left) into a noncentrosymmetric structure (upper right) through selective excitation with a dual-frequency beam and into a birefringent structure (lower right) through excitation with a single linearly polarized beam.

a)Electronic mail: matti.virkki@tut.fi.

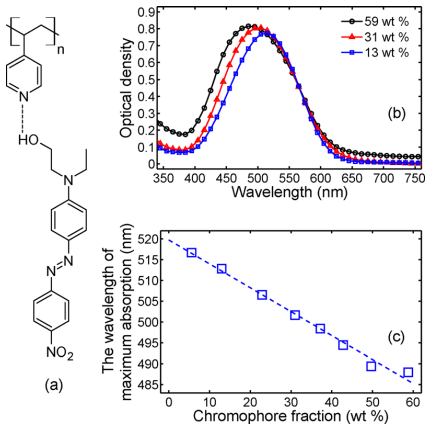

FIG. 2. (Color online) (a) Molecular structure of Disperse Red 1 hydrogen bonded to poly(4-vinylpyridine). (b) Absorption spectra for samples with low (13 wt. %), medium (31 wt. %), and high (59 wt. %) chromophore mass fraction. (c) Wavelength of the absorption maximum as a function of chromophore concentration. The dashed line is a linear fit to the data.

Fig. 2(a). The chromophore and polymer were separately dissolved in dimethylformamide and filtered through a syringe filter with 200 nm pore size. The solutions were mixed in different proportions to form eight complex solutions with chromophore mass fraction ranging from 5.6 to 59 wt. %. The solutions were spin-coated on glass substrates. The absorbance of the samples at 532 nm was fixed to ca. 0.7 by controlling the film thickness.

All-optical poling was performed with a similar setup as in Ref. 8. The dual-frequency poling beam was a combination of the fundamental beam (1064 nm) of a Q-switched diode-pumped Nd:YAG laser (8 ns, 100 Hz), and its second-harmonic at 532 nm. The pulse energies were 20 μJ for the fundamental *writing* beam and 0,4 μJ for the second-harmonic *seeding* beam. The same ratio of the writing and seeding beams could be used for all samples due to their equal absorbance at 532 nm.[8] The phase difference between the beams was found to have minimal effect on the photoinduced noncentrosymmetry due to the coherence properties of the multimode laser used, hence no phase optimization was required.

The photoinduced birefringence was measured with a probe beam at small angle to the poling beam line. The probe was produced with a 5 mW diode laser at 780 nm. The sample was placed between crossed polarizers with $\pm 45^\circ$ orientation with respect to the polarization of the poling beams. The transmitted intensity was measured with a photodiode and the birefringence $|\Delta n|$ was obtained from[19]

$$I = I_0 \sin^2\left(\frac{\pi|\Delta n|d}{\lambda}\right), \qquad (1)$$

where I_0 is the photodiode signal with the two polarizers in parallel orientation, d is the film thickness, and λ the wavelength of the probe beam.

The photoinduced noncentrosymmetry was probed by measuring the second-harmonic produced by the sample. The seeding beam was periodically blocked by placing a long-pass filter before the sample. During the brief interruption of poling, the SHG from the sample, I^S_{SHG}, was measured using a photomultiplier tube. A reference signal, I^Q_{SHG}, was measured from the maximum of the Maker fringes of a quartz crystal. The effective second-order susceptibility $\chi^{(2)}_{eff}$ of the sample is then

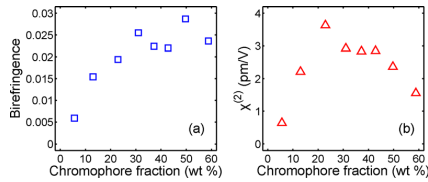

FIG. 3. (Color online) Saturation values of (a) photoinduced birefringence and (b) second-order susceptibility as a function of chromophore concentration during all-optical poling.

$$\chi^{(2)}_{eff} = \chi^{(2)}_{xxx,Q}\left(\frac{n_{\omega,S}}{n_{\omega,Q}d\Delta k_Q}\right)\sqrt{\frac{I^S_{SHG}\, n_{2\omega,S}}{I^Q_{SHG}\, n_{2\omega,Q}}}\, 10^{OD}, \qquad (2)$$

where $\chi^{(2)}_{xxx,Q} = 0.6\,\mathrm{pm/V}$ (Ref. 20) is the relevant susceptibility component of quartz, $n_{\omega,S}$ and $n_{\omega,Q}$ are the refractive indices of the sample and quartz at the fundamental frequency and $n_{2\omega,S}$ and $n_{2\omega,Q}$ at the second-harmonic frequency, $\Delta k_Q = 0.15 \times 10^6\,\mathrm{m}^{-1}$ (Ref. 8) is the wave vector mismatch in quartz, and OD is the optical density of the sample at the second-harmonic wavelength.

The absorption spectra for selected samples are shown in Fig. 2(b) and the wavelengths of maximum absorption in Fig. 2(c). Increasing chromophore concentration leads to broadening and almost linear blue shift of the DR1 absorption maximum at ca. 500 nm. We attribute this gradual blue shift mainly to the fact that the increasing chromophore concentration changes the polarity of the local environment of the chromophores, which gives rise to solvatochromic shift in the absorption maximum.[21] Large-scale chromophore aggregates, on the other hand, would lead to much more pronounced changes in the absorption spectra,[17,22] but here their formation is prevented by the noncovalent coupling between the chromophores and the polymer matrix.

The saturation values for the photoinduced birefringence and second-order susceptibility are shown in Fig. 3. The birefringence increases systematically with chromophore concentration, before leveling off at the highest concentrations (Fig. 3(a)). The maximum value of 0.029 was obtained at 51 wt. % azobenzene concentration. Similar concentration dependence, with a more pronounced drop after 51 wt. %, was found also when the birefringence was induced with a 514 nm beam in separate measurements (data not shown). The concentration dependence of the second-order susceptibility, on the other hand, was very different compared to the birefringence (Fig. 3(b)), with a maximum value of 3.6 pm/V already at 23 wt. % chromophore concentration. Assuming homogeneous chromophore distribution, this corresponds to chromophore number density of $5.3 \times 10^{20}\,1/\mathrm{cm}^3$ and 1.2 nm average distance between the chromophores. Our results are in reasonable agreement with reports for other Disperse Red type molecules.[10]

The notable difference in the concentration dependence of photoinduced birefringence and noncentrosymmetry can

be understood by considering the interactions between the chromophores at high concentrations. For high-dipole-moment chromophores, such as DR1, antiparallel molecular packing is favored over parallel one,[23] and such centrosymmetric packing is detrimental for the second-order response.[24,25] The macroscopic second-order response is thus determined by the competition between the poling field, which drives the molecules into noncentrosymmetric arrangement and the chromophore-chromophore interactions, which drive the molecules into centrosymmetric arrangement.[9] The latter is more prominent at high concentrations, hence decreasing the second-order susceptibility. At the same time, hydrogen bonding between the chromophores and the polymer matrix prevents the formation of large chromophore aggregates. The dipolar interactions that play against noncentrosymmetric chromophore alignment do not prevent their axial ordering, provided that the aggregates remain sufficiently small. We also note that the dynamics and the temporal stability of the photoinduced processes can depend on intermolecular interactions.[15,18] In the present case, however, both the dynamics and stability for different samples were essentially the same.

The results are in good agreement with Refs. 11 and 12 for electrically poled samples as well as with our previous work on photoinduced birefringence, demonstrating (1) that the concentration dependence of the second-order susceptibility is similar in all-optically poled and electrically poled polymer films and (2) that the concentration dependence of photoinduced birefringence is independent of whether it is induced directly with continuous-wave irradiation or during all-optical poling as here.

In conclusion, we have studied the effect of chromophore concentration on photoinduced birefringence and second-order nonlinear response in hydrogen-bonded DR1–P4VP complexes. The two effects exhibit very different concentration dependences even when induced simultaneously during all-optical poling. The second-order response is diminished at high concentrations due to chromophore-chromophore intermolecular interactions, whereas the photoinduced birefringence is more robust against such effects.

This work was supported by Academy of Finland (135043). A.P. acknowledges the support of the Japan Society for the Promotion of Science and the Foundations' Post Doc Pool in Finland. The authors thank Anni Lehmuskero for refractive index measurements.

[1]Z. Sekkat and W. Knoll, *Photoreactive Organic Thin Films* (Academic, San Diego, 2002).
[2]M. Dumont and A. E. Osman, Chem. Phys. **245**, 437 (1999).
[3]N. K. Viswanathan, D. Yu Kim, S. Bian, J. Williams, W. Liu, L. Li, L. Samuelson, J. Kumar, and S. K. Tripathy, J. Mater. Chem. **9**, 1941 (1999).
[4]A. Shishido, Polym. J. **42**, 525 (2010).
[5]U. A. Hrozhyk, S. V. Serak, N. V. Tabiryan, L. Hoke, D. M. Steeves, and B. R. Kimball, Opt. Express **18**, 8697 (2010).
[6]A. Kravchenko, A. Shevchenko, V. Ovchinnikov, A. Priimagi, and M. Kaivola, Adv. Mater. **23**, 4174 (2011).
[7]F. Charra, F. Kajzar, J. M. Nunzi, P. Raimond, and E. Idiart, Opt. Lett. **18**, 941 (1993).
[8]C. Fiorini, F. Charra, J. M. Nunzi, and P. Raimond, J. Opt. Soc. Am. B **14**, 1984 (1997).
[9]L. R. Dalton, A. W. Harper, and B. H. Robinson, Proc. Natl. Acad. Sci. U.S.A. **94**, 4842 (1997).
[10]A. W. Harper, S. Sun, L. R. Dalton, S. M. Garner, A. Chen, S. Kalluri, W. H. Steier, and B. H. Robinson, J. Opt. Soc. Am. B **15**, 329 (1998).
[11]M. J. Banach, M. D. Alexander, S. Caracci, and R. A. Vaia, Chem. Mater. **11**, 2554 (1999).
[12]F. Kajzar, O. Krupka, G. Pawlik, A. Mitus, and I. Rau, Mol. Cryst. Liq. Cryst. **522**, 180 (2010).
[13]G. Pawlik, I. Rau, F. Kajzar, and A. C. Mitus, Opt. Express **18**, 18793 (2010).
[14]A. Priimagi, M. Kaivola, F. J. Rodriguez, and M. Kauranen, Appl. Phys. Lett. **90**, 121103 (2007).
[15]A. Priimagi, J. Vapaavuori, F. J. Rodriguez, C. F. J. Faul, M. T. Heino, O. Ikkala, M. Kauranen, and M. Kaivola, Chem. Mater. **20**, 6358 (2008).
[16]J. Vapaavuori, V. Valtavirta, T. Alasaarela, J.-I. Mamiya, A. Priimagi, A. Shishido, and M. Kaivola, J. Mater. Chem. **21**, 15437 (2011).
[17]A. Priimagi, S. Cattaneo, R. H. A. Ras, S. Valkama, O. Ikkala, and M. Kauranen, Chem. Mater. **17**, 5798 (2005).
[18]A. Priimagi, M. Kaivola, M. Virkki, F. J. Rodríguez, and M. Kauranen, J. Nonlinear Opt. Phys. Mater. **19**, 57 (2010).
[19]T. Todorov, L. Nikolova, and N. Tomova, Appl. Opt. **23**, 4309 (1984).
[20]R. W. Boyd, *Nonlinear Optics* (Academic, San Diego, 2008).
[21]C. Reichardt, Chem. Rev. **94**, 2319 (1994).
[22]A. Priimagi, A. Shevchenko, M. Kaivola, F. J. Rodriguez, M. Kauranen, and P. Rochon, Opt. Lett. **35**, 1813 (2010).
[23]F. Würthner, S. Yao, T. Debaerdemaeker, and R. Wortmann, J. Am. Chem. Soc. **124**, 9431 (2002).
[24]A. Datta and S. K. Pati, J. Chem. Phys. **118**, 8420 (2003).
[25]A. M. Kelley, J. Chem. Phys. **119**, 3320 (2003).

Paper II

Matti Virkki, Ossi Tuominen, Alessandra Forni, Marco Saccone, Pierangelo Metrangolo, Giuseppe Resnati, Martti Kauranen, and Arri Priimagi

"Halogen bonding enhances nonlinear optical response in poled supramolecular polymers"

Journal of Materials Chemistry C, vol. 3, no. 12, pp. 3003–3006, 2015

Journal of
Materials Chemistry C

COMMUNICATION

View Article Online
View Journal

Halogen bonding enhances nonlinear optical response in poled supramolecular polymers†

Cite this: DOI: 10.1039/c5tc00484e

Received 18th February 2015,
Accepted 21st February 2015

DOI: 10.1039/c5tc00484e

www.rsc.org/MaterialsC

Matti Virkki,[a] Ossi Tuominen,[a] Alessandra Forni,[b] Marco Saccone,[c] Pierangelo Metrangolo,[d] Giuseppe Resnati,[d] Martti Kauranen[a] and Arri Priimagi*[cde]

We demonstrate that halogen bonding strongly enhances the nonlinear optical response of poled supramolecular polymer systems. We compare three nonlinear optical chromophores with similar electronic structures but different bond-donating units, and show that both the type and the strength of the noncovalent interaction between the chromophores and the polymer matrix play their own distinctive roles in the optical nonlinearity of the systems.

The halogen bond can be defined as an attractive interaction between an electrophilic region associated with a halogen atom in a molecular entity and a nucleophilic region in another, or the same, molecular entity.[1] Most properties of halogen bonds, such as directionality, strength, and tunability, can be rationalized by considering the anisotropic molecular electrostatic potential (MEP) distribution around halogen atoms. In fact, this is characterized by a region of positive MEP, denoted as the σ-hole,[2] which develops along the extension of the covalent bond involving the halogen atom, and a belt of negative MEP orthogonal to it. Consequently, an electron donor (*e.g.*, a Lewis base) will be attracted by the σ-hole and repelled by the rest of the atom surface. This explains the high directionality and linearity of halogen-bonded structures, both in the gas phase[3] and in the solid state.[4] The strength of the halogen bonding depends on the polarizability of the halogen atom – the higher the polarizability, the greater the interaction strength – and on the moiety attached to the halogen atom.

The benefits of halogen bonding have been recognized in crystal engineering,[5] medicinal chemistry,[6] and more recently in the design of functional materials.[7,8] In particular, halogen-bonded supramolecular complexes provide an excellent platform for inducing macroscopic mechanical movements in azobenzene-containing material systems,[9,10] such as light-induced surface topography patterns in azopolymer films.[11,12] Such patterns are generated through photoinitiated mass transport triggered by *cis–trans* isomerization of the embedded photoactive azobenzene molecules. Halogen-bonded low-molecular-weight complexes were found to allow for an exceptionally efficient mass transport,[9] and halogen-bonded supramolecular polymers were found to surpass similar hydrogen-bonded polymers in surface-patterning efficiency.[12]

Azopolymers are an exceptional platform for organic nonlinear optical materials, due to the high nonlinear optical (NLO) response of push–pull-type azobenzenes that can be tuned through photoisomerization.[13] A purely optical method for controlling the NLO response in azopolymers is all-optical poling,[14] in which a dual-frequency optical field is used to selectively excite azobenzene molecules in a polar fashion (*i.e.*, there is a unique direction in which the molecules need to be oriented for high probability of excitation). After repeated *cis–trans* isomerization cycles, the originally isotropic and thus centrosymmetric structure of an azopolymer is turned into a noncentrosymmetric one. The main motivation for breaking the symmetry are second-order NLO effects, such as second-harmonic generation and the electro-optic effect, that occur only in noncentrosymmetric media.[15] These NLO effects are of high interest in the field of photonics, where they allow several essential functionalities. Cost-effective polymeric materials with high and tunable second-order response would therefore open new possibilities for photonic technology.

Studies on poled polymer systems have largely focused on materials with the light-responsive molecules covalently attached to the polymer backbone.[14,16] However, the tedious synthesis required to prepare such polymers has triggered the search for supramolecular materials with high optical nonlinearities.[17,18] We

[a] *Department of Physics, Tampere University of Technology, P.O. Box 692, FI-33101 Tampere, Finland*
[b] *ISTM-CNR, Institute of Molecular Sciences and Technologies of CNR, Università degli Studi di Milano, Via Golgi 33, I-20133 Milan, Italy*
[c] *Department of Applied Physics, Aalto University, P.O. Box 13500, FI-00076 Aalto, Finland*
[d] *NFMLab, DCMIC "Giulio Natta", Politecnico di Milano, Via Mancinelli 7, I-20131 Milan, Italy*
[e] *Department of Chemistry and Bioengineering, Tampere University of Technology, P.O. Box 541, FI-33101 Tampere, Finland. E-mail: arri.priimagi@tut.fi; Tel: +358-44-515-0300*

† Electronic supplementary information (ESI) available: Sample fabrication, experimental procedures, UV-Vis absorption spectra, results on photoinduced birefringence, computational details and additional theoretical results. See DOI: 10.1039/c5tc00484e

have earlier shown using hydrogen-bonded supramolecular azopolymers that the chromophore content and thereby the photoactive properties can be greatly enhanced through noncovalent interactions.[19] Herein, we show that the benefits of supramolecular interactions in poled polymers can be further boosted by making use of halogen bonds, and that the NLO response inscribed by all-optical poling is superior in halogen-bonded polymer–azobenzene complexes compared to their hydrogen-bonded counterparts. We also demonstrate that the response scales with the strength of halogen bonding, and depends delicately on the ability of the support polymer matrix to act as a noncovalent-bond acceptor. The study is complemented by theoretical calculations that further elucidate the different performance of halogen- and hydrogen-bonded complexes.

The compounds used in this work are shown in Fig. 1. What is unique about the azobenzene molecules employed is that by changing the bond-donor atom X, we profoundly alter the type and strength of noncovalent interaction with the polymer matrix while maintaining the electronic and photochemical properties of the molecules practically unchanged.[11,12] For the support matrix, poly(4-vinylpyridine) (P4VP) was chosen as each of the chromophores is able to interact with the free electron pair of the nitrogen atom in the pyridine ring, giving rise to a R–X···N noncovalent bond. The molecules azo-I and azo-Br form halogen bonds of different interaction strength with P4VP (I > Br) whereas the acidic hydrogen atom of azo-H forms a weak hydrogen bond with P4VP. As a reference polymer, we chose polystyrene (PS), which lacks the electron-donating nitrogen atom and is therefore expected to give rise to weaker and less specific interactions with the chromophores, involving the halogen/hydrogen species and the aromatic ring π electrons arranged in a T-shaped configuration.[20,21] In principle, such R–X···π interaction could take place also in the P4VP matrix but in that case, the stronger R–X···N interaction is expected to prevail.

To verify the formation and characteristics of the involved noncovalent bonds, we modelled the material systems using density functional theory (DFT) at the M062X/6-311++G(d,p) level. We calculated the interaction energies between the azo-X molecules and either 4-methylpyridine or methylbenzene, used as model compounds for P4VP and PS, respectively. In the case of 4-methylpyridine, both collinear and T-shaped arrangements of the interacting molecules were considered. Interaction energies, corrected for Basis Set Superpositions Error (BSSE), were found to be −5.689, −4.248, and −4.128 kcal mol^{-1} for azo-I···N, azo-Br···N, and azo-H···N, respectively. The MEP maps of the azo-X molecules (see Fig. 1) elucidate the different bonding characteristics of azo-I and azo-Br compared to azo-H. The positive electrostatic potential on the halogen species is localized in a small area along the extension of the C–X bond. In contrast, for the azo-H, the area of positive potential is rather hemispherically distributed around the hydrogen atom. This difference accounts for greater directionality of halogen bonding compared to hydrogen bonding.

When considering the azo-X···π interaction, a local energy minimum with T-shaped configuration was obtained only for the halogenated azo-I and azo-Br molecules, with interaction energies amounting respectively to −3.298 and −2.997 kcal mol^{-1} in the case of 4-methylpyridine and to −4.064 and −3.464 kcal mol^{-1} in the case of methylbenzene. These energies are lower than those obtained for the azo-X···N interaction, indicating that the T-shaped configuration is unlikely in P4VP matrix in favour of the collinear one. On the other hand, the azo-X···π interaction, while weaker, is expected to take place in PS matrix, though presumably the optimal T-shaped arrangement is sterically hindered in the real system owing to the presence of the polymeric backbone, making the contribution of such interaction even less significant. Finally, unlike azo-I and azo-Br, azo-H was unable to give rise to a stable T-shaped configuration with either 4-methylpyridine or methylbenzene, indicating that the azo-H molecule interacts with P4VP exclusively through azo-H···N interaction while no directional interaction with PS is to be expected.

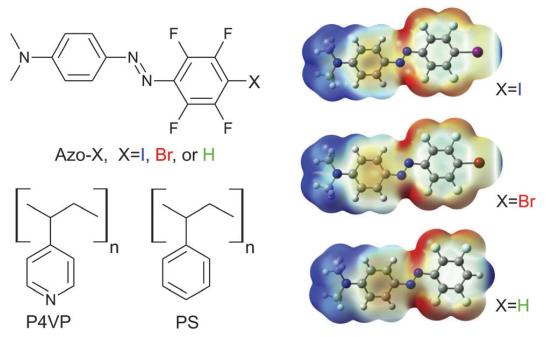

Fig. 1 Chemical structures of the components used in the studied material systems (left) and M062X/6-311++G(d,p) MEP maps (right). Potentials are mapped on the respective isosurfaces (0.001 a.u.) of electron density. Values of electrostatic potential range from −0.03 (red) to 0.03 (blue) a.u., with most positive local values on *X* equal to 0.037, 0.033 and 0.041 a.u. for X = I, Br and H, respectively. Atom color scheme: C, gray; H, light gray; N, dark blue; Br, red; F, sky blue; I, magenta.

The NLO response was studied in spin-coated azopolymer thin films denoted as P4VP(azo-X)$_y$ where *y* stands for the number of azobenzenes per each polymer repeat unit. Prior to the experiments, the samples were verified to be homogeneous and amorphous using optical microscopy. Fig. 2(a) presents the evolution of the second-order nonlinearity during all-optical poling for P4VP(azo-X)$_{0.1}$ samples with thicknesses of 280 nm ± 10%. The poling is performed with 1064 nm fundamental and 532 nm seeding beam wavelengths and the NLO response is measured with 1064 nm fundamental (see ESI,† for details). The nonlinearity is seen to depend drastically on the substituent X, developing in the order I > Br > H. In other words, in samples of equal thickness and containing the same amount of azobenzene chromophores, (i) stronger halogen bonding between the active molecules and the support matrix yields higher optical nonlinearity (azo-I *vs.* azo-Br), and (ii) the halogen-bonded systems surpass the hydrogen-bonded system P4VP(azo-H)$_{0.1}$ in terms of the optical nonlinearity. To the best of our knowledge, this is the first indication of the significance of halogen bonding in developing solid-state organic NLO materials.

To verify the generality of this observation, we prepared another set of samples with lower, 5 mol%, azobenzene

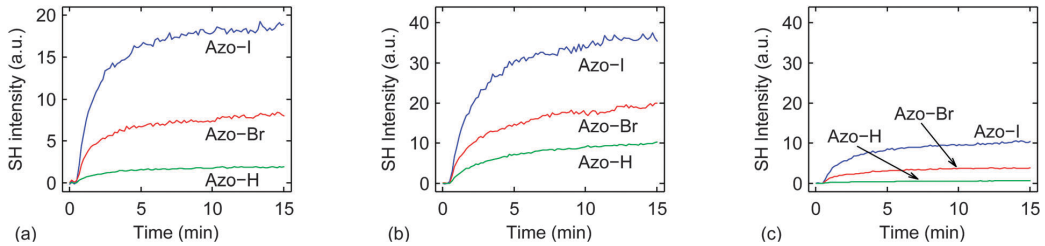

Fig. 2 Evolution of second-order nonlinearity during all-optical poling for P4VP(azo-X)$_{0.1}$ (a), P4VP(azo-X)$_{0.05}$ (b), and PS(azo-X)$_{0.05}$ (c). The poling process is started at 30 s and continued up until 15 min where near-saturation is reached. Generally lower values of NLO response in P4VP(azo-X)$_{0.1}$ compared to P4VP(azo-X)$_{0.05}$ are due to much lower thickness and slight deterioration in the 10 mol% samples due to dozens of poling cycles needed for all-optical poling optimization (see ESI,† for optimization details).

content. Reducing the azobenzene concentration allowed us to compare the NLO response obtained in P4VP to that in a weakly interacting PS matrix: if strong halogen bonds boost the optical nonlinearity, a strong matrix dependence is expected. The poling results for P4VP(azo-X)$_{0.05}$ and PS(azo-X)$_{0.05}$ are presented in Fig. 2(b) and (c), respectively. Two important observations can be made. Firstly, the NLO response still develops in the order I > Br > H. Secondly, the second-order NLO response is greatly diminished when replacing P4VP with PS, becoming negligible with azo-H. Note, however, that the same hierarchy (I > Br > H) still remains following the order of azo-X$\cdots\pi$ interaction energies given by DFT calculations. Overall, this gives us two independent verifications on the significance of halogen bonding on the NLO response: (i) azo-I *vs.* azo-Br in P4VP and (ii) azo-I in P4VP *vs.* PS.

When considering the significance of halogen bonding in all-optical poling, several things have to be accounted for. Firstly, the process is based on photoinduced polar reorientation of the azobenzene molecules and therefore closely related to photoinduction of anisotropic (yet centrosymmetric) chromophore alignment.[22,23] The photoinduced anisotropy can be monitored by measuring the birefringence of the films upon irradiation with linearly polarized light, which we did using 532 nm excitation to match the seeding beam in the poling process. The measurement details and results are presented in the ESI.† The main conclusion from these measurements is that photoinduced birefringence also greatly benefits from stronger chromophore–polymer bonding and halogen bonding yields higher anisotropy compared to hydrogen bonding. The qualitative differences are therefore same as they are for photoinduced NLO effects but the differences between the material systems are smaller.

Secondly, as the optical poling process is driven by repeated cycling between the *trans* and *cis* isomers of the azobenzene units, an accurate comparison between different material systems requires that their spectroscopic/photochemical properties are approximately equal. We verified this for the 5 mol% sample series by pumping the thin films with a 532 nm laser (5 s, 20 mW cm^{-2}), matching the seeding beam wavelength of the poling process. The absorption spectra are given in the ESI† (Fig. S2 and Table S1). For each chromophore, a 14–18 nm blue shift in the peak near 450 nm is seen when moving from P4VP to PS. This shift can be attributed to solvatochromic effects due to change in polarity of the molecular environment.[24,25] After excitation, a 14–23% drop in absorbance at peak and a smaller increase at 350–400 nm are seen. These changes are characteristic for azobenzenes as they isomerize from *trans* to *cis* form[26] and prove that effective photoinduced isomerization takes place during 532 nm excitation. Most of the photoinduced changes were seen to vanish in a few hours. This, together with clearly evident isosbestic points in the spectra reveal that no photodegradation occurs during irradiation. The effective photoisomerization at 532 nm together with lack of permanent changes in the absorption spectra suggest that the results obtained from all-optical poling at 1064/532 nm and photoinduced birefringence at 532 nm truly provide information on the influence of intermolecular interactions and their effects on the efficiency of photoinduced molecular realignment.

Based on the results, we can conclude that stronger halogen bonding leads to enhanced NLO response as well as to higher photoinduced birefringence. In each case, similar-strength hydrogen-bonding is not as beneficial. In each of the chromophores, the bond-donating atom is attached to the highly electronegative tetrafluorinated aromatic ring, due to which the single-atom mutation or a noncovalent bond formation have only minor effects on the molecular properties. Therefore, no significant changes in the photochemical or electronic properties are to be expected within the azo-X series, which is verified by the absorption spectra (Fig. S2, ESI†), computed dipole moments and molecular hyperpolarizabilities (Table S2, ESI†). This leads us to the conclusion that the noncovalent interaction must be the defining factor. Bonding strength has earlier been found to enhance both linear and nonlinear optical properties in supramolecular systems[19] and the comparison of azo-I and azo-Br in this study strongly supports this. Nevertheless, the superior performance of azo-Br compared to azo-H in P4VP is not explained by bonding strength as DFT calculations reveal that the interaction energy is essentially the same. We suggest that the directional nature of the halogen bond leads to a more rigid supramolecular structure that allows the formation of higher molecular order. We note that theoretical calculations have been made that suggest notably modified dipole moments of stilbene-based halogenated NLO molecules in the presence of halogen-bond acceptors.[27] Yet the conclusion of these calculations was that halogen bonding does not significantly

change the molecular-level NLO response. In our future studies, we plan to study the molecular hyperpolarizability through hyper-Rayleigh scattering experiments[28] to (i) gain further understanding on the results presented herein, and (ii) find the limits of halogen bonding in enhancing the NLO response of poled polymer systems.

To summarize, we have studied the second-order NLO response in halogen-bonded supramolecular polymers using all-optical poling. Our results demonstrate that stronger chromophore-polymer halogen bonding results in increased NLO response when the bond strength is the only variable. Furthermore, we have shown that a halogen-bonded supramolecular system is superior to a hydrogen-bonded one even when the bonding strengths are essentially equal. Together, these findings yield the conclusion that both the interaction strength and type have their own distinct effects for NLO response in supramolecular polymer systems and provide new implications for the design of second-order NLO materials.

Acknowledgements

M.V. acknowledges financial support from Tampere University of Technology graduate school and from the Väisälä Foundation. A.F. acknowledges the CINECA Award N. HP10BSXIH2 'XBPi', 2012, for the availability of high performance computing resources and support. P.M. acknowledges the financial support from MIUR for the PRIN 2010–2011 InfoChem project. A.P. acknowledges the Politecnico di Milano International Fellowship Program, the Emil Aaltonen Foundation, and the Academy of Finland for financial support.

References

1 G. R. Desiraju, P. S. Ho, L. Kloo, A. C. Legon, R. Marquardt, P. Metrangolo, P. Politzer, G. Resnati and K. Rissanen, *Pure Appl. Chem.*, 2013, **85**, 1711–1713.
2 T. Clark, *Wiley Interdiscip. Rev.: Comput. Mol. Sci.*, 2013, **3**, 13–20.
3 A. C. Legon, *Angew. Chem., Int. Ed.*, 1999, **38**, 2686–2714.
4 M. Saccone, G. Cavallo, P. Metrangolo, A. Pace, I. Pibiri, T. Pilati, G. Resnati and G. Terraneo, *CrystEngComm*, 2013, **15**, 3102–3105.
5 R. W. Troff, T. Mäkelä, F. Topić, A. Valkonen, K. Raatikainen and K. Rissanen, *Eur. J. Org. Chem.*, 2013, **2013**, 1617–1637.
6 R. Wilcken, M. O. Zimmermann, A. Lange, A. C. Joerger and F. M. Boeckler, *J. Med. Chem.*, 2013, **56**, 1363–1388.
7 A. Priimagi, G. Cavallo, P. Metrangolo and G. Resnati, *Acc. Chem. Res.*, 2013, **46**, 2686–2695.
8 F. Meyer and P. Dubois, *CrystEngComm*, 2013, **15**, 3058–3071.
9 A. Priimagi, M. Saccone, G. Cavallo, A. Shishido, T. Pilati, P. Metrangolo and G. Resnati, *Adv. Mater.*, 2012, **24**, OP345–OP352.
10 O. S. Bushuyev, T. C. Corkery, C. J. Barrett and T. Friscic, *Chem. Sci.*, 2014, **5**, 3158–3164.
11 A. Priimagi, G. Cavallo, A. Forni, M. Gorynsztejn-Leben, M. Kaivola, P. Metrangolo, R. Milani, A. Shishido, T. Pilati, G. Resnati and G. Terraneo, *Adv. Funct. Mater.*, 2012, **22**, 2572–2579.
12 M. Saccone, V. Dichiarante, A. Forni, A. Goulet-Hanssens, G. Cavallo, J. Vapaavuori, G. Terraneo, C. J. Barrett, G. Resnati, P. Metrangolo and A. Priimagi, *J. Mater. Chem. C*, 2015, **3**, 759–768.
13 S. K. Yesodha, C. K. S. Pillai and N. Tsutsumi, *Prog. Polym. Sci.*, 2004, **29**, 45–74.
14 C. Fiorini, F. Charra, J. M. Nunzi and P. Raimond, *J. Opt. Soc. Am. B*, 1997, **14**, 1984–2003.
15 R. W. Boyd, *Nonlinear Optics*, Academic Press, San Diego, 2008.
16 G. Xu, J. Si, X. Liu, Q. Yang, P. Ye, Z. Li and Y. Shen, *Opt. Commun.*, 1998, **153**, 95–98.
17 M. J. Banach, M. D. Alexander, S. Caracci and R. A. Vaia, *Chem. Mater.*, 1999, **11**, 2554–2561.
18 A. Facchetti, E. Annoni, L. Beverina, M. Morone, P. Zhu, T. J. Marks and G. A. Pagani, *Nat. Mater.*, 2004, **3**, 910–917.
19 A. Priimagi, M. Kaivola, M. Virkki, F. J. Rodríguez and M. Kauranen, *J. Nonlinear Opt. Phys. Mater.*, 2010, **19**, 57–73.
20 D. Hauchecorne, N. Nagels, B. J. van der Veken and W. A. Herrebout, *Phys. Chem. Chem. Phys.*, 2012, **14**, 681–690.
21 N. Nagels, D. Hauchecorne and W. A. Herrebout, *Molecules*, 2013, **18**, 6829–6851.
22 A. Natansohn, S. Xie and P. Rochon, *Macromolecules*, 1992, **25**, 5531–5532.
23 J. A. Delaire and K. Nakatani, *Chem. Rev.*, 2000, **100**, 1817–1846.
24 C. Reichardt, *Chem. Rev.*, 1994, **94**, 2319–2358.
25 E. Rusu, D.-O. Dorohoi and A. Airinei, *J. Mol. Struct.*, 2008, **887**, 216–219.
26 Z. Sekkat and W. Knoll, *Photoreactive organic thin films*, Academic Press, San Diego, 2002.
27 E. Cariati, A. Forni, S. Biella, P. Metrangolo, F. Meyer, G. Resnati, S. Righetto, E. Tordin and R. Ugo, *Chem. Commun.*, 2007, 2590–2592.
28 K. Clays and A. Persoons, *Phys. Rev. Lett.*, 1991, **66**, 2980–2983.

Electronic Supplementary Material (ESI) for Journal of Materials Chemistry C.

Halogen Bonding Enhances Nonlinear Optical Response in Poled Supramolecular Polymers

Matti Virkki, Ossi Tuominen, Alessandra Forni, Marco Saccone,
Pierangelo Metrangolo, Giuseppe Resnati, Martti Kauranen and Arri Priimagi

February 12, 2015

Supplementary information

1 Sample fabrication

The synthesis of the Azo-X chromophores has been described earlier[1]. Thin-film samples of the polymer-azobenzene complexes were prepared by spin coating from DMF (P4VP) or from a 50/50 mixture of acetone/dichloroethane (PS). The chromophore concentrations used were 10 mol-% (P4VP) and 5 mol-% (both PS and P4VP). The samples are denoted as P4VP/PS(Azo-X)$_y$ where y stands for the number of azobenzenes per each polymer repeat unit (0.05 in PS; 0.05 or 0.1 in P4VP). All samples were homogeneous and amorphous as verified by optical microscopy. The sample thicknesses were measured using Dektak 150 surface profiler.

2 All-optical poling

The nonlinear optical response was studied using all-optical poling, a technique based on the polar orientational excitation of the chromophores [2, 3]. In our experiments, polar selectivity is reached due to interference between two-photon excitation at the fundamental 1064 nm wavelength and one-photon excitation at the seeding 532 nm wavelength that are present in the poling field. The poling process is periodically halted by blocking the seeding beam. During this time, the fundamental 1064 nm beam is still passed to the sample and the second-harmonic (SH) signal at 532 nm generated by the sample is measured using a photomultiplier tube. The poling light source is a mode-locked diode-pumped Nd:YAG laser with 1064 nm wavelength, 100 Hz repetition rate and 28 ps pulse length. The 532 nm seeding beam is produced by frequency-doubling a small portion of the fundamental beam using a DKDP crystal.

All-optical poling is highly sensitive to the relative phase and intensity between the fundamental (frequency ω) and seeding (frequency 2ω) fields. The optimal relative intensity, i.e. seeding ratio, is reached when the probability of two-photon absorption at the fundamental wavelengthis as high as the probability of single-photon absorption at the seeding wavelength. It has been shown that the optimum ratio can be written as [3]

$$\left|\frac{E_{2\omega}}{E_{\omega}^2}\right| = \frac{\Delta\mu}{2\sqrt{3}\hbar\omega} \tag{1}$$

where E_ω refers to the electric field at the fundamental frequency ω and $E_{2\omega}$ to the field at the seeding frequency 2ω and $\Delta\mu$ is the difference between the dipole moments in the ground and excited states of the chromophore molecules within the two-level approximation. The seeding ratio was optimized by fixing the fundamental beam power to 800 mW and performing the poling experiment with seeding beam powers ranging from 12.5 µW to 400 µW. The poling time for the lowest seed power was 25 minutes and for the highest seed power 5 minutes respectively. These times were chosen in order to let the second-harmonic response saturate during each measurement as the speed of the poling process increases with increasing seeding beam power.

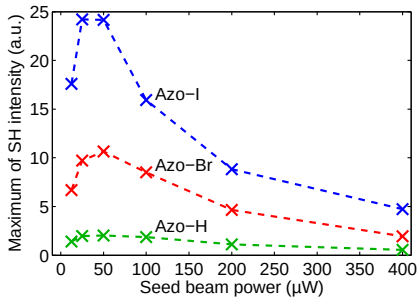

Figure S1: Second-harmonic (SH) intensities reached for different seeding ratios in all-optical poling for the studied chromophores in P4VP matrix. Dashed lines have been drawn to guide the eye.

While the exact phase difference between the fields is unknown, additional phase shift was introduced by rotating a 4 mm thick piece of BK7 glass in the beam line just before the sample. Four phase shifts $\Delta\Phi$ between 0 and $3\pi/4$ in $\pi/4$ steps were studied for each seeding ratio and sample separately. The second-harmonic signal from a thin film depends on the relative phase $\Delta\Phi$ as $1 + \cos(2\Delta\Phi)$ [3]. Therefore, one of our relative phases will show at least 85 % of the maximum second-harmonic signal even in the worst case that is found when the total phase difference is $\pi/8$ for zero additional phase shift.

The optimization results are shown in Fig. S1. The data points for a single sample represent the highest level of second-harmonic response that was reached in the phase optimization for each seeding beam power. The maximum second-harmonic intensity is reached at either 25 or 50 μW power for each sample. It is evident that the qualitative differences between the samples remain even when far away from the optimal seeding ratio. It is worthwhile to mention that according to Eq.1, in our experiments 25 μW seed power corresponds to $\sim 0.8 \times 10^{-10}$ m/V and 50 μW to $\sim 1.1 \times 10^{-10}$ m/V seeding ratio. These values are in excellent agreement with the optimum ratio of $\sim 0.9 \times 10^{-10}$ m/V found for another azobenzene chromophore [3].

The extensive optimization measurements revealed that the same poling parameters are optimal for each of the studied chromophores. Therefore, the results presented in the main article have been acquired by using the seed power of 50 μW and additional phase of $\pi/2$ that were found to yield the highest second-harmonic responses.

3 Spectral characteristics

The photoinduced changes in the absorption spectrum were measured with a setup built around a multi-channel fiber spectrometer (AvaSpec-ULS2048L) with 0.6 nm resolution in the range of 175–1100 nm. The excitation source was a continuous-wave diode-pumped solid-state laser at 532 nm wavelength. Circular polarization was used in order to avoid photoinduced rearrangement of the chromophores. The excitation beam was expanded to about 20 mm diameter and cut to 6 mm using an iris in order to achieve a top-hat profile and equally efficient photoactivation in the whole studied sample area. The excitation beam power reaching the sample was adjusted to 5.65 mW which leads to 20 mW/cm^2 intensity. For the white light probe beam, a balanced deuterium halogen light source (AvaLight-HD-S-BAL) was used. The probe beam power was adjusted to less than 0.1 mW and its diameter was 4.6 mm at the sample. The small peak found at 486 nm in some of the absorption spectra can be attributed to the strong emission line of deuterium at this wavelength together with slight nonlinearity of the spectrometer.

A single spectral measurement was averaged over a 1.1 second interval. The spectrum was first measured just before the excitation light was focused on the sample. The excitation time was 5 s and the second measurement was carried out 10 s after the excitation was ended. The following measurements were carried out after 1, 3, 10, 30, 90 and 180 minutes after the excitation was ended. The absorption spectra measured are shown in Fig. S2. The wavelength and absorbance at the peak near 450 nm were found by fitting a second-order polynomial to 41 data points nearest to the maximum value found in the range 400–500

Table S1: Spectral characteristics and thicknesses of 5 mol-% samples. λ_{peak}: Wavelength of lowest energy peak in absorbance, A_{peak}: absorbance at λ_{peak}, ΔA_{peak}: relative change in absorbance after 532 nm excitation, A_{532}: absorbance at 532 nm, d: thickness

material	P4VP(Azo-I)	P4VP(Azo-Br)	P4VP(Azo-H)	PS(Azo-I)	PS(Azo-Br)	PS(Azo-H)
λ_{peak} (nm)	462	463	449	449	445	435
A_{peak}	0.5668	0.5560	0.6600	0.8511	0.8163	0.8780
ΔA_{peak} (%)	23	20	18	21	19	14
A_{532}	0.2061	0.2111	0.1522	0.1674	0.1529	0.0996
d (nm)	470	480	570	900	700	740

nm. The fitting was done as measurement noise could cause a few nanometer errors in the locations of the spectral peaks due to the broad nature of the lowest energy peak found with azobenzene molecules. The largest difference between the fitting result and the data point with highest absorbance was 3 nm. For the isosbestic points the sum of least square deviations from the average value was calculated for each wavelength in the range of 350–450 nm and the minimum was chosen.

The absorption spectra of the 5 mol-% P4VP(Azo-X) and PS(Axo-X) samples are shown in Fig. S2 and the essential data is gathered to table S1. The photoexcitation experiments reveal that efficient isomerization is achieved for each material system. In each case, a notable drop in absorbance is found near the 450 nm peak accompanied with an increase in the range 350–400 nm. Such a change is characteristic for azobenzene derivatives as they isomerize into the *cis* form [4]. The isosbestic points (marked with dashed lines) were found in the range 389–401 nm following the order of the locations of the absorbance peaks. The time series reveals that thermal relaxation of the *cis* isomer back to the thermally stable *trans* isomer is rather slow in the studied systems, particularly in the PS matrix but the differences between chromophores are small. Furthermore, some of the samples were studied approximately 22 h after excitation and the absorption spectrum was found to regain the dark-adapted profile in this time frame proving that no permanent changes occur at the molecular level.

(a) P4VP(Azo-I)$_{0.05}$

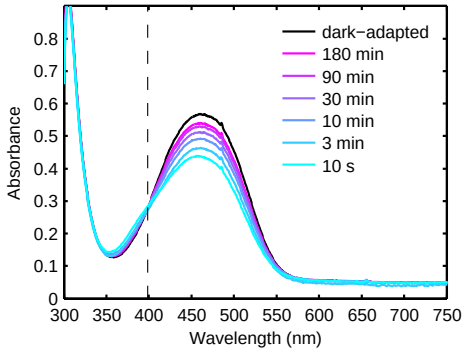

(b) PS(Azo-I)$_{0.05}$

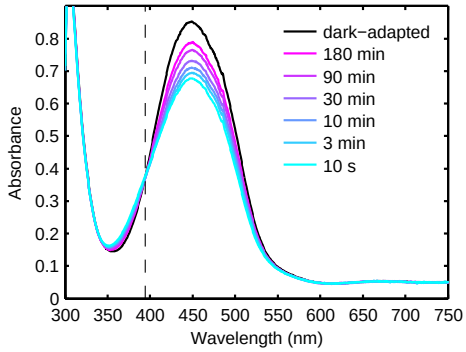

(c) P4VP(Azo-Br)$_{0.05}$

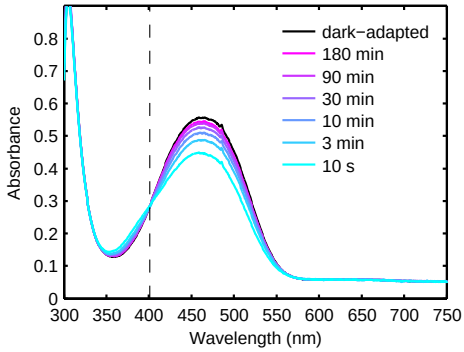

(d) PS(Azo-Br)$_{0.05}$

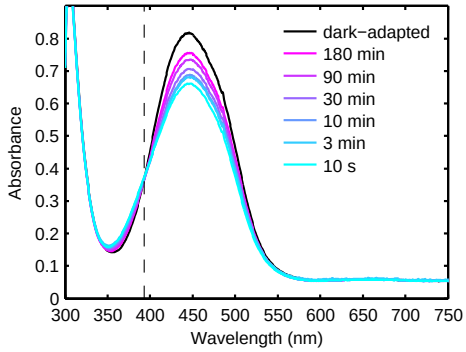

(e) P4VP(Azo-H)$_{0.05}$

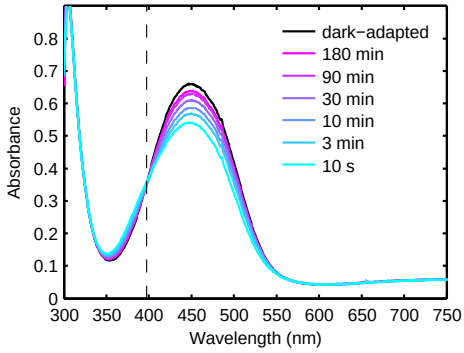

(f) PS(Azo-H)$_{0.05}$

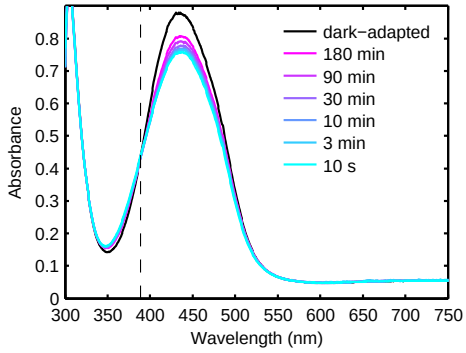

Figure S2: Spectral changes in 5 mol-% Azo-X samples before and after 5 s excitation at 20 mW cm^{-1} 532 nm.

4 Birefringence with 532 nm excitation

Photoinduced birefringence was achieved by directing a vertically polarized beam from a continuous-wave diode-pumped solid-state laser at 532 nm wavelength with 16 mW/cm^2 intensity onto the samples. The induced birefringence due to orientation-dependent photoexcitation and following angular redistribution was studied in real-time with a probe beam at 780 nm. The probe beam was directed onto the sample through a polarizer at +45° angle with respect to the excitation beam polarization. After the sample, the beam was directed onto a photodiode through an analyzing polarizer at -45° angle. Such a setup allows the intensity I measured with the photodiode to be connected to the absolute difference in refractive index $|\Delta n|$ by [5]

$$I = I_0 \sin^2\left(\frac{\pi|\Delta n|l}{\lambda}\right), \tag{2}$$

where I_0 is the reference intensity measured with the polarizer and analyzer parallel, l is the thickness of the sample and λ is the wavelength of the probe beam. The time evolution of the photoinduced birefringence in 5 mol-% Azo-X samples is shown in Fig. S3.

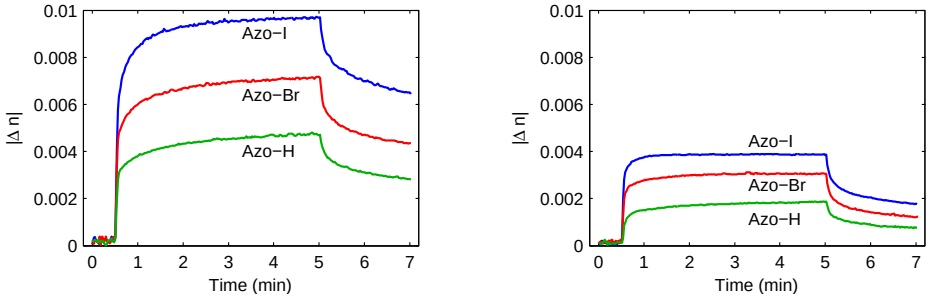

Figure S3: Photoinduced birefringence of 5 mol-% Azo-X samples in P4VP matrix (left) and PS matrix (right).

The birefringences follow the qualitative order (I > Br > H and P4VP > PS) presented in the main article for second-harmonic generation but quantitative differences are notably smaller.

5 Computational methods and additional theoretical results

The molecular dimers of compounds Azo-X with either 4-methylpyridine or methylbenzene were optimized at the M062X/6-311++G** level of theory *in vacuo*. The basis set for iodine[6] was downloaded from the Basis Set Exchange site.[7, 8] The M062X functional has been chosen in view of its optimal performance in treating noncovalent interactions,[9] including in particular halogen bonding with both lone pairs of heteroatoms[10] and π electron systems.[11] Interaction energies have been computed by optimization on the BSSE-free potential energy surface as the difference between the energy of the dimer and the sum of the energies of the single monomers. BSSE correction was made by the standard counterpoise method.[12] All calculations were performed with the Gaussian suite of programs.[13]

Molecular hyperpolarizabilities and dipole moments of the Azo-X chromophores are shown in table S2. Hyperpolarizabilities were obtained with the coupled-perturbed Kohn-Sham method at 1064 nm wavelength. The (99,590) grid, referred to as the ultrafine grid in Gaussian09, has been used for the DFT numerical integrations.

Table S2: M062X/6-311++G(d,p) computed dipoles and hyperpolarizabilities along the dipole direction of the Azo-X series.

Compound	μ(D)	$\beta_z(\times 10^{-30})$esu
Azo-I	6.72	271
Azo-Br	6.90	296
Azo-H	5.87	225

References

[1] A. Priimagi, G. Cavallo, A. Forni, M. Gorynsztejn-Leben, M. Kaivola, P. Metrangolo, R. Milani, A. Shishido, T. Pilati, G. Resnati, and G. Terraneo, "Halogen Bonding versus Hydrogen Bonding in Driving Self-Assembly and Performance of Light-Responsive Supramolecular Polymers," Adv. Funct. Mater. **22**, 2572 (2012).

[2] N. B. Baranova and B. Y. Zel'dovich, "Physical effects in optical fields with nonzero average cube, $< E >^3 \neq 0$," J. Opt. Soc. Am. B **8**, 27 (1991).

[3] C. Fiorini, F. Charra, J. M. Nunzi, and P. Raimond, "Quasi-permanent all-optical encoding of noncentrosymmetry in azo-dye polymers," J. Opt. Soc. Am. B **14**, 1984 (1997).

[4] Z. Sekkat and W. Knoll, *Photoreactive organic thin films*, Academic Press, San Diego (2002).

[5] T. Todorov, L. Nikolova, and N. Tomova, "Polarization holography. 1: A new high-efficiency organic material with reversible photoinduced birefringence," Appl. Opt. **23**, 4309 (1984).

[6] M. N. Glukhovtsev, A. Pross, M. P. McGrath, and L. Radom, "Extension of Gaussian-2 (G2) theory to bromine- and iodine-containing molecules: Use of effective core potentials," J. Chem. Phys. **103**, 1878 (1995).

[7] D. Feller, "The role of databases in support of computational chemistry calculations," J. Comput. Chem. **17**, 1571 (1996).

[8] K. L. Schuchardt, B. T. Didier, T. Elsethagen, L. Sun, V. Gurumoorthi, J. Chase, J. Li, and T. L. Windus, "Basis Set Exchange: A Community Database for Computational Sciences," J. Chem. Inf. Model. **47**, 1045, pMID: 17428029 (2007).

[9] Y. Zhao and D. Truhlar, "The M06 suite of density functionals for main group thermochemistry, thermochemical kinetics, noncovalent interactions, excited states, and transition elements: two new functionals and systematic testing of four M06-class functionals and 12 other functionals," Theor. Chem. Acc. **120**, 215 (2008).

[10] S. Kozuch and J. M. L. Martin, "Halogen Bonds: Benchmarks and Theoretical Analysis," J. Chem. Theory Comput. **9**, 1918 (2013).

[11] A. Forni, S. Pieraccini, S. Rendine, and M. Sironi, "Halogen bonds with benzene: An assessment of DFT functionals," J. Comput. Chem. **35**, 386 (2014).

[12] S. F. Boys and F. d. Bernardi, "The calculation of small molecular interactions by the differences of separate total energies. Some procedures with reduced errors," Mol. Phys. **19**, 553 (1970).

[13] M. J. Frisch, G. W. Trucks, H. B. Schlegel, G. E. Scuseria, M. A. Robb, J. R. Cheeseman, G. Scalmani, V. Barone, B. Mennucci, G. A. Petersson, H. Nakatsuji, M. Caricato, X. Li, H. P. Hratchian, A. F. Izmaylov, J. Bloino, G. Zheng, J. L. Sonnenberg, M. Hada, M. Ehara, K. Toyota, R. Fukuda, J. Hasegawa, M. Ishida, T. Nakajima, Y. Honda, O. Kitao, H. Nakai, T. Vreven, J. A. Montgomery, Jr., J. E. Peralta, F. Ogliaro, M. Bearpark, J. J. Heyd, E. Brothers, K. N. Kudin, V. N. Staroverov, R. Kobayashi, J. Normand, K. Raghavachari, A. Rendell, J. C. Burant, S. S. Iyengar, J. Tomasi, M. Cossi, N. Rega, J. M.

Millam, M. Klene, J. E. Knox, J. B. Cross, V. Bakken, C. Adamo, J. Jaramillo, R. Gomperts, R. E. Stratmann, O. Yazyev, A. J. Austin, R. Cammi, C. Pomelli, J. W. Ochterski, R. L. Martin, K. Morokuma, V. G. Zakrzewski, G. A. Voth, P. Salvador, J. J. Dannenberg, S. Dapprich, A. D. Daniels, . Farkas, J. B. Foresman, J. V. Ortiz, J. Cioslowski, and D. J. Fox, "Gaussian 09 Revision D.01," Gaussian Inc. Wallingford CT 2013.

Paper III

Matti Virkki, Ossi Tuominen, Martti Kauranen, and Arri Priimagi

"Photoinduced nonlinear optical response in azobenzene-functionalized molecular glass"

Optics Express, vol. 24, no. 5, pp. 4964–4971, 2016

Photoinduced nonlinear optical response in azobenzene-functionalized molecular glass

Matti Virkki,[1,*] **Ossi Tuominen,**[1] **Martti Kauranen,**[1] **and Arri Priimagi**[2]

[1]*Department of Physics, Tampere University of Technology, P.O. Box 692, FI-33101 Tampere, Finland*

[2]*Department of Chemistry and Bioengineering, Tampere University of Technology, P.O. Box 541, FI-33101 Tampere, Finland*

[*]*matti.virkki@tut.fi*

Abstract: We show that mexylaminotriazine molecular glass functionalized with the azobenzene derivative Disperse Red 1 shows equally strong second-order nonlinear optical response as well-known polymers with the same photoactive component. Furthermore, even high chromophore loading does not adversely affect the nonlinear response. This suggests that chromophore-chromophore intermolecular interactions do not greatly limit the response of such molecular glasses, which therefore provide an excellent materials platform for nonlinear optical applications.

OCIS codes: (190.0190) Nonlinear optics; (190.2620) Harmonic generation and mixing; (190.4710) Optical nonlinearities in organic materials.

References and links

1. H. M. D. Bandara and S. C. Burdette, "Photoisomerization in different classes of azobenzene," Chem. Soc. Rev. **41**, 1809–1825 (2012).
2. T. Ikeda, J.-i. Mamiya, and Y. Yu, "Photomechanics of liquid-crystalline elastomers and other polymers," Angew. Chem. Int. Ed. **46**, 506–528 (2007).
3. K. Viswanathan, Nirmal, D. Yu Kim, S. Bian, J. Williams, W. Liu, L. Li, L. Samuelson, J. Kumar, and S. K. Tripathy, "Surface relief structures on azo polymer films," J. Mater. Chem. **9**, 1941–1955 (1999).
4. A. Natansohn and P. Rochon, "Photoinduced motions in azo-containing polymers," Chem. Rev. **102**, 4139–4176 (2002).
5. R. D. Schaller, R. J. Saykally, Y. R. Shen, and F. Lagugné-Labarthet, "Poled polymer thin-film gratings studied with far-field optical diffraction and second-harmonic near-field microscopy," Opt. Lett. **28**, 1296–1298 (2003).
6. F. Lagugné-Labarthet, C. Sourisseau, R. D. Schaller, R. J. Saykally, and P. Rochon, "Chromophore orientations in a nonlinear optical azopolymer diffraction grating: even and odd order parameters from far-field raman and near-field second harmonic generation microscopies," J. Phys. Chem. B **108**, 17059–17068 (2004).
7. C. Fiorini, F. Charra, J. M. Nunzi, and P. Raimond, "Quasi-permanent all-optical encoding of noncentrosymmetry in azo-dye polymers," J. Opt. Soc. Am. B **14**, 1984–2003 (1997).
8. R. W. Boyd, *Nonlinear Optics* (Academic, 2008).
9. T. Fuhrmann and T. Tsutsui, "Synthesis and properties of a hole-conducting, photopatternable molecular glass," Chem. Mater. **11**, 2226–2232 (1999).
10. P. Strohriegl and J. Grazulevicius, "Charge-transporting molecular glasses," Adv. Mater. **14**, 1439–1452 (2002).
11. Y. Shirota, "Organic materials for electronic and optoelectronic devices," J. Mater. Chem. **10**, 1–25 (2000).
12. Y. Shirota, K. Moriwaki, S. Yoshikawa, T. Ujike, and H. Nakano, "4-[di(biphenyl-4-yl)amino]azobenzene and 4,4'-bis[bis(4'-tert-butylbiphenyl-4-yl)amino]azobenzene as a novel family of photochromic amorphous molecular materials," J. Mater. Chem. **8**, 2579–2581 (1998).

#255771 Received 17 Dec 2015; revised 11 Feb 2016; accepted 12 Feb 2016; published 26 Feb 2016

13. E. Ishow, R. Camacho-Aguilera, J. Gurin, A. Brosseau, and K. Nakatani, "Spontaneous formation of complex periodic superstructures under high interferential illumination of small-molecule-based photochromic materials," Adv. Funct. Mater. **19**, 796–804 (2009).
14. A. Perschke and T. Fuhrmann, "Molecular azo glasses as grating couplers and resonators for optical devices," Adv. Mater. **14**, 841–843 (2002).
15. E. Ishow, C. Bellaïche, L. Bouteiller, K. Nakatani, and J. A. Delaire, "Versatile synthesis of small NLO-active molecules forming amorphous materials with spontaneous second-order NLO response," J. Am. Chem. Soc. **125**, 15744–15745 (2003).
16. A. Carella, R. Centore, L. Mager, A. Barsella, and A. Fort, "Crosslinkable organic glasses with quadratic nonlinear optical activity," Org. Electron. **8**, 57–62 (2007).
17. K. Traskovskis, I. Mihailovs, A. Tokmakovs, A. Jurgis, V. Kokars, and M. Rutkis, "Triphenyl moieties as building blocks for obtaining molecular glasses with nonlinear optical activity," J. Mater. Chem. **22**, 11268–11276 (2012).
18. N. Tsutsumi and K. Nakatani, "$\chi^{(2)}$ polarization induced in molecular glass of conjugated compound by all-optical poling," Opt. Commun. **259**, 852–855 (2006).
19. M. Virkki, M. Kauranen, and A. Priimagi, "Different chromophore concentration dependence of photoinduced birefringence and second-order susceptibility in all-optical poling," Appl. Phys. Lett. **99**, 183309 (2011).
20. O. Lebel, T. Maris, M.-E. Perron, E. Demers, and J. D. Wuest, "The dark side of crystal engineering: creating glasses from small symmetric molecules that form multiple hydrogen bonds," J. Am. Chem. Soc. **128**, 10372–10373 (2006).
21. J. D. Wuest and O. Lebel, "Anarchy in the solid state: structural dependence on glass-forming ability in triazine-based molecular glasses," Tetrahedron **65**, 7393–7402 (2009).
22. R. N. Eren, A. Plante, A. Meunier, A. Laventure, Y. Huang, J. G. Briard, K. J. Creber, C. Pellerin, A. Soldera, and O. Lebel, "One ring to rule them all: effect of aryl substitution on glass-forming ability in mexylaminotriazine molecular glasses," Tetrahedron **68**, 10130–10144 (2012).
23. A. Laventure, A. Soldera, C. Pellerin, and O. Lebel, "Heads vs. tails: a double-sided study of the influence of substituents on the glass-forming ability and stability of aminotriazine molecular glasses," New J. Chem. **37**, 3881–3889 (2013).
24. A. Meunier and O. Lebel, "A glass forming module for organic molecules: Making tetraphenylporphyrin lose its crystallinity," Org. Lett. **12**, 1896–1899 (2010).
25. R. Kirby, R. G. Sabat, J.-M. Nunzi, and O. Lebel, "Disperse and disordered: a mexylaminotriazine-substituted azobenzene derivative with superior glass and surface relief grating formation," J. Mater. Chem. C **2**, 841–847 (2014).
26. O. R. Bennani, T. A. Al-Hujran, J.-M. Nunzi, R. G. Sabat, and O. Lebel, "Surface relief grating growth in thin films of mexylaminotriazine-functionalized glass-forming azobenzene derivatives," New J. Chem. **39**, 9162–9170 (2015).
27. M. Virkki, O. Tuominen, A. Forni, M. Saccone, M. Pierangelo, G. Resnati, M. Kauranen, and A. Priimagi, "Halogen bonding enhances nonlinear optical response in poled supramolecular polymers," J. Mater. Chem. C **3**, 3003–3006 (2015).
28. L. R. Dalton, A. W. Harper, and B. H. Robinson, "The role of london forces in defining noncentrosymmetric order of high dipole moment–high hyperpolarizability chromophores in electrically poled polymeric thin films," Proc. Natl. Acad. Sci. U. S. A. **94**, 4842–4847 (1997).
29. A. W. Harper, S. Sun, L. R. Dalton, S. M. Garner, A. Chen, S. Kalluri, W. H. Steier, and B. H. Robinson, "Translating microscopic optical nonlinearity into macroscopic optical nonlinearity: the role of chromophore chromophore electrostatic interactions," J. Opt. Soc. Am. B **15**, 329–337 (1998).
30. M. J. Banach, M. D. Alexander, S. Caracci, and R. A. Vaia, "Enhancement of electrooptic coefficient of doped films through optimization of chromophore environment," Chem. Mater. **11**, 2554–2561 (1999).
31. F. Kajzar, O. Krupka, G. Pawlik, A. Mitus, and I. Rau, "Concentration variation of quadratic NLO susceptibility in PMMA-DR1 side chain polymer," Mol. Cryst. Liq. Cryst. **522**, 180–190 (2010).
32. P. Prêtre, L.-M. Wu, A. Knoesen, and J. D. Swalen, "Optical properties of nonlinear optical polymers: a method for calculation," J. Opt. Soc. Am. B **15**, 359–368 (1998).
33. A. Priimagi, M. Kaivola, M. Virkki, F. J. Rodríguez, and M. Kauranen, "Suppression of chromophore aggregation in amorphous polymeric materials: towards more efficient photoresponsive behavior," J. Nonlinear Opt. Phys. Mater. **19**, 57–73 (2010).

1. Introduction

Azobenzenes are a well-known trigger for controlling material properties with light thanks to their reversible photoinduced *cis-trans* isomerization [1]. The isomerization process can drive photomechanical movement such as bending [2] and formation of surface relief gratings (SRGs) [3] as well as photoinduced molecular realignment into highly asymmetric structures

#255771 Received 17 Dec 2015; revised 11 Feb 2016; accepted 12 Feb 2016; published 26 Feb 2016

[4], each controlled by the properties of the excitation light. Even the combination of SRGs and asymmetric molecular order has been proven effective [5, 6]. Azobenzene-based materials are therefore under intense study for applications in optical data storage, photonic circuitries and energy conversion. A particular example of photoinduced asymmetry is all-optical poling (AOP) [7], where a coherent superposition of a dual-frequency optical field leads to photoexcitation with polar selectivity. After repeated *trans-cis-trans* cycles, the process leads to broken inversion symmetry enabling second-order nonlinear optical (NLO) properties [7, 8].

For many applications, a stable amorphous phase of the photoactive moiety is preferred. Pure azobenzenes are brittle crystalline materials, which has lead to the practice of embedding them into a polymer forming an amorphous support structure [4]. These azo-polymers inherit their photoactive properties from the azobenzene while maintaining the rigidity and ease or processing of the parent polymer. While azo-polymers have shown their value as a platform for light-controlled materials, a less used alternative strategy is provided by small molecules capable of forming stable amorphous structures. Such materials, referred to as molecular glasses, have the advantage that the molecular structure and mass are well known in contrast to polymers, which yields easier purification, characterization and better reproducibility [9, 10].

While some small molecules capable of forming amorphous phase have been known for decades, intense study of molecular glasses started in the 1990s focusing on organic charge-transporting materials for electroluminescence [10, 11]. Photochromic glassy materials using azobenzenes were soon demonstrated [12], allowing photoinduced birefringence and surface-relief grating formation [9]. High groove depth and complex patterning [13] as well as efficient coupling into a waveguide [14] have been demonstrated with photoinduced SRGs in azobenzene molecular glasses. Attempts have been made to create molecular glasses with NLO response by combining push-pull type azobenzenes [15, 16], and other suitable nonlinear optical chromophores [17] with functional groups that promote the formation of an amorphous phase. To date, a single attempt of AOP in a non-polymeric organic glass has been reported [18]. Molecular glasses functionalized with azobenzenes have not been studied by AOP although the method is known to be well-suited for azo-polymers [7, 19].

A few years ago, a glass-forming group named mexylaminotriazines was developed by Lebel and coworkers [20, 21]. This group can be easily modified [22, 23] allowing for facile control of its properties, most importantly the glass transition temperature T_g. The mexylaminotriazines possess relatively high symmetry, rigid structure and possibility to self-assemble through hydrogen bonding, all of which defy the traditional design features of molecular glasses. Yet their ability to form stable amorphous phases is remarkable even when functionalized with compounds that readily form crystalline structures when pure [24]. Recently, a mexylaminotriazine functionalized with Disperse Red 1 (DR1) azobenzene was synthesized and shown to be equally good as DR1-PMMA functionalized polymer system for surface-relief grating inscription [25, 26].

In this study, we show that this new mexylaminotriazine functionalized with DR1 provides an ideal candidate for all-optical poling. We find that the DR1 glass reaches an NLO response that is as high as that of similar polymer counterparts while maintaining the benefits of the well-known structure and better repeatability inherent to molecular glasses. Furthermore, we show that chromophore-chromophore intermolecular interactions do not compromize the nonlinear properties with this material even at fairly high chromophore concentrations.

2. Materials and methods

The NLO response was studied with AOP using 1064 nm as the fundamental *writing* field and its second harmonic at 532 nm from a KDP crystal as the weak *seeding* field. The source for the fundamental field was an Ekspla PL2231 diode-pumped Nd:YAG solid-state laser producing 10 mJ, 28 ps pulses at 100 Hz repetition rate. Both fields were linearly polarized with pulse

#255771 Received 17 Dec 2015; revised 11 Feb 2016; accepted 12 Feb 2016; published 26 Feb 2016

energies of 7 mJ and 1 μJ for the fundamental and seeding fields, respectively, at the sample plane. This seeding ratio of 7000:1 was chosen after careful optimization for the sample series. The optimization process has been explained in detail in [27]. In the poling process, two-photon absorption of the writing field and one-photon absorption of the seeding field interfere creating polar selective excitation for the DR1 moieties which gradually results in an in-plane polar order. The increasing order is monitored by blocking the seeding field periodically and by measuring the second-harmonic produced by the sample as the writing field is still applied on the sample.

The first sample series consists of the DR1-functionalized mexylaminotriazine molecular glass (DR1MG) and of two well-known reference polymers (Fig. 1). The first one is the homopolymer Poly(Disperse Red 1 acrylate) (PDR1A) and the second is the copolymer Poly[(methyl methacrylate)-co-(Disperse Red 1 acrylate)] (P(MMA-co-DR1A)). DR1MG was acquired from Solaris Chem and the polymers from Sigma-Aldrich. All components were used without further purification. The homopolymer represents a polymer material with one of the highest possible

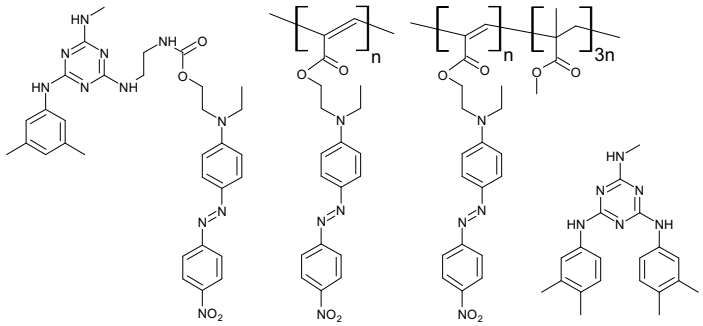

Fig. 1. Chemical structures of the materials used in experiments. From left: DR1MG, PDR1A, P(MMA-co-DR1A), NAMG.

DR1 mass fractions (85 %) for an amorphous material. The copolymer, on the other hand, was chosen as its DR1 fraction is 47 wt%. This fraction is very close to the value of 50 wt% calculated for the molecular glass. The absorption spectra of the materials in 1,2-dichloroethane are shown in Fig. 2(a).

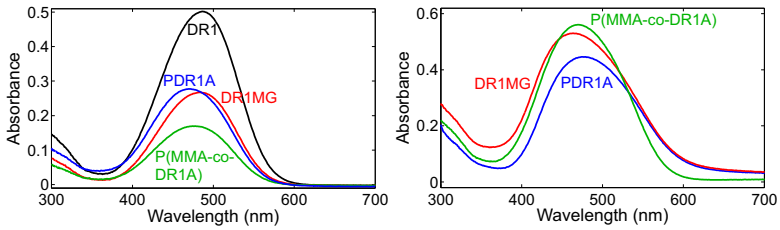

Fig. 2. UV-Vis Absorption spectra of DR1, DR1MG, P(MMA-co-DR1A) and PDR1A in 4×10^{-4} wt% 1,2-dichloroethane solutions (a) and of the sample films (b).

Thin film samples of the molecular glass and polymers were spin-coated on clean microscope glass slides. Solutions with 2 % of the compounds in 1,2-dichloroethane were prepared and filtered through 0.45 μm filter. The spinning rate was set to 1000 rpm for P(MMA-co-DR1A)

#255771 Received 17 Dec 2015; revised 11 Feb 2016; accepted 12 Feb 2016; published 26 Feb 2016

and 3000 rpm for PDR1A and DR1MG in order to reach absorbance of 0.3 at 532 nm which is well suited for AOP. After the poling experiments, the thicknesses of the samples were measured with Dektak 6M stylus profiler. The absorption spectra of the samples are shown in Fig. 2(b). The thicknesses of the samples were 100 nm, 87 nm and 152 nm for DR1MG, PDR1A and P(MMA-co-DR1A), respectively. The homogeneity and stability of the samples was confirmed with polarized optical microscopy where little to no signs of crystallization were seen several months after the experiments. The density of DR1MG was determined using small flakes from a thick drop-cast film which were placed in a concentrated sucrose water solution where they float. The solution density was lowered in small steps by dilution with water until the flakes sink. The density of the solution was measured before and after the flakes sink which gives the DR1MG density 1.25 ± 0.04 g cm^{-3}.

3. Results

The evolution of second-harmonic (SH) signal during the poling process was monitored for 15 minutes after which all of the samples nearly reached saturation. Next, the decay of the signal was monitored for 15 minutes without further poling. In a film shorter than the coherence length for second-harmonic generation, the SH intensity scales quadratically with the sample thickness [8]. Therefore, in order to access the material properties, the measured SH signals were normalized with the sample thicknesses squared. The evolution of the thickness-normalized SH intensities are shown in Fig. 3. From the results, it can be concluded that, within experimental uncertainties, the second-order response of DR1MG is identical to the reference polymers. It should be noted that the T_g-values of the reference polymers PDR1A (79 °C) and P(MMA-co-DR1A) (102 °C) are somewhat higher than 71 °C [25] found in the molecular glass. This could lower the stability of the asymmetric molecular order in the molecular glass compared to the polymers. However, in the case SRGs, it has been found that the thermal stability of DR1MG is similar to a reference polymer with 20 °C higher T_g possibly owing to the hydrogen bonding present in the glass [25]. This makes the comparison with the chosen polymers well justified and the results in Fig. 3 hint towards slightly slower dynamics in the glass compared to the polymers.

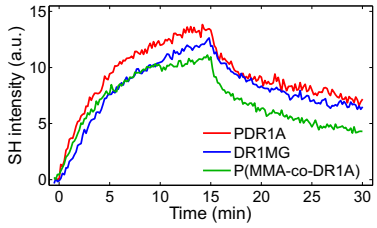

Fig. 3. Evolution of SH signals during AOP normalized with squares of sample thicknesses.

Much of the work on polymers for NLO applications has focused on increasing the concentration of the nonlinear chromophores in order to reach higher NLO response. However, for polar push-pull type molecules, the interchromophore interactions start to play against this goal well before the mechanical properties become compromised [28, 29]. For DR1-PMMA guest-host system the optimum concentration is 20-30 wt% [30], while in a copolymer P(MMA-co-DR1MA), similar to the one used here, the maximum NLO response is reached at 30-40 wt% [31]. Therefore, the optimum concentration for the DR1 molecular glass is also of great interest and was studied in our second series of experiments. In order to vary the DR1 concentration, DR1MG was mixed with another mexylaminotriazine acquired from Solaris Chem Inc. (see

#255771 Received 17 Dec 2015; revised 11 Feb 2016; accepted 12 Feb 2016; published 26 Feb 2016

Fig. 1) with no absorption in the visible range. Otherwise, the properties of this non-absorbing molecular glass (NAMG) are expected to be close to DR1MG. For instance, the glass transition temperature of NAMG is 71 °C [23], equal to that of DR1MG [25]. It should be noted that the pure DR1MG contains 50 wt% of DR1. This sets the upper limit for the chromophore loading in our experiments.

A series of molecular glass mixture (MGM) samples with the DR1 mass fraction varying from 0 to 50 % in 10 % steps was fabricated by mixing solutions of NAMG and DR1MG in appropriate ratios and spin coating. The spin coating was performed at varying rates between 600 and 5500 rpm to reach absorbance close to 0.3 at the 532 nm wavelength. This ensures that the AOP seeding ratio need not be changed from sample to sample. The thicknesses and absorbances of the molecular glass mixture samples at 532 nm are shown in Table 1. It should be noted that MGM 0.0 represents pure NAMG and MGM 0.5 pure DR1MG.

Table 1. Absorbances at 532 nm (A) and thicknesses (d) of the molecular glass mixture samples

material	MGM 0.5	MGM 0.4	MGM 0.3	MGM 0.2	MGM 0.1	MGM 0.0
A	0.304	0.288	0.267	0.284	0.286	0.019
d	85	95	126	180	380	385

All-optical poling was perfomed on the MGM samples as in the first measurement series and the SH signals after 15 minutes were recorded. From these values, the second-order susceptibilities ($\chi^{(2)}$) were calculated using [19]

$$\chi^{(2)}_{eff} = \chi^{(2)}_{xxx,Q}\left(\frac{n_{\omega,S}}{n_{\omega,Q} d \Delta k_Q}\right)\sqrt{\frac{I^S_{SHG}\, n_{2\omega,S}}{I^Q_{SHG}\, n_{2\omega,Q}}}\, 10^A, \tag{1}$$

where $\chi^{(2)}_{xxx,Q} = 0.6$ pm/V [8] is the susceptibility of a Y-cut quartz reference, $n_{\omega,S}$ and $n_{\omega,Q}$ and are the refractive indices of the sample and quartz at the fundamental frequency and $n_{2\omega,S}$ and $n_{2\omega,Q}$ at the second-harmonic frequency, $\Delta k_Q = 0.15 \times 10^6\,\mathrm{m}^{-1}$ [7] is the wave vector mismatch in quartz, A is the absorbance of the sample at the second-harmonic wavelength. The refractive indices of the molecular glass mixtures were approximated with values measured for 10 mol% DR1-PMMA [32], *i.e.* $n_{\omega,S} = 1.55$ and $n_{2\omega,S} = 1.68$. The $\chi^{(2)}$ values are shown in Fig. 4(a). A more or less linear increase is seen in the studied mass fraction range.

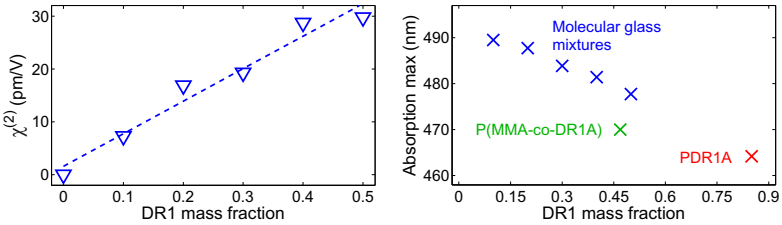

Fig. 4. Second-order susceptibilities after 15 minutes of poling and a linear fit to the data (a) and wavelengths of absorbance peaks of the solid films (b).

#255771 Received 17 Dec 2015; revised 11 Feb 2016; accepted 12 Feb 2016; published 26 Feb 2016

4. Discussion

Second-order susceptibility of 30 pm/V was reached for the DR1 molecular glass. This value is lower but comparable to ∼100 pm/V found for optimal DR1 polymer systems [7, 31]. The fact that the highest second-order susceptibility was reached with the pure DR1MG suggests that, for the molecular glass, the optimum chromophore loading is near or beyond 50 wt%. This is a high loading value compared to the optimum values experimentally found for similar polymer systems. However, it is peculiar that the NLO response only equals that found in the reference polymers as both of the polymers have higher than optimum DR1 loading which is known to decrease the achieved NLO response. With DR1MG density of 1.25 g cm^{-3}, the number density of the DR1 moieties is 1.20×10^{21} cm^{-3}. This value is in good agreement with the optimum value found in simulations taking into account the interchromophore interactions [28], which suggest that higher DR1 loading would not further increase the NLO response. The verification of this prediction is out of experimental reach with the studied molecular glass. However, a molecule with high hyperpolarizability is usually accompanied with high dipole moment. Higher dipole moment brings the optimum chromophore concentration down rapidly [28]. Therefore, in order to estimate the practical limits of the functionalized mexylaminotriazine, substitution with a chromophore with higher hyperpolarizability would be required.

Examination of the spectral properties highlight the feasibility of mexylaminotriazine as a host material. As seen in Fig. 2(a), going from pure DR1 to the DR1 glass a 50 % drop is seen in the absorbance when studied in solutions with equal concentrations by weight. This is in excellent agreement with the fact that DR1 mass fraction is 50 % in this glass. In the polymers, on the other hand, the drop in absorption is much greater than the DR1 mass fraction would suggest. Therefore, it is evident that confinement into polymer side chains affects the properties of DR1 to much greater extent than substitution to the molecular glass. Also, the location of the absorption maximum in the glass at 484 nm wavelength is very close to that found for DR1 at 486 nm. For P(MMA-co-DR1A) and PDR1A, the absorption maxima are found at 476 nm and 471 nm showing much greater blue shift. This comparison is not totally fair as the polymeric structure forces some of the molecules close to one another even in solution. In the solid state, similar effect is to be expected for each material as the intermolecular distances inevitably decrease. Still, as seen in Fig. 2(b), the molecular glasses show less blue shift also in the solid state even when the DR1 concentration exceeds that found in P(MMA-co-DR1A). This is an indication of less pronounced chromophore-chromophore intermolecular interactions which are known to be detrimental to many optical properties [33].

5. Conlusions

In conclusion, we have studied the second-order nonlinear optical properties of mexylaminotriazine molecular glass functionalized with a photoactive nonlinear optical chromophore Disperse Red 1 using all-optical poling. The photoinduced nonlinearity of the molecular glass was found to be identical to that found in polymers functionalized with the same chromophore. Our results point that this new molecular glass is well-suited for a host structure for nonlinear optical materials. In addition, the optical properties of the chromophores are less affected by the molecular glass than by the polymers. The desired optical nonlinearity is reached with no adverse effect on the advantageous properties of molecular glasses. The results suggest that high chromophore loading with strongly dipolar chromophores can be reached in the molecular glass without compromised nonlinear optical response due to chromophore-chromophore intermolecular interactions. This leads to the conclusion that this platform would allow high optical nonlinearities to be reached by replacing Disperse Red 1 with a nonlinear optical chromophore with higher hyperpolarizability.

#255771 Received 17 Dec 2015; revised 11 Feb 2016; accepted 12 Feb 2016; published 26 Feb 2016

Acknowledgments

M.V. acknowledges the financial support from Tampere University of Technology Graduate School, the Väisälä Foundation and the Graduate School of Modern Optics and Photonics. A.P. acknowledges the financial support of the Academy of Finland (Academy Research Fellowship program, project number 277091) and the Emil Aaltonen Foundation. Semen Chervinskii is acknowledged for technical assistance.

#255771 Received 17 Dec 2015; revised 11 Feb 2016; accepted 12 Feb 2016; published 26 Feb 2016

Paper IV

Arri Priimagi, Keiji Ogawa, Matti Virkki, Jun-ichi Mamiya, Martti Kauranen, and Atsushi Shishido

"High-contrast photoswitching of nonlinear optical response in crosslinked ferroelectric liquid-crystalline polymers"

Advanced Materials, vol. 24, no. 48, pp. 6410–6415, 2012

ADVANCED MATERIALS
www.advmat.de

High-Contrast Photoswitching of Nonlinear Optical Response in Crosslinked Ferroelectric Liquid-Crystalline Polymers

*Arri Priimagi, Keiji Ogawa, Matti Virkki, Jun-ichi Mamiya, Martti Kauranen, and Atsushi Shishido**

Organic materials are anticipated as inexpensive and easily processable successors to inorganic crystals as high-performance nonlinear optical (NLO) materials.[1] For controllable photonic devices, organic materials possess a further advantage at the nanometer-scale: their molecular NLO response can be reversibly switched by photochemical or electrochemical modification.[2,3] However, efficient and reversible switching in the solid state remains a challenge, particularly for second-order NLO response because macroscopic noncentrosymmetric alignment of the NLO moieties must be reversibly controlled. Solid-state switching of second-harmonic generation (SHG) has been previously demonstrated in poled polymers containing photochromic dyes,[4,5] organic photochromic crystals,[6,7] and Langmuir–Blodgett (LB) thin films of organometallic complexes.[8] In all cases, the modulation reported has been ≤50%. Moreover, both photochromic SHG switching in poled polymers[4,5] and redox-based switching in LB films[8] suffer from switching-induced irreversible changes in the initial chromophore alignment, which severely limits the number of "on"/"off" cycles that can be obtained in these materials. Common to the aforementioned schemes is that they are all based on reversible modification of molecular hyperpolarizability, which is then ideally transferred into efficient switching of the bulk second-order NLO response. Here, we employ a different scheme and present a new concept for switchable second-order NLO response, based on two-photon isomerization of azobenzene moieties in crosslinked ferroelectric liquid-crystalline polymers.[9,10] Such polymers possess thermodynamically stable net polar order, which allows us to overcome the repeatability problems inherent to the aforementioned switching schemes. Distinct from the previous reports we rely on macroscopic photoinduced change in molecular alignment as opposed to controlling the molecular-level response of the NLO moieties. With this conceptually novel switching scheme we achieve reversible isothermal photocontrol of second-order NLO response with superior contrast of up to 20.

The high performance of organic NLO materials arises from their strong and fast molecular-level NLO response as described by the molecular hyperpolarizabilities.[1] Conventional molecules for second-order NLO effects, such as second-harmonic generation (SHG), consist of strong electron donor (D) and acceptor (A) moieties that are coupled by a π-conjugated bridge. Molecular-level switching of the NLO response is based on modifying the electronic properties of this D–π–A structure by external stimuli.[11] This can be obtained through, for example, photochromic reactions,[12,13] redox interconversion,[14,15] or proton transfer.[16] For device applications, however, molecular-level switching itself is insufficient. Bulk second-order response requires the molecular units to be arranged in a noncentrosymmetric fashion, and efficient and reversible control of the NLO response within macroscopic solid-state structures remains a challenge. The first examples of reversible SHG switching in bulk samples were demonstrated using poled azobenzene- and spiropyran-containing polymers.[4,5] The main problem in such systems is their nonequilibrium nature: the net polar alignment of the chromophores tends to thermally randomize, and this randomization is further boosted by photochemical reactions. Later on, reversible SHG switching in organic photochromic crystals was demonstrated and photomodulation of about 30% was achieved owing to enol–keto intramolecular tautomerism.[6,7] Recently, Coe et al. reported on redox-switchable Langmuir–Blodgett films, where SHG can be modulated by 50%, corresponding to a contrast ratio of 1.[8] In their case, however, the SHG activity was lost already after two oxidation–reduction cycles.

All the aforementioned schemes rely on molecular-level switching of the hyperpolarizability, which is then ideally transferred into efficient switching of the bulk NLO response. In practice, although complete "on"/"off" switching has been demonstrated in solution,[14] efforts towards obtaining this in the solid state have fallen short. Recently, a different approach was introduced by Mercier et al. who showed that noncentrosymmetric-to-centrosymmetric structural transition in organic–inorganic hybrid materials does allow thermally-induced "on"/"off" switching of SHG.[17] The obvious drawback is that the effect is

Dr. A. Priimagi, K. Ogawa, Dr. J. Mamiya, Prof. A. Shishido
Chemical Resources Laboratory
Tokyo Institute of Technology
R1-12, 4259 Nagatsuta, Midori-ku
Yokohama 226-8503, Japan
E-mail: ashishid@res.titech.ac.jp
Dr. A. Priimagi
Department of Applied Physics
Aalto University
P.O. Box 13500, FI-00076 Aalto, Finland
M. Virkki, Prof. M. Kauranen
Department of Physics
Tampere University of Technology
P.O. Box 692, FI-33101 Tampere, Finland

DOI: 10.1002/adma.201203369

ADVANCED MATERIALS
www.advmat.de

Materials Views
www.MaterialsViews.com

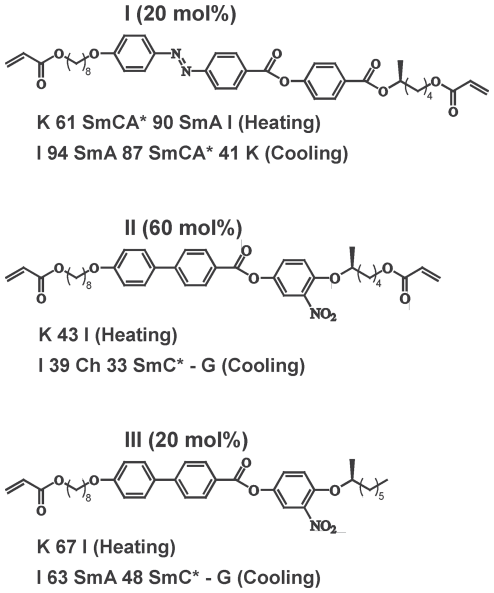

Figure 1. Chemical structures and phase transition temperatures of the azobenzene crosslinker I and the NLO moieties (II and III). The mixture I: II: III exhibited a smectic C* phase at room temperature, allowing facile preparation of SSFLC polymer films.

driven by temperature change: achieving efficient and reversible SHG switching isothermally still remains a great challenge and an attractive goal.

Our conceptually different SHG switching scheme is based on photoinduced change in molecular alignment in azobenzene-containing surface-stabilized ferroelectric liquid-crystalline (SSFLC) polymers. FLCs are an intriguing class of materials for second-order NLO due to their thermodynamically stable net polar order.[9] Due to this property, effort has been put in designing FLCs incorporating D–π–A moieties with high second-order hyperpolarizabilities,[18,19] and also in preparing polymeric SSFLCs with high second-order NLO response.[20,21] On the other hand, incorporation of photochromic units into FLCs provides a pathway towards photochemical control of the spontaneous polarization, through changes in molecular alignment resulting from the photochromic reaction.[22–24] It has also been shown that azobenzene-containing FLC polymers can undergo rapid and efficient photoinduced bending upon irradiation with UV light.[25] Hence, FLCs and FLC polymers are attractive as both photoswitchable materials and NLO materials, but to the best of our knowledge no efforts in combining these two features have been taken up to date.

Our design strategy is based on decoupling the photoresponsive and the NLO-active units (see **Figure 1**): the azobenzene crosslinker **I** serves to modify the molecular alignment within the polymer network through *trans-cis* photoisomerization, whereas compounds **II** and **III** are non-photochromic but second-order NLO active due to the presence of the electron-accepting nitro group, as first shown by Walba et al.[26] The constituent compounds were synthesized according to previously reported methods.[20,21,25] The samples were prepared by photopolymerization of the monomer mixture of **I**: **II**: **III** in a composition ratio of 20 mol%: 60 mol%: 20 mol% (see the Experimental Section for further details). The resulting crosslinked polymer film showed a very low glass-transition temperature of ca. –10 °C, and a high order parameter of molecular alignment of approximately 0.75 as deduced from **Figure 2**a. The tilt angle between the rubbing direction and the direction of molecular alignment was 35° (Figure 2). No ferroelectric switching could be induced in the polymerized state, indicating that the chiral smectic C phase was "locked", with polar axis in the direction of the sample normal.

The sample exhibited stable SHG without applying an external electric field. The SHG response was first studied using a picosecond Nd:YAG laser (1064 nm, 60 ps, 1 kHz, 0.6 W/cm^2) using similar measurement geometries as have been previously employed for characterizing planar-aligned FLCs (see **Figure 3**a for the experimental setup used).[27,28] This wavelength-pulse length combination induces no two-photon isomerization of the azobenzene moieties; hence these measurements address the basic structural properties of the sample. For these experiments we used a sample with 5-µm thickness. This is thinner than the coherence length of SHG for corresponding FLC polymers,[27] the polarization dependence of which could

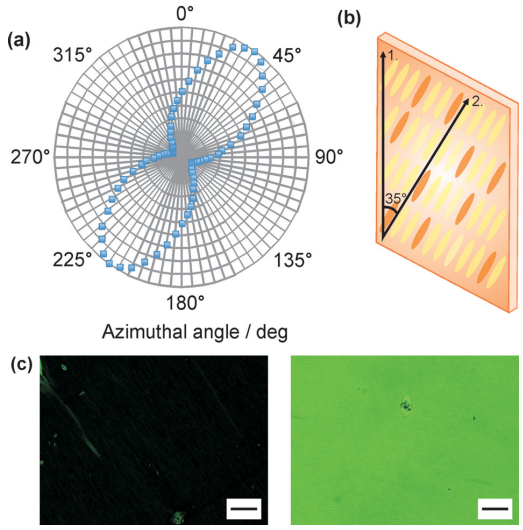

Figure 2. a) The relative absorbance of the crosslinked SSFLC polymer film (thickness 10 µm) at 455 nm as a function of the angle between the plane of polarization and the rubbing direction (set as 0°). b) Schematic illustration of the molecular alignment within the crosslinked SSFLC polymer films. (1.) and (2.) correspond to the rubbing direction and the molecular alignment direction, respectively, and the polar axis lies in the direction of sample normal. c) Polarized optical micrographs of the crosslinked SSFLC polymer film, taken at 35° (left) and 80° (right) angles between the polarizer transmission direction and the rubbing direction. The scale bar corresponds to 100 µm.

Adv. Mater. **2012**,
DOI: 10.1002/adma.201203369

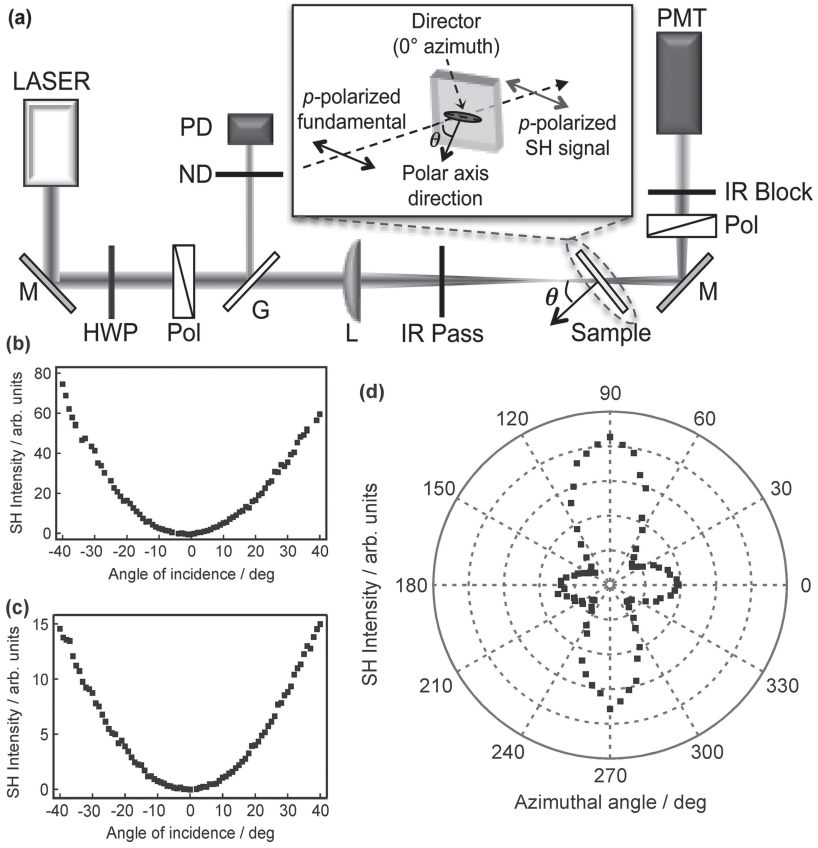

Figure 3. a) Schematic of the experimental setup. Abbreviations: M, mirror; HWP, half-wave plate; Pol, polarizer; G, microscope slide; ND, neutral-density filter; PD, photodiode; L, lens (+ 150 mm); IR Pass, a filter to block any second-harmonic generated by the optical components; IR block, a combination of filters and a lens tube to block the strong fundamental beam from reaching the photomultiplier tube (PMT). b,c) SHG at varying angles of incidence for a *p*-polarized input and *p*-polarized second-harmonic in a 5-μm crosslinked SSFLC polymer film with the director set vertically (b) and horizontally (c) with respect to the polarization plane. d) The dependence of the SHG signal on the director azimuthal angle at a fixed angle of incidence of 20° for *p*-polarized fundamental and second-harmonic beams.

significantly complicate the interpretation of the results. At the same time, we minimize any polarization changes as light propagates through the highly birefringent sample. The results are summarized in Figure 3. As the polar axis lies in the direction of the sample normal, no SHG could be detected at normal incidence, and the SH intensity increased significantly with increasing angle of incidence irrespective of whether the sample director was set perpendicular or parallel to the plane of incidence (Figure 3b,c). The azimuth angle dependence of SHG, shown in Figure 3d depicts four distinct SHG maxima, found when the sample director is parallel (0°, 180°) or perpendicular (90°, 270°) to the plane of polarization, as expected based on previous literature reports.[28] Hence, the results are in agreement with the earlier reports on similar samples,[27,28] suggesting that the net polar order inherent to SSFLC polymers is essentially undisturbed by the azobenzene crosslinkers.

The SHG switching experiments were carried out using a femtosecond Ti:sapphire laser (800 nm, 1 kHz, 100 fs, ≈3.5 W/cm^2), which served not only to produce the SHG but also to induce two-photon isomerization of the azobenzene derivatives as verified by UV-vis spectroscopy.[29,30] The key results are shown in **Figure 4**a. The results are obtained for a 20-μm-thick sample, but the same effect was observed also for samples with thicknesses of 5 and 10 μm. When the sample director was set perpendicular to the *p*-polarized pump beam, the SH intensity remained steady. Upon rotating the sample by 90° (director parallel to the pump beam polarization), SH intensity decreased to 10% of the initial value within 10 min irradiation period. Upon longer irradiation, SHG was further suppressed, saturating to 5% of the initial value within 20 min irradiation. As shown in Figure 3b, the suppression of SHG is accompanied by an increase in the absorbance of the azobenzene nπ^* transition,

ADVANCED MATERIALS
www.advmat.de

Materials Views
www.MaterialsViews.com

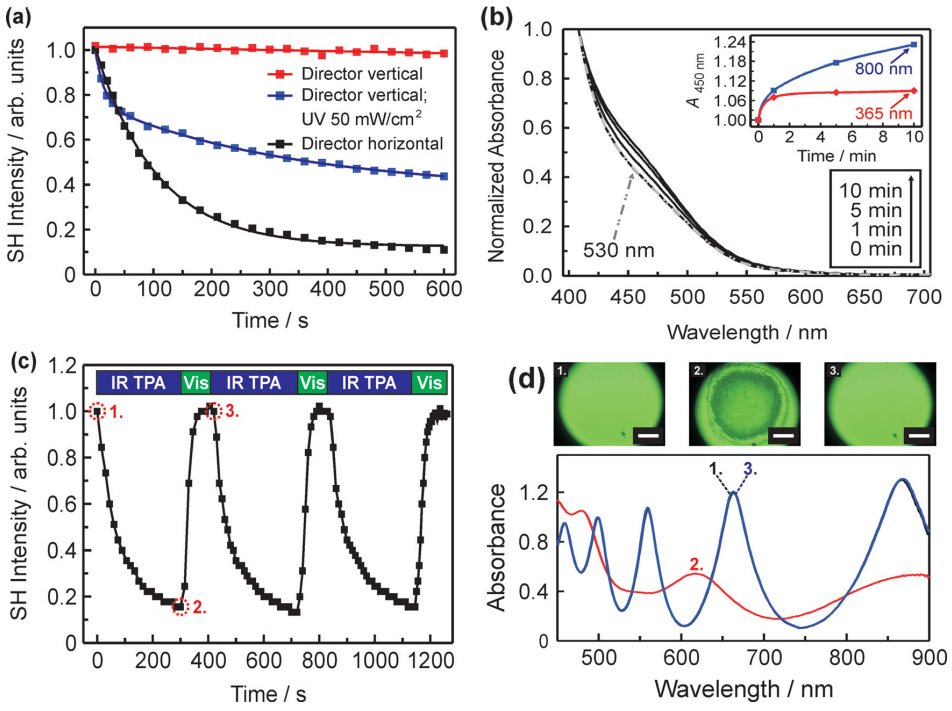

Figure 4. a) Photoinduced suppression of SHG in a 20-µm crosslinked SSFLC polymer film upon UV excitation and two-photon excitation. b) UV-vis spectral changes of the 20-µm crosslinked SSFLC polymer film, arising from two-photon isomerization. Inset: *trans-cis* isomerization-induced increase in the absorbance at 450 nm upon UV excitation (red curve) and two-photon excitation (blue curve). c) The two-photon isomerization-induced switching of SHG is completely reversible, and the initial SHG can be rapidly restored upon irradiation with a 530 nm LED. "IR TPA" refers to the period of irradiation with 800 nm; "Vis" refers to the 530 nm irradiation period. d) Top: The polarized-optical micrographs illustrate the decreased molecular alignment of the initially aligned film (1.) by two-photon isomerization (2.), and the restoration of the initial molecular alignment by irradiating with 530 nm LED (3.). The scale bar corresponds to 400 µm. Bottom: The birefringence of the samples at the initial and the SHG-suppressed states were determined from the UV-vis spectra, taken between two parallel-aligned polarizers with the sample director set to 45° angle with respect to the polarizer transmission direction. The birefringence Δn can be deduced form the wavelengths of the subsequent absorption maxima (λ and λ') as $\Delta n = (\lambda\lambda')/[d(\lambda\text{-}\lambda')]$, where d is the sample thickness.

proving that the phenomenon is triggered by *trans-cis* photoisomerization of the azobenzene moieties. When the sample was irradiated with 530 nm LED (10 mW/cm^2), the initial spectrum was quickly restored due to reverse *cis-trans* isomerization (Figure 4b).

As a comparison, we studied the SHG switching also by exciting the azobenzenes with a UV-LED (365 nm, 50 mW/cm^2), when the director was set perpendicular to the pump beam polarization. In this case, the SHG decreased only by a factor of 2 upon 10 min irradiation (Figure 4a), and the isomerization-induced spectral changes were less pronounced than for the two-photon excitation scheme (Figure 4b, inset). This can be attributed to the low penetration depth of the UV light into the samples, which confines the isomerization into the vicinity of the surface. Two-photon excitation, on the other hand, isomerizes the azobenzene moieties uniformly throughout the whole of the sample, rendering the nonlinear excitation scheme more efficient than the UV excitation.

The isomerization-induced SHG switching is completely reversible, as brought out in Figure 4c: *trans-cis* isomerization efficiently suppresses the SHG, reverse *cis-trans* isomerization induced by the 530 nm LED restores the SH intensity to the initial value. No fatigue was observed over at least 6 cycles. Hence, the thermodynamically stable polar order inherent to SSFLC polymers, in combination with the chemical crosslinking of the liquid-crystalline polymer, allows us to overcome the stability problems arising in conventional poled polymer systems,[4,5] and enables efficient and reversible control over the second-order NLO response.

The switching scheme can be explained as follows. When the azobenzenes are in the *trans*-form, the mesogens are highly aligned, and the birefringence of the sample is ca. 0.18. Two-photon absorption converts part of the azobenzene moieties into non-mesogenic *cis*-form due to which the initial molecular alignment is disturbed, as evidenced by the decreased contrast of the polarized-optical micrographs shown in Figure 4d. As

Adv. Mater. **2012**,
DOI: 10.1002/adma.201203369

a result, the birefringence decreased from ca. 0.18 to ca. 0.10 (Figure 4d). This decrease in the molecular alignment is very large compared to values we have previously reported,[31] and it efficiently disturbs the non-centrosymmetric ordering of the NLO-active moieties and suppresses the SHG, whereas the initial high net polar order of the SSFLC polymers is perfectly restored thermally or photochemically thanks to memory effect of the molecular alignment set by the crosslinkers.

All in all, the limits of our switching scheme are yet to be tested, and various tracks can be followed to enhance the process further. The molecular-level second-order NLO response of the present NLO-phores could be increased by addition of electron-donating group in the *para* position of the electron-accepting nitro group,[32] or by using laterally azo-bridged, highly non-linear dimesogens.[18,19] The NLO response of SSFLC polymers has also been reported to depend on crosslinking density,[21] and lower crosslinking density or higher azobenzene concentration may yield more efficient and faster SHG switching. One drawback of the present material system is that it is not bistable, but the azobenzenes thermally reconvert to the *trans*-form within a time scale of a few hours. This restores the mesogen alignment as well as the SHG to the initial state. This limitation could be addressed by replacing the azobenzene units with bistable diarylethene derivatives, which have been shown to yield bistable photoswitching of the spontaneous polarization of FLCs.[33,34]

Surface-stabilized FLC polymers have significant advantages compared to other materials in which a switchable second-order nonlinear response has been demonstrated. First, by relying on photoinduced change in molecular alignment rather than controlling the molecular-level hyperpolarizability we achieve a significant improvement in the reversibility and repeatability of the switching. Decoupling of the photochromic units and the NLO moieties also increases the flexibility of the system, allowing one to combine and optimize the material composition in order to meet the needs for a specific target. In addition, by relying on two-photon photomodification the switching beam interacts with the whole sample, enabling high switching contrast to be reached. By further optimization of materials design, we envisage SSFLC polymers to provide a route towards stable and reversible control over the second-order NLO response in the solid-state, with the possibility of setting the operation point anywhere between zero and the maximum by controlling the extent of photochromic reaction. Altogether, our concept constitutes a versatile platform for externally controllable NLO-active solid-state materials and a step towards device applications in all-optical switching and signal processing.

Experimental Section

The photopolymerization was carried out as follows. First, the monomer mixture (Figure 1) containing 1 mol% of a photoinitiator (LUCIRIN TPO) was injected at 55 °C (above the isotropization temperature of the mixture) into an ITO-coated glass cell with unidirectionally rubbed polyimide layers. Cell thicknesses of 5, 10, and 20 μm were used. The mixture was subsequently cooled to room temperature (smectic C^* phase of the polymerizable mixture) under AC electric field (5 V/μm, 1 Hz) at a cooling rate of 1 °C/min as the AC field has been reported to improve the alignment order of the smectic layers.[21] The photopolymerization was carried out under a DC field (10 V/μm), using light polarized perpendicularly to the direction of molecular alignment to prevent photoisomerization of the azobenzene units. The light source was a high-pressure mercury lamp equipped with proper filters to obtain polymerization wavelength of 400 nm and irradiation intensity of 10 mW/cm^2. The polymerization time was 5 h. In some cases, the samples were removed from the glass cells after irradiation in order to confirm successful photopolymerization; the NLO experiments were carried out using the sandwich-type samples.

Acknowledgements

This work was supported by JSPS KAKENHI Grant Numbers 19050010, 22550109, 22·00831, and by Academy of Finland (Project number 135043). A.P. acknowledges the financial support by the Foundations' Post Doc Pool in Finland.

Received: August 14, 2012
Published online:

[1] P. N. Prasad, D. J. Williams, *Introduction to Nonlinear Optical Effects in Molecules and Polymers*, John Wiley and Sons, New York **1991**.
[2] J. A. Delaire, K. Nakatani, *Chem. Rev.* **2000**, *100*, 1817.
[3] I. Asselberghs, K. Clays, A. Persoons, M. D. Ward, J. McCleverty, *J. Mater. Chem.* **2004**, *14*, 2831.
[4] R. Loucïf-Saibi, K. Nakatani, J. A. Delaire, M. Dumont, Z. Sekkat, *Chem. Mater.* **1993**, *5*, 229–236.
[5] Y. Atassi, J. A. Delaire, K. Nakatani, *J. Phys. Chem.* **1995**, *99*, 16320.
[6] K. Nakatani, J. A. Delaire, *Chem. Mater.* **1997**, *9*, 2682.
[7] M. Sliwa, S. Létard, I. Malfant, M. Nierlich, P. G. Lacroix, T. Asahi, H. Masuhara, P. Yu, K. Nakatani, *Chem. Mater.* **2005**, *17*, 4727.
[8] L. Boubekeur-Lecaque, B. J. Coe, K. Clays, S. Foerier, T. Verbiest, I. Asselberghs, *J. Am. Chem. Soc.* **2008**, *130*, 3286.
[9] S. T. Lagerwall, *Ferroelectric and Antiferroelectric Liquid Crystals*, John Wiley and Sons, New York **1999**.
[10] M. Brehmer, R. Zentel, *Macromol. Chem. Phys.* **1994**, *195*, 1891.
[11] B. J. Coe, *Chem. Eur. J.* **1999**, *5*, 2464.
[12] S. L. Gilat, S. H. Kawai, J. M. Lehn, *Chem. Eur. J.* **1995**, *1*, 275.
[13] V. Aubert, V. Guerchais, E. Ishow, K. Hoang-Thi, I. Ledoux, K. Nakatani, H. Le Bozec, *Angew. Chem. Int. Ed.* **2008**, *47*, 577.
[14] B. J. Coe, S. Houbrechts, I. Asselberghs, A. Persoons, *Angew. Chem. Int. Ed.* **1999**, *38*, 366.
[15] M. Malaun, Z. R. Reeves, R. L. Paul, J. C. Jeffery, J. A. McCleverty, M. D. Ward, I. Asselberghs, K. Clays, A. Persoons, *Chem. Commun.* **2001**, 49.
[16] I. Asselberghs, Y. Zhao, K. Clays, A. Persoons, A. Comito, Y. Rubin, *Chem. Phys. Lett.* **2002**, *364*, 279.
[17] W. Bi, N. Louvain, N. Mercier, J. Luc, I. Rau, F. Kajzar, B. A. Sahraoui, *Adv. Mater.* **2008**, *20*, 1013.
[18] D. M. Walba, D. J. Dyer, T. Sierra, P. L. Cobben, R. Shao, N. A. Clark, *J. Am. Chem. Soc.* **1996**, *118*, 1211.
[19] Y. Zhang, J. Martinez-Perdiguero, U. Baumeister, C. Walker, J. Etxebarria, M. Prehm, J. Ortega, C. Tschierske, M. J. O'Callaghan, A. Harant, M. Handschy, *J. Am. Chem. Soc.* **2009**, *131*, 18386.
[20] M. Trollsås, C. Orrenius, F. Sahlén, U. W. Gedde, T. Norin, A. Hult, D. Hermann, P. Rudquist, L. Komitov, S. T. Lagerwall, J. Lindström, *J. Am. Chem. Soc.* **1996**, *118*, 8542.
[21] C. Artal, M. B. Ros, J. L. Serrano, N. Pereda, J. Etxebarría, C. L. Folcia, J. Ortega, *Macromolecules* **2001**, *34*, 4244.
[22] T. Ikeda, T. Sasaki, K. Ichimura, *Nature* **1993**, *361*, 428.
[23] R. P. Lemieux, *Soft Matter* **2005**, *1*, 348.
[24] P. Beyer, M. Krueger, F. Giesselmann, R. Zentel, *Adv. Funct. Mater.* **2007**, *17*, 109.

[25] Y. Yu, T. Maeda, J. Mamiya, T. Ikeda, *Angew. Chem. Int. Ed.* **2007**, *46*, 881.
[26] D. M. Walba, M. B. Ros, N. A. Clark, R. Shao, K. M. Johnson, M. G. Robinson, J. Y. Liu, D. Doroski, *Mol. Cryst. Liq. Cryst.* **1991**, *198*, 51.
[27] D. S. Hermann, P. Rudquist, S. T. Lagerwall, L. Komitov, B. Stebler, M. Lindgren, M. Trollsås, F. Sahlen, A. Hult, U. W. Gedde, C. Orrenius, T. Norin, *Liq. Cryst.* **1998**, *24*, 295.
[28] M. Lindgren, D. S. Hermann, J. Örtegren, P. O. Arntzen, U. W. Gedde, A. Hult, L. Komitov, S. T. Lagerwall, P. Rudquist, B. Stebler, F. Sahlén, M. Trollsås, *J. Opt. Soc. Am. B* **1998**, *15*, 914.
[29] L. Antonov, K. Kamada, K. Ohta, F. S. Kamounah, *Phys. Chem. Chem. Phys.* **2003**, *5*, 1193.
[30] H. Ishitobi, Z. Sekkat, S. Kawata, *J. Opt. Soc. Am. B* **2006**, *23*, 868.
[31] A. Shimamura, A. Priimagi, J. Mamiya, T. Ikeda, Y. Yu, C. J. Barrett, A. Shishido, *ACS Appl. Mater. Interfaces* **2011**, *3*, 4190.
[32] K. Schmitt, R. P. Herr, M. Schadt, J. Fünfschilling, R. Buchecker, X. H. Chen, C. Benecke, *Liq. Cryst.* **1993**, *14*, 1735.
[33] K. E. Maly, M. D. Wand, R. P. Lemieux, *J. Am. Chem. Soc.* **2002**, *124*, 7898.
[34] K. E. Maly, P. Zhang, M. D. Wand, E. Buncel, R. P. Lemieux, *J. Mater. Chem.* **2004**, *14*, 2806.

Adv. Mater. **2012**,
DOI: 10.1002/adma.201203369

Tampereen teknillinen yliopisto
PL 527
33101 Tampere

Tampere University of Technology
P.O.B. 527
FI-33101 Tampere, Finland

ISBN 978-952-15-3811-7
ISSN 1459-2045